博士論文

Near horizon physics of charged black holes and the Jackiw-Teitelboim gravity

（電荷を持つブラックホールの地平線近傍の物理と Jackiw-Teitelboim 重力理論）

氏名　後藤郁夏人

Near horizon physics of charged black holes and the Jackiw-Teitelboim gravity

---

Kanato Goto

A thesis submitted to
the University of Tokyo, Komaba, Graduate school of Arts and Sciences

Contents

Abstract

In this thesis, we perform a comprehensive study of the dimensional reductions from the four-dimensional charged black holes in the near-extremal and the near-horizon limit. We mainly consider dimensionally reducing the magnetically charged black holes in the canonical (fixed charge) ensemble and the electrically charged black holes in the grand canonical (fixed chemical potential) ensemble. For the magnetically charged black holes, the near-extremal and the near-horizon limit of the dimensionally reduced theory leads to the dilaton gravity theory which is called the Jackiw-Teitelboim model. On the other hand for the electrically charged black hole, we obtain a different dilaton gravity theory which is coupled to the two-dimensional Maxwell field. We show that these two theories obey the same equations of motion with respect to the metric and the dilaton after putting the Maxwell field in the latter theory on-shell. We also argue about how the four-dimensional electromagnetic duality is encoded in these two dimensional gravity theories in the semi-classical limit. By investigating the solutions of these theories and performing the thermodynamical arguments, we found that they describe the black holes in the asymptotically two-dimensional AdS spacetime in which the properties of the near-extremal black holes in four dimensions are encoded. We also discuss the relation to the so-called Schwarzian theory which also describes the infrared dynamics of the so-called Sachdev-Ye-Kitaev model, which is a quantum mechanical model of the Majorana fermions and argue about implications for the AdS/CFT correspondence.

We also computed a gravitational quantity, so-called holographic complexity of these two-dimensional models in the AdS/CFT context. This quantity is conjectured to be dual to the computational complexity of the CFT state. We found that these two models lead to completely distinct behavior of the complexity at late times. We compared them with the four-dimensional result of the holographic complexity.

Acknowledgement

First and foremost I want to express my special appreciation and thanks to my supervisor, Mitsuhiro Kato, for the continuous support of my Ph.D. study and for his patience. I would like to thank you for encouraging my research and for allowing me to discuss with researchers at various external institutes. Such experiences helped me to expand the scope of my study and it also led to the research projects related to this thesis.

Besides my advisor, I would especially like to thank my collaborators, Robert C. Myers, Beni Yoshida, Hugo Marrochio and Leonel Queimada for fruitful discussions, as the works done in collaboration with them constitute the most important parts of this thesis. It was a true pleasure to work with all of you.

I would also like to express my gratitude to Tadashi Takayanagi, with whom I often discussed at the early stage of my Ph.D. course. I really enjoyed discussions and learned a lot of things from you. I imagine that I couldn't live a fulfilling research life as now without such experience.

I am also grateful to my collaborators Yoichi Kazama and Takuya Okuda for fruitful discussions. In particular I feel indebted to Yoichi Kazama for innumerable discussions on the black hole physics and AdS/CFT correspondence which are deeply related to the contents of this thesis.

I also extend my gratitude to the secretary of our group, Toko Sasaki, who is always concerned about students in our group including myself and supported us in all aspects of our research lives.

During the course of my Ph.D. studies, I have benefited also from discussions with various other people. As it is impossible to list them all, let me particularly thank to Thomas Hartman, Alice Bernamonti and Federico Galli for discussions on the topics related to the AdS/CFT correspondence.

Finally I would like dedicate my sincere gratitude to Joseph Polchinski, who taught me mysteries of gravity and black holes during my visit of Santa Barbara when I was still an undergraduate student. The fruitful discussions with him led me to start researching the black hole physics in the course of my Ph.D. studies.

1 Introduction

Gravity attracts everything in our world; it has also attracted the greatest interests of many people for a long time. In spite of many efforts, its true identity is still hidden in a veil of mystery.

Albert Einstein, one of the greatest physicists in the 20th century, took a giant step forward understanding the nature of gravity[1–6]. He recaptured gravity as the fabric of the spacetime more than just one of the other forces such as the electromagnetic force. In Einstein's gravity theory, properties of the gravitational force and the principle of relativity are elegantly unified by the spacetime. His idea has changed not only our understanding of gravity but also shed light on the nature of space and time; it is not just a box in which the physical processes occur but it itself is a dynamical object which obeys the laws of physics and causes the gravitational force. Since the radical change of worldview which he made, understanding gravity is strongly tied with one of the most fundamental questions about our universe which people have always wondered '*What are space and time?*'

Black holes, whose existence is also predicted by Einstein's gravity theory, are the most mysterious objects in our world [7]. Though they are objects within a framework of Einstein's theory, the existence of their singularities and horizons highlights the need for altering our current understanding of gravity and the spacetime. According to the Einstein's gravity theory, once an object enters the black hole horizon it inevitably hits the spacetime singularity, but which is the place where Einstein's description of gravity breaks down and we are deprived of the ability to predict anything.

Stephen W. Hawking also showed the limitation of our current understanding of gravity by considering a quantum mechanics near the black hole horizon. He raised a question, so-called 'Hawking's information paradox', by predicting that the quantum fluctuations around the horizon cause the black hole to evaporate and as a result, the gravitational system thermalizes [8, 9]. Such a process is inconsistent with quantum mechanical principle because the quantum pure state should not be turned into the thermal states by the unitary time evolutions. Thermal nature of the black hole is well expressed within his famous formula for the black hole entropy [8, 10]

$$S_{\rm BH} = \frac{A}{4G_N}\,. \tag{1.1}$$

It is known that the black hole has no hair (Hawking and his colleagues had success in growing its hair recently[11, 12], but it is still not so hairy as the formula predicts[1]),

[1]Very recently there was a further development in a special case of three-dimensional BTZ black holes[13].

thus his formula seems to be claiming that the description of gravity in terms of the spacetime is just a kind of the hydrodynamical approximations and we need to refine our current understanding of gravity.

Josef Polchinski and his colleagues refined and redefined Hawking's information paradox recently [14–16]. Through the analyses of quantum effects near the horizon of a black hole, they reached a surprising conclusion which is known as the firewall paradox. They claimed that there is a possibility that the geometrical descriptions of black hole interior break down as long as one persists the quantum mechanical principles! These problems seem to suggest the lack of our knowledge on gravity when it is placed in the quantum mechanical systems.

People have struggled to look for a consistent framework which enables us to understand gravity and quantum mechanics consistently under the spell of the 'quantum gravity'. Physicists who were studying elementary particle theory tried to put this problem into the framework of the quantum field theory which they used to handle (for early work in this direction, see [17–23]). They focused on considering small fluctuations of the metric on a fixed geometry and tried to quantize it just same as other elementary particles. Such a quantum is called *graviton*. String theory is the most successful theory in this approach which doesn't lead to any inconsistencies and gives us finite results of quantum physics of gravity at least within perturbative calculations. However in this approach, the notion of the spacetime geometry, which plays the most important role in the Einstein's theory, is broken up into small quanta of graviton and we cannot tell what position spacetime geometry occupies in the framework of quantum gravity and how it emerges from its Hilbert space. In order to gain a deeper understanding of the quantum nature of gravity and resolve black hole paradoxes described above, it seems that we need to recapture the concept of "spacetime" itself (rather than graviton) from the perspective of quantum mechanics instead of presupposing its existence as we usually do in the classical theory.

AdS/CFT correspondence, which was discovered by Juan Maldacena about twenty years ago [24], is considered to give us a suitable stage on which we can pursue this problem. It is a correspondence between the quantum gravity in $d+1$-dimensional Anti de-Sitter (AdS) spacetime and certain kinds of d-dimensional conformal field theories [24–26]. This enables us to analyze quantum gravity in AdS by using the CFT which has a well-defined Hilbert space. In the context of AdS/CFT, the CFT is defined on the boundary of AdS spacetime, thus the bulk geometry is expected to emerge from quantum degrees of freedom in the CFT. People have been trying to understand the bulk geometric quantities from the CFT perspective. One of the most famous formula in this direction is so-called Ryu-Takayanagi formula [27], which relates the entanglement

entropy and the area of the bulk co-dimension two surface as follows

$$S_{\mathrm{E}} = \frac{A}{4G_N} \,. \tag{1.2}$$

Very recently Leonard Susskind proposed an interesting connection between the computational complexity of the CFT [28, 29]and the volume of the bulk co-dimension one region, which we will also explain in detail in the main body of the thesis.

The key to the understanding of the quantum nature of gravity and spacetime must be hidden in understanding the basic mechanism of the AdS/CFT correspondence. AdS/CFT correspondence is expected to hold in several dimensions. In the $\mathrm{AdS}_3/\mathrm{CFT}_2$ correspondence, the conformal symmetry is enhanced to the infinite dimensional symmetry, so-called Virasoro symmetry which governs the behavior of the excitations of the gravitons in the AdS side. Taking the full advantage of the enhanced symmetry, many fruitful results on the gravitational physics have obtained via CFT calculations [30–34].

One might expect that the simplest example of the AdS/CFT would be "$\mathrm{AdS}_2/\mathrm{CFT}_1$" which is the lowest dimensional one. However contrary to our expectations, "$\mathrm{AdS}_2/\mathrm{CFT}_1$" is in a sense the most mysterious and strangest correspondence. One strange thing is that AdS boundary has two disconnected pieces in two dimension. Only through the bulk spacetime, they are causality connected with each other. If two CFTs describing the holography lives on these boundaries independently, how such CFTs communicate with each other without knowing about the existence of the bulk spacetime? Another weird thing is that AdS_2 spacetime seems to be unable to describe finite energy excitations. From the CFT side, the reason can be explained simply as follows. When the theory has one dimensional conformal (reparametrization) symmetry which is infinite dimensional, the traceless condition is imposed on the energy-momentum tensor. However for CFT_1, it implies the vanishing Hamiltonian. Therefore one-dimensional CFT is just a theory of a constraint and has no dynamics. Next we will give a brief explanation about this problem from the gravitational point of view.

Near-Horizon Limit of the Charged Black Hole and AdS_2

Maldacena, Michelson and Strominger [35] found the 'finite energy excitation' problem described above by performing a comprehensive study the near horizon limit of the four-dimensional charged black hole from which AdS_2 geometry appears. Now let us review their arguments. Let us consider the magnetically charged black hole in four

dimension[2]

$$
\begin{aligned}
ds^2 &= -\frac{(r-r_+)(r-r_-)}{r^2}dt^2 + \frac{r^2}{(r-r_+)(r-r_-)}dr^2 + r^2 d\Omega_2 \\
F &= \frac{g\tilde{Q}}{\sqrt{4\pi G_N}} \sin\theta d\phi \wedge d\theta \\
r_\pm &= g\tilde{Q}\ell_P + E\ell_p^2 \pm \sqrt{2g\tilde{Q}E\ell_P^3 + E^2\ell_P^4},
\end{aligned}
\tag{1.3}
$$

where $\ell_P = \sqrt{G_N}$ is the Plank length. We can take the near horizon limit of the geometry by taking $\ell_P \to 0$ while fixing the combination $z = g^2\tilde{Q}^2\ell_p^2/(r-r_+)$. The geometry ends up to be $AdS_2 \times S^2$ as we will explain in section 2. Let us investigate how the physical quantities behave in the $\ell_P \to 0$ limit. The excitation energy of the extremality and the charge are related as

$$
E = M - \frac{g\tilde{Q}}{\ell_P}\,. \tag{1.4}
$$

Taking the near extremal case, we can find the energy E and the Hawking temperature T_H are related to each other as

$$
E \sim 2\pi^2 g^3 \tilde{Q}^3 T_H^2 \ell_P \tag{1.5}
$$

One can see that we cannot take the $\ell_P \to 0$ limit while keeping the values $E, \tilde{Q}$ and T_H to be finite. If we fix $\tilde{Q}$, the system only has the ground state, which corresponds to the extremal black hole. Let us remind ourselves that the Hawking radiations typically have energies of order $\sim T_H$. The semi-classical description breaks down when $E \sim T_H$ which occurs at

$$
E_{\text{gap}} \sim \frac{1}{g^3\tilde{Q}^3\ell_P}\,. \tag{1.6}
$$

This corresponds to the energy of the lowest-lying excitation above the ground state. taking the limit $\ell_P \to 0$ leads to the infinite energy gap and no excitations above the ground state. On the other hand, a higher dimensional AdS spacetime can be obtained by taking the near horizon limit of the black p-brane geometry. In this case, the brane has the transverse spatial volume of the brane V_p, then we have a relation

$$
E \sim V_p T_H^{p+1}\,. \tag{1.7}
$$

[2]Here we just give a brief explanation. In section 2, we will study the near horizon limit in detail including the asymptotically AdS case.

Here we can take the limit $\ell_P \to 0$ safely in contrast to the AdS_2 case. Similarly to the arguments above, we have the energy gap

$$E_{\text{gap}} \sim \frac{1}{V^{\frac{1}{p-1}}}\,, \tag{1.8}$$

which is finite even after taking the limit $\ell_P \to 0$. The difference comes from the fact that the zero-dimensional object has zero volume, then we have a gapped spectrum while a finite volume of the higher dimensional object leads to the continuous spectrum.

These arguments imply that in order to include the excitations above the gap, we must not take the strict decoupling limit. This corresponds to moving a little bit from the CFT fixed point [36]. In the AdS language, since we have UV/IR relation between the CFT and the AdS, this corresponds to moving the AdS boundary a little bit into the bulk. As we will explain later in section 4, it seems that so-called Jackiw-Teitelboim gravity model (JT model in short) [37–39] in two dimensions which can describe the near-extremal black holes actually taking this procedure. In this model, we have a dynamical dilaton whose on-shell value diverges near the AdS boundary. In the usual AdS/CFT dictionary, such a "non-normalizable mode" takes us away from the CFT fixed point. In the AdS side, this corresponds to the fact that we have to cut off the AdS spacetime at a finite radius to avoid the divergence [40]. It is known that the dynamics of such a cut-off surface is controlled by the so-called Schwarzian action as we will explain in subsection 4.2. As a result, we instead have the correspondence between the nearly AdS and the nearly CFT, or $NAdS_2/NCFT_1$ in short.

This ingenious mechanism to obtain $NAdS_2/NCFT_1$ was first found in the CFT side by the analyses of the so-called Sachdev-Ye-Kitaev (SYK) model [42–45]. Sachdev-Ye-Kitaev model is a quantum mechanical model of Majorana fermions. The SYK model has been extensively studied in recent years since it can be solvable in the strong coupling (IR) limit while it shows a chaotic behavior then it can be an interesting toy model of the holography. The SYK model has a reparametrization (one dimensional conformal) symmetry at the strict IR point, but where physical quantities diverge. In order to get their finite results, we must move away a little it from the CFT fixed point, then the reparametrization symmetry is slightly broken. This is nothing but the mechanism I explained above. It also turns out that the pattern of the breaking symmetry is again controlled by the Schwarzian action the same as the JT model [36, 45]. This mechanism also is expected to shed new light on the higher dimensional holography and might lead to some generalizations of the AdS/CFT correspondence which we currently know.

Main Aim of This Thesis

As described above, the analyses of the Jackiw-Teitelboim model are quite important for a deeper understanding of the mechanism of the holography and they also might lead us beyond the framework of the AdS/CFT correspondence which we currently know. Jackiw-Teitelboim model is derived from the Einstein-Maxwell theory describing the charged near-extremal black holes by the dimensional reduction. The main aim of this thesis is to perform the comprehensive study of the dimensional reduction of the four-dimensional charged black holes. In the literature, people have mainly discussed the JT model in the $NAdS_2/NCFT_1$ context, but we found that another dimensionally reduced theory describing AdS_2 geometry can be derived from the four-dimensional charged black holes under a certain different situation. We will analyze both theories in details and compare their actions, equations of motions and thermodynamic quantities. In four dimension, we have the electromagnetic duality between the magnetic solutions and the electric solutions of the black holes [46–48]. We will discuss how the duality is encoded in the dimensionally reduced theories which we derived. We will also see that both theories lead to the Schwarzian action.

As we also explained above, recently people found interesting connections between the quantum-information-theoretic quantities and the gravitational properties in the AdS/CFT correspondence (for a review on recent progress, see also [49]). The most famous connection is represented in the so-called Ryu-Takayanagi formula [27] which relates the entanglement in CFT and the connectedness of the bulk spacetime [50, 51]. Very recently Susskind found that the properties of the entanglement are not enough to explain the properties of some bulk geometrical quantity [28, 29, 53]. He conjectured that the notion of the "computational complexity" of the CFT plays a role of explaining such a bulk quantity. In the literature, corresponding bulk quantity is called "holographic complexity," whose behavior has been extensively computed on various geometries using various prescriptions a part of which we will explain later (for a non-extensive list, see [28, 29, 53–73]). Despite many attempts [75–88], a satisfactory definition of the computational complexity for generic QFTs has not known yet. Motivated by that, we holographically computed the complexity of the SYK model using the JT model and another dimensionally reduced model which we derived. Our analysis gives us information about the complexity of SYK model. It becomes a starting point to look for a suitable definition of complexity in higher dimensional CFTs and will shed light on the fundamental role of the complexity in AdS/CFT.

Outline of This Thesis

This thesis is organized as follows.

In section 2, we will review the charged black hole also called the Reissner-Nordström black hole described by the Einstein-Maxwell theory in four dimensions and analyze its near-extremal near-horizon geometry. We compute the first corrections of the gravitational quantities in the near-extremal limit. We will see that the AdS geometry appears at the leading order in the near horizon limit, and we also compute the first order correction of it. We will also review how the electromagnetic duality holds semi-classically for the Einstein-Maxwell theory. We give additional arguments for the duality which has not discussed in the literature in subsection 2.2.

Section 3 is one of the main parts of this thesis, where we performed a comprehensive study of the dimensional reduction of the four dimensional charged black holes. We will analyze the dimensional reductions from the magnetically charged black holes as well as electrically charged black holes described by the four dimensional Einstein-Maxwell action. They lead to different two dimensional dilaton gravity theories. We analyze them in the near-horizon and near-extremal limit and obtain the linearized model which captures the leading order behavior of the near-extremal near-horizon geometry of the four dimensional charged black holes. we will see that one of them is equivalent to the JT model, but the other is a different dilaton gravity model which is coupled to the two dimensional Maxwell field. In subsection 3.5, we will argue the universality of the JT model from a more general perspective. In subsection 3.6, we will discuss the solutions of the dimensionally reduced theories and describe their thermodynamics.

In section 4, we will see the relation between the SYK model and our two dimensional dilaton gravity models. We first review the thermodynamics of the SYK model and see that they share common properties with the thermodynamics of the black hole solutions in AdS_2 of the dilaton gravity theories. We discuss that though the SYK model has the emergent conformal (reparametrization) symmetry at the strict IR limit, it is spontaneously and explicitly broken to a smaller subgroup of the original symmetry. We review that the dynamics of the symmetry breaking pattern is governed by the so-called Schwarzian action. In subsection 4.2, it is found that the same action effectively governs the gravitational dynamics of the AdS_2 spacetime in the dilaton gravity theories. We explain the gravitational interpretation of the conformal symmetry breaking.

In section 5, we compute the holographic complexity using the two dimensional dilaton gravity models we derived in section 3. Surprisingly while these two theories

lead to the same geometry, we will find the late time behavior of the complexity is completely distinct with each other. In order to investigate the origin of the difference, we also compute the holographic complexity in the four dimensional electrically and magnetically charged Reissner-Nordström black hole solution described by the Einstein-Maxwell theory and see the coincidence with the two dimensional results. W will also explain how the electromagnetic duality is successfully interfaced with this distinct behavior of the complexity.

In section 6, we will summarize our arguments and describe the future directions. The contents of this thesis are mainly based on the joint work [89, 90].

2 Reissner-Nordström Black Hole in AdS

We start with the discussion of the charged black holes in four dimension (for related arguments, see for example [93–95]). The following arguments can be easily generalized to higher dimensions if one further couples the gravitational theory to a $(d-2)-$form field strength $F_{\mu_1\cdots\mu_{d-2}}$ which is the Hodge dual of the two-form Maxwell field strength $F_{\mu\nu}$. For detailed arguments, see Appendix B. We are especially interested in the holography, thus we mainly consider the spacetime with a negative cosmological constant $\Lambda < 0$, but almost all the discussions below are still valid in the asymptotically flat spacetime by taking the cosmological constant a special value $\Lambda = 0$. Reissner-Nordström black holes are solutions of the Einstein-Maxwell theory which has the following action

$$\begin{aligned} I_{EM} =& \frac{1}{16\pi G_N}\int_{\mathcal{M}} d^4x\sqrt{-\hat{g}}(\hat{R}-2\Lambda) + \frac{1}{8\pi G_N}\int_{\partial\mathcal{M}}\sqrt{-\hat{\gamma}}\hat{K} \\ & - \frac{1}{4g^2}\int_{\mathcal{M}} d^4x\sqrt{-\hat{g}}F_{\mu\nu}F^{\mu\nu}\,, \end{aligned} \tag{2.1}$$

where the terms in the first line are Einstein-Hilbert action with so-called Gibbons-Hawking-York boundary term [91, 92] which is needed for the variational principle to be well defined. Λ is the cosmological constant in four dimensions and as explained above we assume $\Lambda < 0$ in the most part of this section. In the second line, we have the bulk action for the Maxwell field $F_{\mu\nu}$. In this section, we don't consider a boundary term for the Maxwell field. We will introduce it in the later section and describe the role of such a boundary term.

This Einstein-Maxwell action yields the following Einstein equation

$$\hat{R}_{\mu\nu} - \frac{1}{2}\hat{g}_{\mu\nu}\hat{R} + \Lambda\hat{g}_{\mu\nu} = 8\pi G_N T_{\mu\nu} \tag{2.2}$$

where $T_{\mu\nu}$ is the stress tensor of the Maxwell field

$$T_{\mu\nu} = \frac{1}{g^2}(\hat{g}^{\alpha\beta}F_{\mu\alpha}F_{\nu\beta} - \frac{1}{4}\hat{g}_{\mu\nu}\hat{g}^{\alpha\beta}\hat{g}^{\rho\sigma}F_{\sigma\alpha}F_{\rho\beta})\,, \tag{2.3}$$

and the equation for the Maxwell field

$$\partial_\mu(\sqrt{-\hat{g}}F^{\mu\nu}) = 0\,. \tag{2.4}$$

Throughout this thesis, we use the rescaled field strength $F^2/g^2 \to F^2/G_N$ and identify the couple constant g for the Maxwell field with the Newton's constant G_N for simplicity of the notation. These equations admit the Reissner-Nordström black hole solutions. The metric takes the following form

$$ds^2 = -f(r)dt^2 + \frac{1}{f(r)}dr^2 + r^2 d\Omega_2^2 \tag{2.5}$$

with the blackening factor $f(r)$ defined as

$$f(r) = 1 - \frac{2G_N M}{r} + \frac{Q_{e,m}^2}{4\pi r^2} + \frac{r^2}{L^2}\,, \tag{2.6}$$

where M is the mass of the black hole and $Q_{e,m}$ is the electric or magnetic charge the solution carries. L is the radius of the AdS_4 spacetime which is related to the cosmological constant as

$$L = \sqrt{\frac{3}{|\Lambda|}}\,. \tag{2.7}$$

$d\Omega_2$ is the line element of the unit two sphere and can be parametrized as

$$d\Omega_2^2 = \sin^2\theta d\theta^2 + d\phi^2\,. \tag{2.8}$$

The solution of the Maxwell field takes the following form

$$F_e = \frac{Q_e}{4\pi r^2} dr \wedge dt\,,\ F_m = \frac{Q_m}{4\pi}\sin\theta d\phi \wedge d\theta, \tag{2.9}$$

for the electric solution and the magnetic solution respectively. Notice that we rescaled the field strength, thus the natural definition of the charge $\tilde{Q}$ associated to the original field strength is related to the charge above as

$$\tilde{Q} = \sqrt{\frac{G_N}{4\pi g^2}} Q\,. \tag{2.10}$$

The solution has a symmetry under exchanging the electric charge and the magnetic charge, which is nothing but electromagnetic dually. More generally we can mix both charges by the rotation in the (Q_e, Q_m) plane. We will use this symmetry to work on the purely magnetic case below. Notice that by taking the limit $L \to \infty$, the solution becomes the Reissner-Nordström black hole in the asymptotically flat spacetime, and $Q \to 0$ limit reproduces the neutral AdS-Schwarzschild black hole.

It is interesting to rewrite the blackening factor as [95]

$$f(r) = 1 - \frac{r_+}{r} - \frac{r_+^3}{L^2 r} - \frac{Q^2}{4\pi r_+ r} + \frac{Q^2}{4\pi r^2} + \frac{r^2}{L^2} \tag{2.11}$$

and the mass of the black hole

$$M = \frac{1}{2G_N}\left(r_+ + \frac{r_+^3}{L^2} + \frac{Q^2}{r_+}\right)\,. \tag{2.12}$$

in terms of the charge Q and a largest real positive root of $f(r)$; r_+ which we will identify with the outer horizon of the black hole. The temperature is calculated via surface gravity $\kappa = \partial f(r_+)/2$

$$T = \frac{\kappa}{2\pi} = \frac{1}{4\pi r_+}\left(1 - \frac{Q^2}{r_+^2} + \frac{3r_+^2}{L^2}\right) \tag{2.13}$$

In order for the Reissner-Nordström metric to describe a charged black hole with a non-singular horizon at $r = r_+$, the following condition should be satisfied

$$\frac{3r_+^4}{L^2} + r_+^2 \geq Q^2\,. \tag{2.14}$$

If this condition is violated, the black hole has a naked curvature singularity at $r = 0$. We are interested in the case where the above condition is satisfied. As we can see easily, such a solution has zero temperature. When the inequality is saturated, we have the extremal black hole whose the horizon is degenerate. In this case, we have the extremal values of the mass and the charge

$$M_{\text{ext}} = \frac{r_h}{G_N}\left(1 + \frac{2r_h^2}{L^2}\right)\,, \tag{2.15}$$

$$Q_{\text{ext}}^2 = 4\pi\left(r_h^2 + \frac{3r_h^4}{L^2}\right) = 4\pi\left(r_h^2 - \Lambda r_h^4\right)\,, \tag{2.16}$$

as well as the blackening factor

$$f(r) = \frac{(r - r_h)^2}{r^2 L^2}(L^2 + 3r_h^2 + 2r_h r + r^2)\,, \tag{2.17}$$

where we specially write r_+ as r_h for the extremal solution. The inequality (2.14) and the expression (2.12) imposes the bound on the black hole mass of the form $M \geq M_{\text{ext}}(Q)$. One might think that if the theory is embedded in a supersymmetric theory, the extremal state with $M = M_{\text{ext}}$ would give the supersymmetric state. However, the BPS bound which comes from the supersymmetric algebra is instead $M \geq Q/\sqrt{4\pi}G_N$[3]. For a finite L the inequality $M_{\text{ext}} > Q/\sqrt{4\pi}G_N$ is always satisfied and one can find that the extremal state is non-supersymmetric. On the other hand, if we take the flat limit $L \to \infty$, since we have an equality $M_{\text{ext}} = Q/\sqrt{4\pi}G_N$ instead of the inequality, thus the extremal state can be supersymmetric when the theory is embedded in a supersymmetric theory. For the supersymmetric solution with a finite L, we have a blackening factor [96]

$$f(r) = \left(1 - \frac{Q}{4\pi r}\right)^2 + \frac{r^2}{L^2} \tag{2.18}$$

[3]This is the condition for the electric solutions. For the magnetic solutions, we have magnetic BPS solutions [96] with $M = 0$ and $Q_m = \pm 2\pi L$.

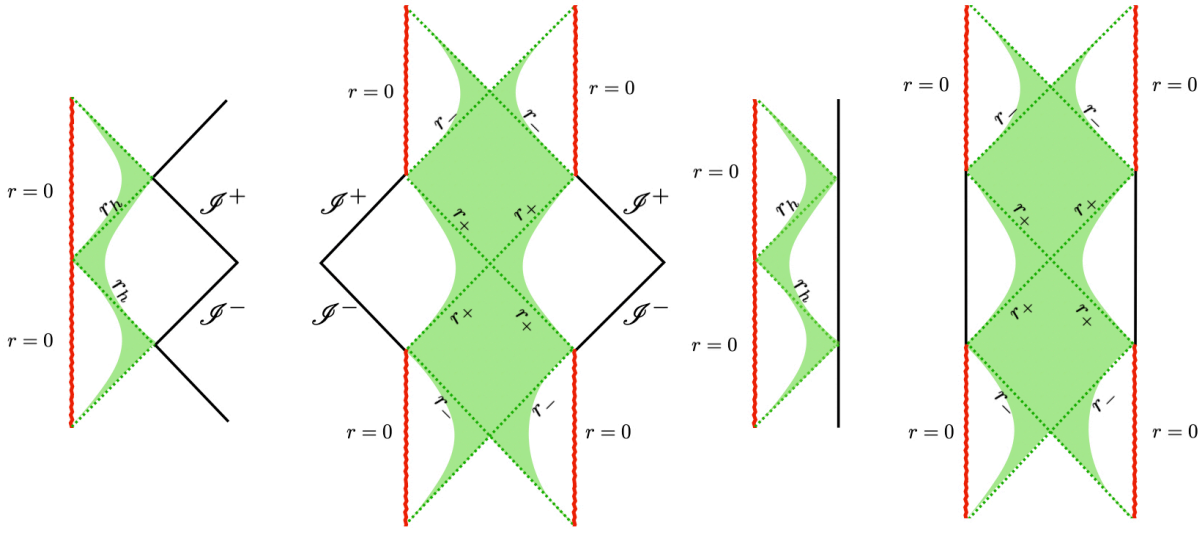

Figure 1: The Penrose diagrams of the extremal and near-extremal Reissner-Nordström black holes in the asymptotically flat and asymptotically AdS spacetimes. The most left panel corresponds to the extremal black hole in the asymptotically flat spacetime and the figure in the middle is for the near-extremal black hole in the asymptotically flat spacetime. The singularity is represented as the zigzag lines colored in red. Black real lines represent the spacetime infinity: $\mathscr{I}^+$ is the future null infinity and $\mathscr{I}^-$ is the past null infinity. The right two figures are extremal and near-extremal Reissner-Nordström black holes in the asymptotically AdS spacetime.Black real lines represent the AdS boundary placed at the spacetime infinity. In both flat and AdS black holes, the causal structures are drastically changed when we go from the extreme ones to non-extreme ones. The near-extremal black hole has two horizons: $r = r_\pm$ the outer horizon and the inner horizon while the extremal black hole has a degenerate horizon r_h. The near horizon region is colored in the green. Each region leads to the (nearly) AdS_2 spacetime (times S^2).

which is always positive, then the solution has the naked singularity. Next let us consider the near horizon geometry of the extremal black hole. In the near horizon region we have $r - r_h \ll r_h$, thus we expand the metric in $(r - r_h)/r_h$ then we find that the metric can be approximated to the AdS_2 metric up to $\mathcal{O}(\frac{r-r_h}{r_h})$ corrections

$$ds^2 = -\frac{(r-r_h)^2}{L_2^2}dt^2 + \frac{L_2^2}{(r-r_h)^2}dr^2 + r_h^2 d\Omega_2^2\,, \tag{2.19}$$

with the radius of the two dimensional AdS defined by

$$L_2^2 = \frac{L^2}{6 + \frac{L^2}{r_h^2}} \,. \tag{2.20}$$

Notice that this radius is finite even we take the asymptotically flat space limit $L \to \infty$, thus the near horizon geometry of the extremal solution of the Reissner-Nordström black hole in the asymptotically AdS or flat spacetime approaches $AdS_2 \times S^2$. AdS_2 geometry has the radius L_2 while that of sphere S^2 is r_h. In the flat space limit $L \to \infty$, they become equivalent and the AdS part and the sphere of the geometry have the same radius. It might be interesting to rewrite (2.20) as

$$|\Lambda_2| = |\Lambda| + \frac{Q_{\text{ext}}^2}{4\pi r_h^2} \,, \tag{2.21}$$

where $|\Lambda_2| = 1/L_2^2$. We can see that the two dimensional cosmological constant can be expressed as a sum of the four dimensional cosmological constant and the charge of the black hole.

Near-Extremal Black Holes

We explained features of extremal black holes, but our interest lies in near extremal ones. The non-extremal solutions satisfy the inequality (2.14) has two horizons, that is outer horizon expressed as r_+ and the inner horizon r_- which is the smaller real positive root of $f(r)$. Causal structure of the non-extremal black hole are drastically different from the extremal one as depicted in Figure 1. From the Penrose diagram in Figure 1, we can see that the inner horizon r_- as well as the horizon r_h in the extremal black hole is the Cauchy horizon which lies at the lightlike boundary of the validity of a Cauchy surface while the outer horizon r_+ is the event horizon beyond which physical objects cannot escape. It is known that the Cauchy horizon is unstable due to the averaged weak energy condition and any small perturbation on the Cauchy surface grows infinitely at this horizon. This implies that we cannot go outside of the their horizons even if the causal structures of the Penrose diagrams seem to allow.

We will now consider near-extremal black holes by taking the horizons to be

$$r_\pm = r_h \pm \delta r_h \tag{2.22}$$

with an assumption

$$\frac{\delta r_h}{r_h} \ll 1 \,, \tag{2.23}$$

to make sure the temperature very small. The temperature and the entropy of the system increase proportionally to δr_h and they are given by

$$T \approx \frac{\delta r_h}{2\pi L_2^2}\,, \tag{2.24}$$

$$S = \frac{\pi r_+^2}{G_N} \approx \frac{\pi r_h^2}{G_N} + \frac{2\pi \delta r_h r_h}{G_N}\,. \tag{2.25}$$

Moreover, if we are considering a near-extremal black hole, it means that we need to slightly deviate from the parameters of the extremal black hole. We choose to work in an ensemble of fixed charge, hence what changes with respect to extremality is the mass

$$M = M_{\text{ext}} + \delta M\,, \tag{2.26}$$

where

$$\delta M = \frac{r_h \delta r_h^2}{2G_N L_2^2} = \frac{2\pi^2}{G_N} r_h T^2 L_2^2\,. \tag{2.27}$$

Notice that the deviation of the mass comes at the order δr_h^2 and hence it is proportional to T^2. This feature is common with the so-called Jackiw-Teitelboim model, which is two-dimensional dilaton gravity theory derived from the four-dimensional charged black holes by the dimensional reduction of the action (2.1). We will discuss it in detail later. The choice of a fixed charge ensemble is encoded in action (2.1) and the use of a magnetic charge as we will explain in the later section.

Finally we consider the first order corrections from $AdS_2 \times S^2$ for the near horizon geometry of the near-extremal black hole. Up to the order $\mathcal{O}(((r-r_h)/r_h)^2)$ and $\mathcal{O}((\delta r_h/r_h)^2)$, we can find the metric of the following form

$$\begin{aligned} ds^2 &= -f(r)dt^2 + \frac{dr^2}{f(r)} + r_h^2\left(1 + \frac{2(r-r_h)}{r_h}\right) d\Omega_2^2\,, \\ f(r) &= \frac{(r-r_+)(r-r_-)}{L_2^2}\left(1 - \frac{4}{3}\frac{r-r_h}{r_h}\right)\,, \end{aligned} \tag{2.28}$$

where we focus on the large black hole $r_h \gg L$ and omit terms negligible in this limit. The leading order of this geometry is again given by $AdS_2 \times S^2$. In section 3, we integrate out the S^2 factor of the geometry by dimensionally reducing our spacetime, and obtain the two-dimensional theories which can capture the near horizon geometry of the near extremal Reissner-Nordström black holes. We dimensionally reduce both electrically charged and magnetically charged black holes described by the four dimensional action (2.1). We will see that the geometry (2.28) is correctly reproduced from the analyses of the dimensionally reduced theories.

2.1 Electriomagnetic Duality

We saw that the Einstein-Hilbert action coupled a Maxwell field in the four dimensions admits the electrically charged black hole and the magnetically charged one. Montonen and Olive [97] conjectured that there is a duality, so-called S-duality between electrically charged elementary particles and magnetically charged monopoles which is shown later to hold in the $d = 4$ $\mathcal{N} = 4$ supersymmetric Yang-Mills theory. They claimed that monopoles in the original theory with the coupling g behave like the elementary electrically charged particles in the original theory with the coupling $g' = 1/g$. S-duality is expected to hold full quantum mechanically. Black holes can be regarded as the solitons of the gravitational theory, on the other hand, it is also known that some extremal black holes are identified with elementary states in string theory. Thus it is natural to wonder whether the electromagnetic duality holds for the magnetically charged black holes and the electrically charged black holes. We can see that the symmetry holds at the level of the equation of the Maxwell field since the duality operation

$$\star F_{\mu\nu} = \frac{1}{2}\epsilon_{\mu\nu\rho\sigma}F^{\rho\sigma} \tag{2.29}$$

which exchanges the role of the electric field and the magnetic field keeps the equation of motion invariant. However, it is not obvious whether it is a symmetry of quantum theory. Maxwell action consists of the term $F^2 \sim B^2 - E^2$, but we can see that the sign changes if we consider the magnetic charge instead of the electric charge. In this section, we will see that we can indeed regard it as a symmetry of the quantum theory of gravity at least when we focus on the parameter region where the semi-classical approximation is valid.

In the semi-classical approximation, the partition function of the gravitational system given by the Euclidean path integral is dominated by the solutions of the equations of motion with the given boundary conditions. These solutions are given by the Reissner-Nordström black holes. Thus the partition function is approximated by exponential of the Euclidean on-shell action evaluated on the Reissner-Nordström black hole solution

$$Z = \int \mathcal{D}g_{\mu\nu}\mathcal{D}A_\mu e^{-I_{\text{EH-Max}}} \sim e^{-I^{\text{RN}}_{\text{EH-Max}}}\,. \tag{2.30}$$

To evaluate the partition function, we consider the solutions of the Einstein-Maxwell system in the Euclidean regime. If we wick rotate the Lorenzian action (2.1) and the

solution (2.5)(2.6)(2.9) by $\tau = it$, the Einstein-Maxwell action can be written as

$$I_{EM} = -\frac{1}{16\pi G_N}\int_{\mathcal{M}} d^4x\sqrt{g_E}(\hat{R}-2\Lambda) - \frac{1}{8\pi G_N}\int_{\partial\mathcal{M}}\sqrt{\gamma_E}\hat{K} + \frac{1}{4G_N}\int_{\mathcal{M}} d^4x\sqrt{g_E}F_{\mu\nu}F^{\mu\nu}\,. \tag{2.31}$$

and the solution for the metic becomes

$$ds^2 = f(r)d\tau^2 + \frac{dr^2}{f(r)} + r^2 d\Omega_2^2\,., \tag{2.32}$$

with

$$f(r) = 1 - \frac{2G_N M}{r} + \frac{Q_{e,m}^2}{(4\pi r)^2} + \frac{r^2}{L^2}\,. \tag{2.33}$$

The electric solution of the Maxwell field can be written as

$$F_e = -i\frac{Q}{4\pi r^2}dr\wedge d\tau\,, \tag{2.34}$$

thus we obtain the on-shell Euclidean action for the electric field as

$$I_{\text{Max}}^{\text{electric}} = \frac{1}{4G_N}\int d^4x\sqrt{g_E}F_{\mu\nu}F^{\mu\nu} = -\frac{Q^2}{2G_N}\int d^4x\sqrt{g_E}\frac{1}{(4\pi r^2)^2} \tag{2.35}$$

On the other hand, the magnetic solution

$$F_m = \frac{Q}{4\pi}\sin\theta d\phi\wedge d\theta\,, \tag{2.36}$$

leads to the on-shell action

$$I_{\text{Max}}^{\text{magnetic}} = \frac{1}{4G_N}\int d^4x\sqrt{g_E}F_{\mu\nu}F^{\mu\nu} = \frac{Q^2}{2G_N}\int d^4x\sqrt{g_E}\frac{1}{(4\pi r^2)^2}, \tag{2.37}$$

thus the sign is flipped if we exchange the magnetic solution with the electric one. To see why the difference in sign of the on-shell action is not inconsistent with the electromagnetic duality, let us remind ourselves of the variation principle of the action (2.1), which gives us

$$\delta I_{\text{Max}} = (\text{terms giving equations of motion}) - \frac{1}{G_N}\int_{\partial\mathcal{M}} d^3x\sqrt{\gamma_E}F^{\mu\nu}n_\mu\delta A_\nu\,, \tag{2.38}$$

where n_μ is the outward directed normal vector to the boundary. Since we want to get rid of the boundary terms coming from the variation, we set $\delta A_i = 0$ at the boundary where i denotes the directions along the boundary In the case of the magnetically charged black hole, this corresponds to fixing the magnetic change since the magnetic charge is given by the integral of F over S^2 on the boundary

$$Q_m = \int_{S^2} F \,. \tag{2.39}$$

and we can determine F purely from the boundary value of A_i. On the other hand, for the electrically charged case, the electric charge is given by the integral of the Hodge dual of F, which is not determined just by the boundary value of A_ν. Instead of fixing the charge, for the electric case the condition $\delta A_\nu = 0$ fixes the chemical potential μ defined on the boundary as

$$\mu = \frac{1}{G_N} \lim_{r\to\infty} A_t \,. \tag{2.40}$$

Therefore magnetically charged black holes described by the action (2.1) are in the canonical ensemble (fixed charge ensemble) while electrically charged black holes are in the grand canonical ensemble (fixed chemical potential ensemble). This is the reason why the different actions (2.37)(2.35) does not necessarily imply the contradiction with the electromagnetic duality. In order to see the quantum equivalence between the electric solution and the magnetic solution, we should compare them by putting them in the same ensemble. It is easier to put the electric solution in the fixed charge (canonical) ensemble. To give the canonical ensemble, we should add a Maxwell boundary term to the original action as [46–48]

$$I'_{\text{Max}} = I_{\text{Max}} - \frac{1}{G_N} \int_{\partial\mathcal{M}} d^3x \sqrt{\gamma_E} F^{\mu\nu} n_\mu A_\nu \,. \tag{2.41}$$

The variation of this action gives us

$$\begin{aligned} \delta I'_{\text{Max}} = &\text{(terms giving equations of motion)} \\ &- \frac{1}{G_N} \int_{\partial\mathcal{M}} d^3x \delta(\sqrt{\gamma_E} F^{\mu\nu} n_\mu) A_\nu \,. \end{aligned} \tag{2.42}$$

Therefore vanishing condition of the boundary term imposes $\delta(\sqrt{\gamma_E} F^{\mu\nu} n_\mu) = 0$ which amounts to fixing the electric charge. Notice that due to the equation of motion $\nabla_\mu F^{\mu\nu} = 0$, we have

$$F^{\mu\nu} F_{\mu\nu} = 2\nabla_\nu F^{\mu\nu} A_\mu \,, \tag{2.43}$$

for the solution of the Maxwell field. Thus if we put the on-shell value of the electric Maxwell field to the Maxwell boundary term, it can be expressed as

$$\begin{aligned} I_{\rm Max}^{\rm electric'} &= I_{\rm Max}^{\rm electric} - \frac{1}{2G_N}\int_{\mathcal{M}} d^2x\sqrt{g_E}F^{\mu\nu}F_{\mu\nu} \\ &= \frac{Q^2}{2G_N}\int d^4x\sqrt{g_E}\frac{1}{(4\pi r^2)^2} \\ &= I_{\rm Max}^{\rm magnetic} \end{aligned} \tag{2.44}$$

when F is on-shell. Thus we proved the equivalence of the on-shell actions between the electric solution and the magnetic solution in the canonical ensemble, which implies the semiclassical approximations to the Euclidean path integral for dual electric and magnetic solutions are identical.

Let us make some comments on the thermodynamics of the charged black holes here. In the semi-classical approximation, the partition function is written as $Z = e^{-I}$ where I is the on-shell action evaluated on the solution. In the canonical ensemble, the partition function $Z_{\rm C}$ is expressed in terms of the Helmholtz free energy as $\log Z_{\rm C} = -\beta F$, i.e, $\beta F \simeq I_{\rm C}$ where $I_{\rm C}$ is the on-shell value of the action in the canonical ensemble (2.44). The Helmholtz free energy is expressed in terms of the mass temperature and the entropy of the black hole solution as

$$F = M - TS\,. \tag{2.45}$$

On the other hand, in the grand canonical ensemble, $\log Z_{GC}$ is given by the Gibbs free energy G which is identified with the on-shell action in the grand canonical ensemble $I_{\rm GC}$ in the semi-classical approximation. The Gibbs free energy is written in terms of the mass temperature and the entropy and the chemical potential of the solution as

$$G = M - TS - \mu Q\,. \tag{2.46}$$

Thus the Helmholtz free energy and the Gibbs energy are related as

$$F = G + \mu Q\,. \tag{2.47}$$

On the other hand, as we saw in the electric case the on-shell action in the canonical ensemble and the grand canonical ensemble are related via the Maxwell boundary term as

$$I_{\rm C}^{\rm electric} = I_{\rm GC}^{\rm electric} + I_{\rm Max,bdy}\,, \tag{2.48}$$

where

$$I_{\rm Max,bdy} = -\frac{1}{G_N}\int_{\partial\mathcal{M}} d^3x\sqrt{\gamma_E}F_e^{\mu\nu}n_\mu A_{e,\nu}\,. \tag{2.49}$$

We have an electric solution

$$A^e_\tau = i\left(\frac{Q_e}{4\pi r} - \mu\right)\,,\quad F^e_{r\tau} = -i\frac{Q_e}{4\pi r^2}\,, \tag{2.50}$$

where μ is the chemical potential defined at infinity

$$\mu = \frac{i}{G_N}\lim_{r\to\infty} A_\tau = \frac{Q_e}{4\pi G_N r_+}\,. \tag{2.51}$$

Here we have chosen the gauge so that the gauge field is regular at the outer horizon. Electric charge is defined as the integral of the Hodge dual of F at the boundary

$$Q_e = \int_{S^2} \star F\,, \tag{2.52}$$

thus we can rewrite the Maxwell boundary term as

$$I_{\text{Max,bdy}} = \beta\mu Q_e\,, \tag{2.53}$$

where we used the fact that the Euclidean time has the periodicity β. Therefore we can write the Helmholtz free energy as

$$\begin{aligned}\beta F &\approx I^{\text{electric}}_{\text{C}}\big|_{\text{on-shell}} \\ &= I^{\text{electric}}_{\text{GC}}\big|_{\text{on-shell}} + I_{\text{Max,bdy}} \\ &= \beta G + \beta\mu Q\,.\end{aligned} \tag{2.54}$$

and we can reproduce the relation between the Helmholtz free energy and the Gibbs free energy $F = G+\mu Q$. As we can see, adding the Maxwell boundary term to the Euclidean action produces the Legendre transform to the Helmholtz free energy, associated with the canonical ensemble where the total (electric) charge Q is held fixed. One can see some related arguments in [46–48, 98] and for the AdS/CFT context in [99, 100]. The thermofield double state dual to the black holes in the canonical ensemble described by I_C reads

$$|TFD(t_L,t_R)\rangle_C = Z^{-1/2}\sum_\alpha e^{-\beta E_\alpha/2}e^{-iE_\alpha(t_L+t_R)}|E_\alpha,-Q\rangle_L|E_\alpha,Q\rangle_R\,, \tag{2.55}$$

where every state has the same charge Q. If we trace out the states in either boundary we get a density matrix corresponding to a canonical ensemble with the inverse temperature β and fixed charge Q. Had we chosen to work with the action I_{GC}, we would be in a fixed chemical potential ensemble. In this case, the dual state reads

$$|TFD(t_L,t_R)\rangle_{GC} = Z^{-1/2}\sum_{\alpha,\sigma} e^{-\beta(E_\alpha-\mu Q_\sigma)/2}e^{-iE_\alpha(t_L+t_R)}|E_\alpha,-Q_\sigma\rangle_L|E_\alpha,Q_\sigma\rangle_R\,. \tag{2.56}$$

Notice that in this case the charge is allowed to fluctuate and so we sum over states which possess different charges. If we trace out the states in either boundary we get a density matrix corresponding to a grand canonical ensemble with the inverse temperature β and fixed chemical potential μ.

2.2 More on the Maxwell Boundary Term

In the previous subsection, we saw that the Einstein-Maxwell theory describing the electric solutions are semi-classically equivalent to the one describing the magnetic solutions by introducing the Maxwell boundary term

$$I_{\text{Max,bdy}} = -\frac{1}{G_N}\int_{\partial\mathcal{M}} d^3x\sqrt{\gamma_E}F^{\mu\nu}n_\mu A_\nu\,, \tag{2.57}$$

to the original action (2.1). In this subsection, we will consider whether we can do the converse arguments, namely we will consider whether the on-shell action with the Maxwell boundary terms such like (2.57) describing the magnetic solutions is the same as the one without it describing the electric solution. To consider the Maxwell boundary term (2.57) for the magnetic field, we should remind ourselves of the existence of the Dirac string. If we would neglect the existence of the Dirac string and assume that the relation $F = dA$ holds globally even for the magnetic solution, by the following manipulation

$$\begin{aligned}\frac{1}{2G_N}\int_{\mathcal{M}} d^4x\sqrt{g_E}F^{\mu\nu}F_{\mu\nu} = \frac{1}{G_N}\int_{\mathcal{M}} d^4x\sqrt{g_E}F^{\mu\nu}\nabla_\mu A_\nu \\ -\frac{1}{G_N}\int_{\mathcal{M}} d^4x\sqrt{g_E}\nabla_\mu F^{\mu\nu}A_\nu\end{aligned} \tag{2.58}$$

and using the equation of motion

$$\nabla_\mu F^{\mu\nu} = 0 \tag{2.59}$$

and Stokes' theorem, we could write

$$\frac{1}{2G_N}\int_{\mathcal{M}} d^4x\sqrt{g_E}F^{\mu\nu}F_{\mu\nu} = \frac{1}{G_N}\int_{\partial\mathcal{M}} d\Sigma_\mu F^{\mu\nu}A_\nu\,. \tag{2.60}$$

However this leads a contradiction: for the magnetic solutions F only has support on angular directions and therefore the right-hand side (2.60) will always vanish if we simply take $\partial\mathcal{M}$ to be the boundary and has no effect in the action of magnetically charged black holes, while on the left-hand side, it does not vanish. This problem arises because $F = dA$ is not globally well defined for a magnetic monopole and hence we must be careful when using Stokes' theorem.

Let us remind ourselves that the magnetic solution of the Maxwell field takes the following form

$$A = \frac{Q_m}{4\pi}(1-\cos\theta)\,d\phi\,,\;\; F = \frac{Q_m}{4\pi}\sin\theta d\phi\wedge d\theta\,. \tag{2.61}$$

The existence of the Dirac string can be easily seen from the fact that the vector field $v^\mu = (4\pi)^2 F^{\mu\nu}A_\nu$ for the magnetic solution in which we are applying the Stokes' theorem, can be expressed as

$$v = \frac{Q_m^2}{r^4\sin\theta}(1-\cos\theta)\frac{\partial}{\partial\theta}\,. \tag{2.62}$$

Clearly, v has a singularity at $\theta=\pi$. This could be a coordinate artifact but for this reason, it is problematic to apply the divergence theorem to v. In order to solve this problem, we will have to split the spheres S^2 at each point of spacetime into two open hemispheres S^2_N with $0\leq\theta<\pi/2$ and S^2_S with $\pi/2<\theta\leq\pi$ and define a different gauge field for each one such that we can safely apply the divergence theorem on each hemisphere. Namely, we will take the gauge fields to be

$$\begin{aligned} A^N &= \frac{Q_m}{4\pi}(1-\cos\theta)\,d\phi\,,\\ A^S &= -\frac{Q_m}{4\pi}(1+\cos\theta)\,d\phi\,. \end{aligned} \tag{2.63}$$

in each hemisphere. Notice that F is the same for both gauge fields through $F=dA$. Now, the vector fields in each hemisphere are given by

$$\begin{aligned} v^N &= \frac{Q_m^2}{r^4\sin\theta}(1-\cos\theta)\,\frac{\partial}{\partial\theta}\,,\\ v^S &= -\frac{Q_m^2}{r^4\sin\theta}(1+\cos\theta)\,\frac{\partial}{\partial\theta}\,. \end{aligned} \tag{2.64}$$

We can see that both vector fields are well defined over the corresponding hemisphere. Therefore, we can apply the divergence theorem separately on each hemisphere. Since the surface $\theta=\pi/2$ is a set of zero measure for the bulk integral, we can write

$$\frac{1}{2G_N}\int_{\mathcal{M}} d^4x\sqrt{g_E}F^{\mu\nu}F_{\mu\nu} = \frac{1}{2G_N}\int_{\mathcal{M}_N\cup\mathcal{M}_S} d^4x\sqrt{g_E}F^{\mu\nu}F_{\mu\nu}\,, \tag{2.65}$$

where $\mathcal{M}_N=\mathcal{N}\times S^2_N$, $\mathcal{M}_S=\mathcal{N}\times S^2_S$ and $\mathcal{N}$ is the rest of the manifold apart from the sphere. Using (2.58), (2.59) and Stokes' theorem for the region $\mathcal{M}_N\cup\mathcal{M}_S$, it follows that

$$\frac{1}{2G_N}\int_{\mathcal{M}} d^4x\sqrt{g_E}F^{\mu\nu}F_{\mu\nu} = \frac{1}{G_N}\int_{\partial(\mathcal{M}_N\cup\mathcal{M}_S)} d\Sigma_\mu F^{\mu\nu}A_\nu\,. \tag{2.66}$$

Thus we see that the boundary that should enter the Stokes' theorem is not just the boundary of the manifold $\mathcal{M}$ but also an additional boundary at $\theta = \pi/2$. In particular, for the magnetic solution (2.61), this is the only boundary that contributes. For consistency, let us check that (2.66) indeed holds. We have

$$\frac{1}{G_N}\int_{\partial(\mathcal{M}_N\cup\mathcal{M}_S)} d\Sigma_\mu F^{\mu\nu}A_\nu = \frac{1}{G_N}\int_{\theta=\frac{\pi}{2}} d\Sigma^N_\mu F^\mu_\nu A^\nu_N + \frac{1}{G_N}\int_{\theta=\frac{\pi}{2}} d\Sigma^S_\mu F^\mu_\nu A^\nu_S\,, \tag{2.67}$$

where

$$d\Sigma^N = r^2\sin\theta d\theta\,,\ d\Sigma^S = -r^2\sin\theta d\theta\,. \tag{2.68}$$

It follows that

$$\frac{1}{G_N}\int_{\partial(\mathcal{M}_N\cup\mathcal{M}_S)} d\Sigma_\mu F^{\mu\nu}A_\nu = \frac{Q_m^2}{G_N}\int_{\mathcal{N}} d^2x\frac{1}{(4\pi r^2)^2}\,, \tag{2.69}$$

which matches the left-hand side integral of (2.66) after we integrate over the sphere S^2.

Thus we can see that the on-shell action with the Maxwell boundary term

$$I_{\text{Max,bdy}} = -\frac{1}{G_N}\int_{\partial(\mathcal{M}_N\cup\mathcal{M}_S)} d^3x\sqrt{\gamma_E}F^{\mu\nu}n_\mu A_\nu\,. \tag{2.70}$$

for the magnetic solution gives

$$\begin{aligned} I^{\text{magnetic}}_{\text{Max}} + I_{\text{Max,bdy}} &= \frac{1}{4G_N}\int d^4x\sqrt{g_E}F_{m,\mu\nu}F_m^{\mu\nu} - \frac{1}{2G_N}\int d^4x\sqrt{g_E}F_{m,\mu\nu}F_m^{\mu\nu} \\ &= -\frac{1}{4G_N}\int d^4x\sqrt{g_E}F_{m,\mu\nu}F_m^{\mu\nu} \\ &= \frac{Q^2}{2G_N}\int d^4x\sqrt{g_E}\frac{1}{(4\pi r^2)^2}, \\ &= \frac{1}{4G_N}\int d^4x\sqrt{g_E}F_{e,\mu\nu}F_e^{\mu\nu}\,. \end{aligned} \tag{2.71}$$

Thus semi-classically the theory which describes the magnetic solution with the Maxwell boundary term (2.57) is equivalent to the one which describes the electric solution without the boundary term.

3 Dimensional Reduction

In this section, we study the dimensional reduction of the four-dimensional Einstein-Maxwell theory

$$\begin{aligned} I_{EM} =& \frac{1}{16\pi G_N}\int_{\mathcal{M}} d^4x\sqrt{-\hat{g}}(\hat{R}-2\Lambda)+\frac{1}{8\pi G_N}\int_{\partial\mathcal{M}}\sqrt{-\hat{\gamma}}\hat{K} \\ & -\frac{1}{4G_N}\int_{\mathcal{M}} d^4x\sqrt{-\hat{g}}F_{\mu\nu}F^{\mu\nu}\,. \end{aligned} \tag{3.1}$$

by compactifying S^2 part of the AdS_4 metric. We assume the metric of the form

$$\begin{aligned} ds^2 &= \hat{g}_{\mu\nu}dx^\mu dx^\nu \\ &= g_{\mu\nu}dx^\mu dx^\nu + \Psi^2 d\Omega_2^2\,, \end{aligned} \tag{3.2}$$

and derive the two-dimensional theories which capture the spherically symmetric dynamics of the near-extremal near-horizon of the black hole. From the analysis in section 2, the near horizon geometry is approximated to $AdS_2\times S^2$, thus we expect that the dimensionally reduced theories can describe the AdS_2 geometry. Before starting to discuss the dimensional reduction, we introduce the coordinate systems in AdS_2 spacetime.

3.1 Coordinate Systems of AdS_2

In this subsection, we introduce coordinate systems in the AdS_2 spacetime which we will use in the later arguments. It is convenient to use the embedding coordinates $X=(X^M)_{M=-1,0,1}$ in $\mathbb{R}^{2,1}$ which obeys the constraint

$$-(X^{-1})^2-(X^0)^2+(X^1)^2=-L_2^2\,, \tag{3.3}$$

where L_2 is the AdS_2 scale. The induced metric on the surface (3.3) is given by

$$ds^2=-(dX^{-1})^2-(dX^0)^2+(dX^1)^2\,. \tag{3.4}$$

This embedding surface is invariant under $so(2,1)=sl(2,\mathbb{R})$ rotation,which means that AdS spacetime has an isometry of $sl(2,\mathbb{R})$. The surface (3.3) represents only a part of the AdS spacetime: we have to take the universal cover of this manifold. The surface is originally periodic under the 2π rotation on the (X^{-1},X^0) plane, but in order to take the universal cover, we should unroll this timelike cycle. It is convenient to introduce the global AdS coordinate which covers the whole AdS_2 spacetime to see how taking the universal cover of (3.3) works.

The global AdS_2 coordinate (τ, η) can be obtained by the following parametrization

$$X^{-1} = L_2 \frac{\cos\tau}{\cos\eta}\,,\ X^0 = L_2 \frac{\sin\tau}{\cos\eta}\,,\ X^1 = L_2 \tan\eta\,. \tag{3.5}$$

The metric of the global coordinate is written as

$$ds^2 = L_2^2 \frac{-dt^2 + d\eta^2}{\cos^2\eta}\,, \quad -\frac{\pi}{2} \le \eta \le \frac{\pi}{2}\,. \tag{3.6}$$

The original hyperboloid is covered with $\tau \in [-\pi, \pi]$, but to avoid closed timelike curves, we instead take $\tau \in \mathbb{R}$ by taking the universal cover of the manifold. As a result, the global coordinate covers the entire AdS spacetime. Notice that the boundary of the AdS spacetime is located at $\eta = \pm\pi/2$. Thus the boundary of AdS_2 has two disconnected pieces. This is a contrast to the higher dimensional AdS_d spacetime, which has a single conformally cylindrical boundary $\mathbb{R} \times S^{d-2}$.

We introduce another convenient coordinate system (t, r) as

$$X^{-1} = \frac{L_2^2}{\sqrt{\mu}} \frac{r - r_h}{L_2}\,,\ X^0 = \frac{L_2^2}{\sqrt{\mu}} \sqrt{f(r)} \sinh\frac{\sqrt{\mu}}{L_2^2} t\,,\ X^1 = \frac{L_2^2}{\sqrt{\mu}} \sqrt{f(r)} \cosh\frac{\sqrt{\mu}}{L_2^2} t\,, \tag{3.7}$$

where we defined

$$f(r) \equiv \frac{(r - r_+)(r - r_-)}{L_2^2}\,,\ r_\pm = r_h \pm \sqrt{\mu}\,. \tag{3.8}$$

$\sqrt{\mu}$ parametrizes the positions of the outer and inner horizons $r_\pm$. The metric is expressed as

$$ds^2 = -\frac{(r - r_+)(r - r_-)}{L_2^2} dt^2 + \frac{L_2^2}{(r - r_+)(r - r_-)} dr^2\,. \tag{3.9}$$

This coordinate system is especially convenient when we relate our two-dimensional system to the higher dimensional Reissner-Nordström black holes. Thus we sometimes call this coordinate as the Reissner-Nordström-like coordinate of AdS_2. In the section 2, we already discussed how this AdS_2 coordinate arises from the near horizon geometry of the four dimensional Reissner-Nordström metric.

Notice that if we shift the radial coordinate by r_h as $r' = r - r_h$, we obtain the so-called Rindler(-AdS) coordinate (t, r'), whose metric is expressed as

$$ds^2 = -\frac{r'^2 - \mu}{L_2^2} dt^2 + \frac{L_2^2}{r'^2 - \mu} dr'^2\,. \tag{3.10}$$

If we wick rotate the Lorentzian time t into the Euclidean time $\tau = it$, it can be seen from (3.7) that the coordinate τ is periodic under $\beta = 2\pi L_2^2/\sqrt{\mu}$. Thus these coordinate

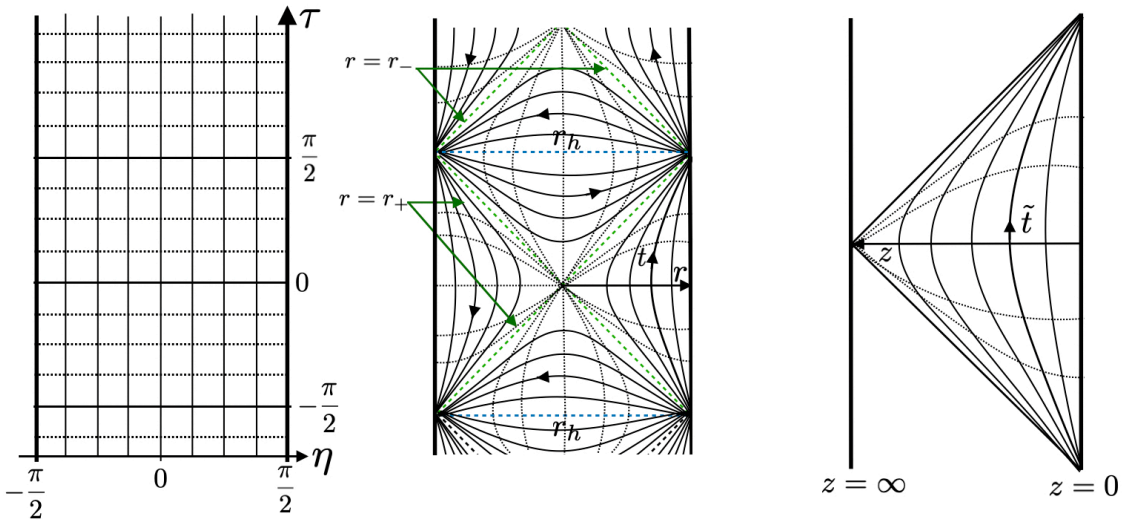

Figure 2: The figures correspond to the global AdS coordinate (3.6), thermal (Reissner-Nordström-like) coordinate (3.9) and the Poincaré coordinate (3.11) from the left. The arrows of the time flow are depicted in the real lines in each figure. The spacelike surfaces (radial axes) are depicted in the dotted lines. The Reissner-Nordström coordinate has two horizons $r_\pm$ just the same as the Reissner-Nordström black hole. The Poincaré coordinate only covers a part of the AdS spacetime.

systems look like thermal with temperature $T = \sqrt{\mu}/2\pi L_2^2$. This is just the artifact of the coordinate choice, but as we will see in subsection 3.6, the solutions of the dilaton gravity theories which we will introduce nicely fit these coordinates and the systems actually become thermal (black holes).

We also introduce the Poincaré coordinate $(\tilde{t}, z)$ given by the following embedding

$$X^{-1} = \frac{L_2^2 + z^2 - \tilde{t}^2}{2z}\,,\quad X^0 = L_2\frac{\tilde{t}}{z}\,,\quad X^1 = \frac{L_2^2 - z^2 + \tilde{t}^2}{2z}\,, \tag{3.11}$$

where the coordinates $(\tilde{t}, z)$ ranges as $z \in [0, \infty]$ and $\tilde{t} \in \mathbb{R}$. The metric becomes

$$ds^2 = L_2^2\frac{-d\tilde{t}^2 + dz^2}{z^2}\,. \tag{3.12}$$

Seen from the Figure 2 that the Poincaré coordinate only covers a part of the entire AdS spacetime, which is called Poincaré patch. We will use this coordinate system in subsection 4.2.

3.2 Magnetically Charged Black Hole in the Canonical Ensemble

We first consider the dimensional reduction of the Einstein-Maxwell theory in a near-extremal magnetically charged black hole in the canonical ensemble. We make the following ansatz for the metric and the magnetic gauge field

$$\begin{aligned} &ds^2 = g_{ab}dx^a dx^b + \Psi^2 d\Omega_2^2\,, \\ &F_{\phi\theta} \neq 0, (\text{other components of } F) = 0\,. \end{aligned} \tag{3.13}$$

where Ψ parametrize the radius of the charged black hole. We can use this ansatz to solve the equation of motion for F and obtain the solution of the form

$$F = \frac{Q}{4\pi}\sin\theta d\phi \wedge d\theta\,. \tag{3.14}$$

As we explained, the magnetically charged black holes described by the action (2.1) are in the canonical (fixed charge) ensemble, thus we take the charge to be the extremal one $Q = Q_{\text{ext}}$. We want to integrate out the spherical degrees of freedom and obtain the dimensionally reduced action. In this procedure, we fix the metric of the sphere while we leave the metric g_{ab} and the radius of the sphere Ψ as dynamical degrees of freedom in two dimensions. For the magnetically charged black hole with $F_{\phi\theta} = \frac{1}{4\pi}Q_{\text{ext}}\sin\theta$, we have

$$4\pi F^2 = \frac{Q_{ext}^2}{2\pi\Psi^4}\,. \tag{3.15}$$

In general, if we have the warped product geometry given by

$$ds^2 = ds_{(1)}^2 + e^{2\tau(x^{(1)})}ds_{(2)}^2\,, \tag{3.16}$$

then we can decompose the Ricci curvature as

$$\hat{R} = R_{(1)} + e^{-2\tau}R_{(2)} - 2d\nabla_{(1)}^2\tau - d(d+1)g^{ab}\partial_a\tau\partial_b\tau\,, \tag{3.17}$$

where d is the dimensionality of the $ds_{(2)}^2$ part. In our case, $\Psi = e^{\tau}$ and $d = 2$, thus the Ricci scalar can be decomposed as

$$\hat{R} = R + \frac{2}{\Psi^2} - 4\nabla^2\log\Psi - \frac{6}{\Psi^2}(\nabla\Psi)^2\,, \tag{3.18}$$

where not-hatted quantities refer to the two-dimensional geometry which survives after integrating out the spherical part of the metric. The determinant of the metric $\sqrt{-\hat{g}}$ is written in terms of the one in two dimension $\sqrt{-g}$ as

$$\sqrt{-\hat{g}} = \Psi^2\sqrt{-g}\sin\theta\,. \tag{3.19}$$

Then dimensionally reduced theory from a magnetically charged black hole is written as

$$I_C^{\text{magnetic}} = \frac{1}{4G_N}\int_{\mathcal{M}} d^2x\sqrt{-g}\left(\Psi^2 R + 2(\nabla\Psi)^2 + 2 - 2\Psi^2\Lambda - \frac{Q_{ext}^2}{2\pi\Psi^2}\right) - \frac{1}{2G_N}\int_{\partial\mathcal{M}} dx\sqrt{-\gamma}n^\mu\nabla_\mu\Psi^2\,. \tag{3.20}$$

where the surface term comes from the integration by parts which we performed to get the above action and it is canceled with the dimensionally reduced GHY-term

$$\begin{aligned} I_{\text{GHY}} &= \frac{1}{8\pi G_N}\int_{\partial\mathcal{M}}\sqrt{-\hat{\gamma}}\hat{K} \\ &= \frac{1}{4G_N}\int_{\partial\mathcal{M}}\sqrt{-\gamma}\Psi^2 K + \frac{1}{2G_N}\int_{\partial\mathcal{M}} dx\sqrt{-\gamma}n^\mu\nabla_\mu\Psi^2\,. \end{aligned} \tag{3.21}$$

Near-Horizon Expansion at the Level of Equations of Motion

Now that we have the dimensionally reduced action (3.20) derived from the magnetic solution, then we will next derive the equations of motion from the full action (3.20) and take the near-horizon expansion around the horizon at the level of the equation of motion. The equations of motion derived from the action (3.20) are given by

$$0 = R - 2\Lambda + \frac{Q_{ext}^2}{2\pi\Psi^4} - \frac{\nabla^2\Psi}{\Psi}\,, \tag{3.22}$$

$$0 = \nabla_\mu\nabla_\nu\Psi^2 - g_{\mu\nu}\nabla^2\Psi^2 - g_{\mu\nu}\left(\Lambda\Psi^2 - 1 + \frac{Q_{ext}^2}{4\pi\Psi^2}\right) - 2\nabla_\mu\Psi\nabla_\nu\Psi + g_{\mu\nu}(\nabla\Psi)^2\,. \tag{3.23}$$

We now expand Ψ^2 as

$$\Psi^2 = \frac{\Phi_0 + \Phi}{4\pi}\,. \tag{3.24}$$

around some constant Φ_0 and express the equations (3.22)(3.23) at the leading order of Φ/Φ_0. We choose the value of the extremal dilaton Φ_0 as the area of the extremal black hole

$$\Phi_0 = 4\pi r_h^2 \tag{3.25}$$

and introduce the radius of the AdS_2 geometry

$$\Lambda_2 \equiv \Lambda - Q_{\text{ext}}^2/(4\pi r_h^4) = 2\Lambda - \frac{1}{r_h^2}\,. \tag{3.26}$$

The above definition is the same as one we considered in (2.21). Notice that for the large black holes, we obtain a simple relation $\Lambda_2 \simeq 2\Lambda$.

Then expanding Ψ in (3.22)(3.23) around $\Phi_0 = 4\pi r_h^2$, we can obtain the following form of the equations of motions

$$0 = R - 2\Lambda_2 + 2\left(\Lambda_2 - \frac{1}{r_h^2}\right)\frac{\Phi}{\Phi_0} - \frac{\nabla^2\Phi}{\Phi_0}\,, \tag{3.27}$$

$$0 = \nabla_\mu\nabla_\nu\Phi - g_{\mu\nu}\nabla^2\Phi - g_{\mu\nu}\Lambda_2\Phi\,, \tag{3.28}$$

up to the order $\mathcal{O}((\Phi/\Phi_0)^2)$. At the leading order in Φ/Φ_0, the first equation reduces to

$$R = 2\Lambda_2 + \mathcal{O}(\Phi/\Phi_0)\,. \tag{3.29}$$

Since $\Lambda_2 < 0$, this implies that we have an AdS_2 solution at the leading order. Our strategy to solve these coupled equations with respect to the metric and the dilaton is as follows. We first solve the equation (3.27) at the order $\mathcal{O}(1)$ and then using the leading order solution for the metric we solve the second equation (3.28) for the dynamical dilaton Φ at the leading order, then finally we take into account of the back reaction to the metric at order Φ/Φ_0 according to the equation (3.27) by using the leading order solution for Φ. Using the metric of the AdS_2 (3.9), we can solve the second equation for the dilaton Φ as

$$\Phi = \Phi_b\frac{r - r_h}{r_h}\,. \tag{3.30}$$

If we take a normalization as $\Phi_b = 2\Phi_0$ with $\Phi_0 = 4\pi r_h^2$, we obtain a simple expression for the combination $\Psi = (\Phi_0 + \Phi)/4\pi$ of the following form

$$\Psi^2 = r_h^2\left(1 + \frac{2(r - r_h)}{r_h}\right) \simeq r^2\,, \tag{3.31}$$

which nicely fits the spherical part of near horizon geometry (2.28), which can be expressed as $\Psi^2 d\Omega_2^2$. Since the equation (3.28) implies $\nabla^2\Phi = -2\Lambda_2\Phi$, thus using the solution (3.30) with $\Phi_b = 2\Phi_0, \Phi_0 = 4\pi r_h^2$, we can write the first equation as

$$R + \frac{2}{L_2^2} = \frac{8}{L_2^2}\frac{r - r_h}{r_h}\,. \tag{3.32}$$

where we consider a large four-dimensional black hole and neglect terms suppressed by L/r_h. The metric deviates from AdS_2 according to this equation due to the existence of the dynamical dilaton Φ according to the above equation. By solving the above equation, we can find that the metric deviates from the AdS_2 at the order $\mathcal{O}(\Phi/\Phi_0)$ as

$$\begin{aligned} ds^2 &= -f(r)dt^2 + \frac{1}{f(r)}dr^2\,, \\ f(r) &= \frac{(r - r_+)(r - r_-)}{L_2^2}\left(1 - \frac{4}{3}\frac{r - r_h}{r_h}\right)\,. \end{aligned} \tag{3.33}$$

This is consistent with the (t, r) part of the metric (2.28) which we directly derived by taking the near-horizon limit of the near-extremal Reissner-Nordström black hole metric.

Near-Horizon Expansion at the Level of Action

Next, we consider expanding the action itself in Φ instead of doing so at the level of the equation of motion. We keep the linear order of Φ and neglect the kinetic term of Φ, then we end up with the following action

$$I_{\rm JT} = \frac{\Phi_0}{16\pi G_N}\int_{\mathcal{M}} d^2x\sqrt{-g}R + \frac{1}{16\pi G_N}\int_{\mathcal{M}} d^2x\sqrt{-g}\Phi\left(R - 2\Lambda_2\right) . \tag{3.34}$$

This action is nothing but the one of the Jackiw-Teitelboim (JT) model [37–39]. Thus we confirmed that the JT model can be derived from the four-dimensional magnetically charged black holes in the canonical ensemble. For more general arguments to derive the JT action, see subsection 3.5 and Appendix B.

This action yields the following equations of motion

$$0 = R - 2\Lambda_2 \,, \tag{3.35}$$

$$0 = \nabla_\mu\nabla_\nu\Phi - g_{\mu\nu}\nabla^2\Phi - g_{\mu\nu}\Lambda_2\Phi \,. \tag{3.36}$$

Notice that the first equation deviates from (3.27) at the linear order in Φ. The term $2\Lambda_2\frac{\Phi}{\Phi_0}$ comes from the quadratic term in Φ of the action (3.20) and $\frac{\nabla^2\Phi}{\Phi_0}$ from the kinetic term of Ψ, thus they do not appear in the equation of motion from the action of the JT model. Therefore, the linearized action (3.34) only captures the geometry and the dilaton profile both at the leading order. The important feature of the action (3.34) is that it truncates higher order terms of the original action "self-consistently": even after plugging the solution of the equations of motion back into the action, the action is still the order of $\mathcal{O}(\Phi/\Phi_0)$ and higher order terms do not show up.

3.3 Electrically Charged Black Hole in the Grand Canonical Ensemble

Next we consider the dimensionally reduced theory of the Einstein-Maxwell action (2.1) derived from the near-extremal electrically charged black hole. Let us remind ourselves that the electric solutions described by the action (2.1) is in the grand canonical ensemble. Thus in this subsection, we try to obtain the dimensionally reduced theory which captures the near-horizon geometry of the near-extremal electrically charged black holes in the grand canonical ensemble.

We make the following ansatz for the four-dimensional solution

$$\begin{aligned} &ds^2 = g_{ab}dx^a dx^b + \Psi^2 d\Omega_2^2\,, \\ &F_{ab} \neq 0, (\text{other components of } F) = 0\,. \end{aligned} \tag{3.37}$$

When we dimensionally reduce the Einstein-Maxwell theory, we leave the metric g_{ab} and the radius of the sphere Ψ as dynamical degrees of freedom. In contrast to the magnetic case, in order to solve the equation for the Maxwell field F_{ab}, we need the information of the components of the metric g_{ab} which remain the dynamical degrees of freedom in two dimensions. Thus when deriving the action of the reduced theory, we should also leave the Maxwell field to be off-shell degrees of freedom[4].

Performing the same procedure of the dimensional reduction, we end up with the following dimensionally reduced action

$$I_{\rm GC}^{\rm electric} = \frac{1}{4G_N}\int_{\mathcal{M}} d^2x\sqrt{-g}\left(\Psi^2 R + 2(\nabla\Psi)^2 + 2 - 2\Psi^2\Lambda - 4\pi\Psi^2 F^2\right)\,, \tag{3.38}$$

up to the surface term appeared in (3.20), which is absorbed by the dimensionally reduced GHY-boundary term. Notice that in addition to the metric and the dilaton Ψ, there is also a term for the Maxwell field $F_{\mu\nu}$ in two dimensions. Thus the dimensionally reduced theory is a system where the metric, the dilaton and the Maxwell field are coupled with each other.

Near-Horizon Expansion at the Level of Equations of Motion

We have the dimensionally reduced action (3.38) derived from the electric solution, then we will next derive the equations of motion from the full action (3.38) and take the near-horizon expansion around the horizon at the level of the equation of motion and try to solve this coupled system as we did in the magnetic case.

[4]For related arguments, see [101]

From the action (3.38), we obtain the following equations of motions

$$0 = \partial_\mu(\sqrt{-g}\Psi^2 F^{\mu\nu}) \tag{3.39}$$

$$0 = R - 2\Lambda - 4\pi F^2 - \frac{\nabla^2\Psi}{\Psi} \tag{3.40}$$

$$\begin{aligned} 0 = \nabla_\mu\nabla_\nu\Psi^2 - g_{\mu\nu}\nabla^2\Psi^2 - g_{\mu\nu}(\Lambda\Psi^2 - 1) + 8\pi\Psi^2(F_{\mu\sigma}F_\nu{}^\sigma - \frac{1}{4}g_{\mu\nu}F^2) \\ - 2\nabla_\mu\Psi\nabla_\nu\Psi + g_{\mu\nu}(\nabla\Psi)^2. \end{aligned} \tag{3.41}$$

As we did for the magnetically charged black holes, we expand the dilaton around some constant Φ_0

$$\Psi^2 = \frac{\Phi_0 + \Phi}{4\pi}\,. \tag{3.42}$$

We first solve the equation of motion for F and plug it back into the other equations of motions. In the equation (3.39), the Maxwell field is coupled both to the metric and the dilaton. In order to solve the equation for F, it is reasonable to take an ansatz for the two dimensional metric of the following form

$$\begin{aligned} ds^2 &= -f(r)dt^2 + \frac{1}{f(r)}dr^2\,, \\ f(r) &= \frac{(r-r_+)(r-r_-)}{L_2^2}\left(1 - c\frac{r-r_h}{r_h}\right) \end{aligned} \tag{3.43}$$

with an $\mathcal{O}(1)$ constant c up to $\mathcal{O}((\frac{r-r_h}{r_h})^2)$. Ricci scalar for this metric is computed as

$$R = -\frac{2}{L_2^2} + \frac{6c}{L_2^2}\frac{r-r_h}{r_h}\,. \tag{3.44}$$

With this ansatz, we can solve the equation of motion for the gauge field (3.39) as

$$F_{\mu\nu} = \frac{Q}{4\pi\Psi^2}\epsilon_{\mu\nu}\,,\ F^2 = -\frac{2Q^2}{(4\pi\Psi^2)^2}\,. \tag{3.45}$$

up to $\mathcal{O}((\frac{r-r_h}{r_h})^2)$. Notice that the charge Q can take any values and in general, and it can deviate from the extremal value of the charge Q_{ext}. This represents the fact that we dimensionally reduced the solution in the grand canonical ensemble, so the charge of the solution in four dimensions can fluctuate. We want to obtain the theory which describes the near-extremal black holes, thus we write the deviation of the charge from its extremal value as

$$\delta Q = Q - Q_{\text{ext}} \tag{3.46}$$

and assume that δQ is small, more precisely we assume that the quantity $\delta Q/Q_{\rm ext}$ is at most the same order as Φ/Φ_0. Plugging the solution for $F_{\mu\nu}$ (3.45) back into the equations of motion, and expanding Ψ^2 around a constant

$$\Phi_0 = 4\pi r_h^2\,, \tag{3.47}$$

we obtain the following equations

$$\begin{aligned} 0 &= R - 2\Lambda_2 + 2\left(\Lambda_2 - \frac{1}{r_h^2}\right)\left[\frac{\tilde{\Phi}}{\Phi_0} - \frac{1}{r_h^2\Lambda_2}\frac{\delta Q}{Q_{\rm ext}}\right] - \frac{\nabla^2\tilde{\Phi}}{\Phi_0}\,, \\ 0 &= \nabla_\mu\nabla_\nu\tilde{\Phi} - g_{\mu\nu}\nabla^2\tilde{\Phi} - \Lambda_2 g_{\mu\nu}\tilde{\Phi}\,. \end{aligned} \tag{3.48}$$

up to the order $\mathcal{O}((\frac{r-r_h}{r_h})^2)$ and $\mathcal{O}((\Phi/\Phi_0)^2)$. We introduced the dilaton shifted as $\tilde{\Phi} = \Phi + \Phi_q$ where

$$\Phi_q = -\left(\Lambda_2 - \frac{1}{r_h^2}\right)\frac{\delta Q}{Q_{\rm ext}}\frac{\Phi_0}{\Lambda_2}\,. \tag{3.49}$$

If we consider a four-dimensional black hole large and neglect terms suppressed by L/r_h, then we end up with the same equations of motion as the magnetic case (3.27)(3.28) but with an additional shift of the dilaton by Φ_q. At the leading order in Φ, they also reduce to the equations of motion of the JT model. We have an AdS_2 solution for the metric up to corrections of the order $\mathcal{O}(\frac{r-r_h}{r_h})$ and $\mathcal{O}(\Phi/\Phi_0)$.

Next we try to see how the metric deviates from AdS_2 in the presence of the dilaton $\tilde{\Phi}$. The strategy is the same as the magnetic case. Using the AdS_2 metric (3.9) obtained by solving at the leading order, we can obtain a solution for the dilaton $\tilde{\Phi}$ just like the magnetic case as

$$\tilde{\Phi} = 2\Phi_0\frac{r-r_h}{r_h}\,, \tag{3.50}$$

where we choose the normalization constant Φ_b so that total dilaton Ψ^2 takes a simple form as follows

$$\Psi^2 \simeq \frac{\Phi_0}{4\pi}\left(1 + \frac{\delta Q}{Q_{\rm ext}}\right)\left(1 + 2\frac{r-r_h}{r_h}\right) \simeq \frac{Q}{Q_{\rm ext}}r^2\,. \tag{3.51}$$

When we consider a large black hole in four dimensions, we can show that the deviation of the metric from the AdS_2 obeys the following form

$$\begin{aligned} ds^2 &= -f(r)dt^2 + \frac{1}{f(r)}dr^2\,, \\ f(r) &= \frac{(r-r_+)(r-r_-)}{L_2^2}\left(1 - \frac{4}{3}\frac{r-r_h}{r_h}\right)\,, \end{aligned} \tag{3.52}$$

which is consistent with the ansatz (3.43) by taking the constant c as $c = 4/3$. This is also consistent with (3.33) and (2.28).

Near-Horizon Expansion at the Level of Action

We now construct the linearized action which captures small deviations from the extremal throat for the electric solution in the canonical ensemble just in the same way as we derived the JT model. Linearly expanding the action $I_{\text{GC}}^{\text{electric}}$ and the neglecting the kinetic term of Ψ under the same philosophy as the JT model, we obtain

$$\begin{aligned}\tilde{I}_{\text{JT-Max}} &= \frac{1}{2G_N}\int_{\mathcal{M}} d^2x\sqrt{-g} + \frac{1}{16\pi G_N}\int_{\mathcal{M}} d^2x\sqrt{-g}(\Phi_0+\Phi)\left(R - 2\Lambda - 4\pi F^2\right) \\ &= I_{\text{JT}} - \frac{1}{16\pi G_N}\int_{\mathcal{M}} d^2x\sqrt{-g}(\Phi_0-\Phi)\left(\Lambda_2 - \frac{1}{r_h^2}\right) - \frac{1}{4G_N}\int_{\mathcal{M}} d^2x\sqrt{-g}(\Phi_0+\Phi)F^2\,.\end{aligned} \tag{3.53}$$

This action seems to only contain linear terms in Φ and the higher terms are correctly truncated, but that is not the case. In Appendix A, we performed the analyses of the action (3.53), then we found the equations of motion derived from the action (3.53) inevitably contain the infinitely higher order terms in Φ. Thus this action fails to truncate the higher order terms "self-consistently": if we plug the solution of this "linearized" action back into itself, the higher order terms inevitably come in. The reason why that happens is that the solution for field strength contains the (total) dilaton in its denominator as we saw in (3.45). Then if we expand it around a constant Φ_0, infinitely many higher order terms appear. In this case, we also wish to only capture small corrections (linear order) to the extremal field strength

$$4\pi F_0^2 = -2Q_{\text{ext}}^2/4\pi r_h^4 = \Lambda_2 - \frac{1}{r_h^2}\,. \tag{3.54}$$

Hence, we expand the field strength as

$$F_{\mu\nu} = (F_0)_{\mu\nu} + \tilde{F}_{\mu\nu} = 2\partial_{[\mu}(A_0)_{\nu]} + 2\partial_{[\mu}\tilde{A}_{\nu]} \tag{3.55}$$

by decomposing the gauge potential $A_\mu = (A_0)_\mu + \tilde{A}_\mu$. Here $\tilde{F}$ captures corrections of order Φ/Φ_0 relative to F_0. Then we re-expand the bulk action (3.53) to the linear order in both Φ and $\tilde{F}$, the resulting action takes the following form

$$\begin{aligned}I_{\text{JT-Max}} = I_{\text{JT}} &- \frac{1}{16\pi G_N}\int_{\mathcal{M}} d^2x\sqrt{-g}(\Phi_0-\Phi)\left(\Lambda_2 - \frac{1}{r_h^2}\right) \\ &- \frac{1}{4G_N}\int_{\mathcal{M}} d^2x\sqrt{-g}\left[(\Phi_0+\Phi)F_0^2 + 2\Phi_0 F_0^{\mu\nu}\tilde{F}_{\mu\nu}\right]\,.\end{aligned} \tag{3.56}$$

We treat A_0 as a dynamical field, however, our prescription is that the solution is always chosen to yield precisely the extremal field strength in (3.54). This action (3.56) leads to the following equations of motion

$$0 = \partial_\mu(\sqrt{-g}\Phi_0 F_0^{\mu\nu}) \tag{3.57}$$

$$0 = \partial_\mu(\sqrt{-g}[\Phi_0 F^{\mu\nu} + \Phi(F_0)^{\mu\nu}]) \tag{3.58}$$

$$0 = R - 2\Lambda_2 - \left(4\pi F_0^2 - \Lambda_2 + \frac{1}{r_h^2}\right) \tag{3.59}$$

$$\begin{aligned} 0 = {} & \nabla_\mu\nabla_\nu\Phi - g_{\mu\nu}\nabla^2\Phi - \Lambda_2 g_{\mu\nu}\Phi - \frac{1}{2}\left(\Lambda_2 - \frac{1}{r_h^2}\right) g_{\mu\nu}(\Phi_0 - \Phi) \\ & + 2\pi(\Phi_0 + \Phi)\left(4(F_0)_{\mu\sigma}(F_0)_\nu{}^\sigma - g_{\mu\nu}F_0^2\right) + 4\pi\Phi_0\left(2(F_0)_{\mu\sigma}\tilde{F}_\nu^\sigma + 2\tilde{F}_{\mu\sigma}(F_0)_\nu{}^\sigma - g_{\mu\nu}F_0^{\rho\sigma}\tilde{F}_{\rho\sigma}\right). \end{aligned} \tag{3.60}$$

The first equation comes from the variation of the gauge field $\tilde{A}_\mu$, and the second equation is derived from the variation with respect to $(A_0)_\mu$. The third and the fourth equations are derived from the variations with respect to Φ and $g_{\mu\nu}$ respectively. The first equation can be solved as $(F_0)_{\mu\nu} = C\epsilon_{\mu\nu}$. There is a family of constant solutions parametrized by C, but as we explained above, we are interested in expanding the field strength around its extremal value, then we focus on the solution

$$(F_0)_{\mu\nu} = \frac{Q_{\text{ext}}}{\Phi_0}\epsilon_{\mu\nu}\,, \tag{3.61}$$

where we choose the constant $\Phi_0 = 4\pi r_h^2$. We can see that if we plug this solution into the third equation (3.59), we obtain the equation $R = 2\Lambda_2$, thus the solution (3.61) leads to the AdS_2 geometry with the cosmological constant Λ_2. Moreover, by using the solution for $(F_0)_{\mu\nu}$, we can show the following equality

$$2\pi(\Phi_0 + \Phi)\left(4(F_0)_{\mu\sigma}(F_0)_\nu{}^\sigma - g_{\mu\nu}F_0^2\right) = \frac{1}{2}\left(\Lambda_2 - \frac{1}{r_h^2}\right) g_{\mu\nu}(\Phi_0 + \Phi), \tag{3.62}$$

then the sum over the third term, the fourth term in the first line and the first term in the second line of (3.60) gives $-g_{\mu\nu}\Phi/r_h^2$. The second equation (3.58) for the field strength $\tilde{F}$ gives the solution of the following form

$$\tilde{F}_{\mu\nu} = \left[\frac{\delta Q}{\Phi_0} - \frac{Q_{\text{ext}}}{\Phi_0^2}\Phi\right]\epsilon_{\mu\nu}\,, \tag{3.63}$$

where we used the solution for $(F_0)_{\mu\nu}$ (3.61). Notice that we assumed that $\tilde{F}_{\mu\nu}$ to be very small, at most of the order $\mathcal{O}(\Phi/\Phi_0)$, thus we introduced a small parameter δQ

which scales as $\delta Q/Q_{\rm ext} \lesssim \mathcal{O}(\Phi/\Phi_0)$. It is interesting to see the total field strength $F_{\mu\nu} = (F_0)_{\mu\nu} + \tilde{F}_{\mu\nu}$ is given by

$$F_{\mu\nu} = \frac{Q_{\rm ext}}{\Phi_0}\left[1 + \frac{\delta Q}{Q_{\rm ext}} - \frac{\Phi}{\Phi_0}\right]\epsilon_{\mu\nu} \tag{3.64}$$

then if we define the "total charge" as $Q \equiv Q_{\rm ext} + \delta Q$, this agrees with the solution (3.45) linearly expanded with respect both to Φ and δQ. Since we can find that the following combination gives

$$\begin{aligned} &4\pi\Phi_0\left(2(F_0)_{\mu\sigma}\tilde{F}^{\sigma}_{\nu} + 2\tilde{F}_{\mu\sigma}(F_0)_{\nu}{}^{\sigma} - g_{\mu\nu}F_0^{\rho\sigma}\tilde{F}_{\rho\sigma}\right) \\ &= \left(\Lambda_2 - \frac{1}{r_h^2}\right) g_{\mu\nu}\frac{\delta Q}{Q_{\rm ext}}\Phi_0 - g_{\mu\nu}\left(\Lambda_2 - \frac{1}{r_h^2}\right)\Phi\,, \end{aligned} \tag{3.65}$$

thus we end up the equations

$$0 = R - 2\Lambda_2 \tag{3.66}$$

$$0 = \nabla_\mu\nabla_\nu\tilde{\Phi} - g_{\mu\nu}\nabla^2\tilde{\Phi} - g_{\mu\nu}\Lambda_2\tilde{\Phi}. \tag{3.67}$$

with the background of the Maxwell fields

$$(F_0)_{\mu\nu} = \frac{Q_{\rm ext}}{\Phi_0}\epsilon_{\mu\nu}\,,\ \tilde{F}_{\mu\nu} = -\frac{Q_{\rm ext}}{\Phi_0^2}\left(\tilde{\Phi} - \frac{1}{r_h^2\Lambda_2}\frac{\delta Q}{Q_{\rm ext}}\Phi_0\right)\epsilon_{\mu\nu}\,, \tag{3.68}$$

where we introduced the dilaton shifted as $\tilde{\Phi} = \Phi + \Phi_q$. The equations of motions we obtained reproduce the solution (3.45) and equations for the metric and the dilaton (3.48) at the leading order of Φ. The equations (3.3) (3.48) reduces the equations of the JT model with replacement $\Phi \to \tilde{\Phi}$. Thus we found that the action (3.56) self-consistently truncates the higher order terms in Φ correctly reproduces the equations of motion derived from the full action (3.38) at the leading order. Thus the two-dimensional dilaton gravity theory (3.56) can be regarded as the counterpart of the JT model in the electric case and it correctly captures the physics of the four-dimensional electrically charged black holes in the grand canonical ensemble.

Comments on the Dimensional Reduction of the Dyonic Black Holes

We finally comment on the dimensional reduction of the dyonic black holes which have both the electric and magnetic charges. We take the following ansatz for the metric and the components of the field strength

$$\begin{aligned} &ds^2 = \hat{g}_{\mu\nu}dx^\mu dx^\nu = g_{ab}dx^a dx^b + \Psi^2 d\Omega_2^2\,, \\ &F_{rt} \neq 0\,,\ F_{\phi\theta} \neq 0\,. \end{aligned} \tag{3.69}$$

We can use this ansatz and obtain the solution of the form

$$F = \frac{Q_{\text{ext}}}{4\pi} \sin\theta d\phi \wedge d\theta \,. \tag{3.70}$$

where we set $Q_m = Q_{\text{ext}}$ for simplicity. Then integrating out the spherical degrees part of the integral, we obtain the follwing two-dimensional action

$$I_{\text{dyonic}} = \frac{1}{4G_N} \int_{\mathcal{M}} d^2x\sqrt{-g} \left(\Psi^2 R + 2(\nabla\Psi)^2 + 2 - 2\Psi^2\Lambda - \frac{8\pi Q_{ext}^2}{\Psi^2} - 4\pi\Psi^2 F^2 \right) . \tag{3.71}$$

It might be interesting to explore the following linearized theory

$$I_{\text{dyonic}} = I_{\text{JT}} - \frac{1}{4G_N} \int d^2x\sqrt{-g}(\Phi_0 + \Phi)F^2 \,. \tag{3.72}$$

The action simply describes the JT model coupled to the field strength $F_{\mu\nu}$. This action yields the following equations of motion

$$0 = \partial_\mu(\sqrt{-g}(\Phi_0 + \Phi)F^{\mu\nu}) \tag{3.73}$$

$$0 = R - 2\Lambda_2 - 4\pi F^2 \tag{3.74}$$

$$0 = \nabla_\mu\nabla_\nu\Phi - g_{\mu\nu}\nabla^2\Phi - g_{\mu\nu}\Lambda_2\Phi + 2\pi(\Phi_0 + \Phi)\left(4F_{\mu\sigma}F_\nu{}^\sigma - g_{\mu\nu}F^2\right) . \tag{3.75}$$

Unlike the I_{JT} and $I_{\text{JT}-\text{Max}}$, it seems that these equations do not reduce to the equations of the JT model even after we keep the terms of the linear order in Φ.

If we plug the solution for $F_{\mu\nu}$ back into the action (3.71), the higher order terms show up in the same reason as the electric case. Therefore to obtain self-consistent truncated theory, we further expand the Maxwell field as (3.55) the same as we did for the model $I_{\text{JT-Max}}$. Then we obtain the action

$$I_{\text{dyonic}} = I_{\text{JT}} - \frac{1}{4G_N} \int_{\mathcal{M}} d^2x\sqrt{-g} \left[(\Phi_0 + \Phi)F_0^2 + 2\Phi_0 F_0^{\mu\nu}\tilde{F}_{\mu\nu} \right] . \tag{3.76}$$

This action yields the following equations of motion

$$0 = \partial_\mu(\sqrt{-g}\Phi_0 F_0^{\mu\nu}) \tag{3.77}$$

$$0 = \partial_\mu(\sqrt{-g}[\Phi_0 F^{\mu\nu} + \Phi(F_0)^{\mu\nu}]) \tag{3.78}$$

$$0 = R - 2\Lambda_2 - 4\pi F_0^2 \tag{3.79}$$

$$\begin{aligned} 0 = {} & \nabla_\mu\nabla_\nu\Phi - g_{\mu\nu}\nabla^2\Phi - g_{\mu\nu}\Lambda_2\Phi + 2\pi(\Phi_0 + \Phi)\left(4(F_0)_{\mu\sigma}(F_0)_\nu{}^\sigma - g_{\mu\nu}F_0^2\right) \\ & + 4\pi\Phi_0\left(2(F_0)_{\mu\sigma}\tilde{F}_\nu^\sigma + 2\tilde{F}_{\mu\sigma}(F_0)_\nu{}^\sigma - g_{\mu\nu}F_0^{\rho\sigma}\tilde{F}_{\rho\sigma}\right) . \end{aligned} \tag{3.80}$$

Similarly to the previous arguments, we can find solutions for $(F_0)_{\mu\nu}$ and $\tilde{F}_{\mu\nu}$ as

$$(F_0)_{\mu\nu} = \frac{Q_{\text{ext}}}{\Phi_0}\epsilon_{\mu\nu}\,, \tilde{F}_{\mu\nu} = \left[\frac{\delta Q}{\Phi_0} - \frac{Q_{\text{ext}}}{\Phi_0^2}\Phi\right]\epsilon_{\mu\nu}\,. \tag{3.81}$$

Plugging these solutions back into the equations (3.79) and (3.80)

$$0 = R - 2\tilde{\Lambda}_2 \tag{3.82}$$

$$0 = \nabla_\mu\nabla_\nu\tilde{\Phi} - g_{\mu\nu}\nabla^2\tilde{\Phi} - g_{\mu\nu}\tilde{\Lambda}_2\Phi + \frac{1}{3}g_{\mu\nu}\tilde{\Lambda}_2\Phi_0\,, \tag{3.83}$$

where we redefined the AdS scale as $\Lambda_2 \to \tilde{\Lambda}_2 = \Lambda_2 + 2\pi F_0^2 = 3\Lambda_2/2$ and shifted the dilaton as $\Phi \to \tilde{\Phi} = \Phi - \frac{2\delta Q}{3Q_{\text{ext}}}\Phi_0$. We can see that the second equation differs from that of the JT model at the order $\mathcal{O}(1)$.

3.4 Semiclassical Duality between the Dimensionally Reduced Theories

We dimensionally reduced the action (2.1) in a magnetically and an electrically charged black hole and obtained the action (3.20) and (3.38) respectively. From these actions, we derived linearized actions (3.34)(3.56) which are given by

$$I^E_{\rm JT} = -\frac{\Phi_0}{16\pi G_N}\int_{\mathcal{M}} d^2x\sqrt{g_E}R - \frac{1}{16\pi G_N}\int_{\mathcal{M}} d^2x\sqrt{g_E}\Phi\left(R-2\Lambda_2\right) \tag{3.84}$$

$$\begin{aligned} I^E_{\text{JT-Max}} = I^E_{\rm JT} &+ \frac{1}{16\pi G_N}\int_{\mathcal{M}} d^2x\sqrt{g_E}(\Phi_0-\Phi)\left(\Lambda_2-\frac{1}{r_h^2}\right) \\ &+ \frac{1}{4G_N}\int_{\mathcal{M}} d^2x\sqrt{g_E}\left[(\Phi_0+\Phi)F_0^2 + 2\Phi_0 F_0^{\mu\nu}\tilde{F}_{\mu\nu}\right]. \end{aligned} \tag{3.85}$$

where $I^E_{\rm JT}$ and $I^E_{\text{JT-Max}}$ are the action of the JT model and the linearized action derived from the electric solution in the Euclidean regime respectively. In the previous subsections, we confirmed that these actions reproduce the equations of motions derived from the original action (3.20) and (3.38) at the leading order. We already discussed how the duality between the magnetic solutions and the electric solutions in four dimensions appear in the gravitational system. The important point was that if we put them in the same ensemble, the on-shell actions evaluated on the magnetic and electric solutions are equivalent. Let us remind ourselves that the magnetic solutions described by the Einstein-Maxwell action (2.1) are in the canonical ensemble. Since the action of the JT model is derived from such solutions described by (2.1) in the near-extremal near-horizon limit, thus it is expected to capture the s-wave physics in the near-horizon region of the near extremal black holes in the canonical ensemble. On the other hand, the electrically charged solutions described by the action (2.1) are in the grand canonical ensemble. Since the dimensionally reduced action (3.88) is derived from such solutions, thus it can describe the near horizon physics of near-extremal electrically charged black holes in the grand canonical ensemble. In this subsection, we will compare these two actions and confirm the semi-classical electromagnetic duality is reproduced by the two dimensional actions. Let us take a solution of the two dimensional Maxwell field F with the extremal charge $Q = Q_{\rm ext}$ and then we have the following solutions with respect to $(F_0)_{\mu\nu}$ and $\tilde{F}_{\mu\nu}$

$$\begin{aligned} (F_0)_{\mu\nu} &= \frac{Q_{\rm ext}}{\Phi_0}\epsilon_{\mu\nu}\,, & \tilde{F}_{\mu\nu} &= -\frac{Q_{\rm ext}}{\Phi_0^2}\Phi\epsilon_{\mu\nu}\,, \\ (A_0)_t &= \frac{Q_{\rm ext}}{\Phi_0}(r'-r'_+)\,, & \tilde{A}_t &= -\frac{Q_{\rm ext}}{2\Phi_0^2}\phi_b(r'^2-r'^2_+)\,. \end{aligned} \tag{3.86}$$

We plug the solution back into the original action and obtain the on-shell value of the linearized Maxwell action of the following form

$$\begin{aligned} I_{\text{Max}} &= \frac{1}{4G_N}\int_{\mathcal{M}} d^2x\sqrt{g_E}\left[(\Phi_0+\Phi)F_0^2+2\Phi_0 F_0^{\mu\nu}\tilde{F}_{\mu\nu}\right] \\ &= \frac{1}{16\pi G_N}\int_{\mathcal{M}} d^2x\sqrt{g_E}(\Phi_0-\Phi)\left(\Lambda_2-\frac{1}{r_h^2}\right). \end{aligned} \tag{3.87}$$

This leads to the following on-shell action of the theory $I_{\text{JT-Max}}$

$$I^E_{\text{JT-Max}}\big|_{F_0,\tilde{F}:\text{on-shell}} = I^E_{\text{JT}} + \frac{1}{8\pi G_N}\int_{\mathcal{M}} d^2x\sqrt{g_E}(\Phi_0-\Phi)\left(\Lambda_2-\frac{1}{r_h^2}\right). \tag{3.88}$$

Clearly, it deviates from the action of the JT model. It is not strange since we derived these actions from different ensembles. In four dimension, by introducing the Maxwell boundary term

$$I_{\text{Max,bdy}} = -\frac{1}{G_N}\int_{\partial\mathcal{M}} d^3x\sqrt{\hat{\gamma}_E}F_e^{\mu\nu}n_\mu A_{e,\nu}\,. \tag{3.89}$$

we can describe the electrically charged black holes in the canonical ensemble and confirm the equivalence between the on-shell actions evaluated on the magnetic and the electric solutions. Here we will play the same game in two dimension by introducing the two dimensional counterpart of the Maxwell boundary term in four dimensions. The most natural candidate here is the action

$$I_{\text{Max,bdy}} = -\frac{1}{G_N}\int_{\partial\mathcal{M}} d\tau\sqrt{\gamma_{\tau\tau}}n_\mu\left[(\Phi_0+\Phi)F_0^{\mu\nu}(A_0)_\nu+\Phi_0(F_0^{\mu\nu}\tilde{A}_\nu+\tilde{F}^{\mu\nu}(A_0)_\nu)\right] \tag{3.90}$$

where $\gamma_{\tau\tau}$ is the metric on the boundary of the manifold $\partial\mathcal{M}$. Indeed by the variation of the action $I_{\text{JT-Max}}+I_{\text{Max,bdy}}$ with respect to the Maxwell field gives

$$\begin{aligned} &\delta(I_{\text{JT-Max}}+I_{\text{Max,bdy}}) \\ &= (\text{terms giving equations of motion}) \\ &-\frac{1}{G_N}\int_{\partial\mathcal{M}} d\tau\sqrt{\gamma_{\tau\tau}}\left[\delta(F_0^{\mu\nu}n_\mu)[(\Phi_0+\Phi)(A_0)_\nu+\Phi_0\tilde{A}_\nu]+\delta(\tilde{F}^{\mu\nu}n_\mu)\Phi_0(A_0)_\nu\right], \end{aligned} \tag{3.91}$$

Thus vanishing condition of the boundary term fixes the electric charge both for F_0 and $\tilde{F}$. Thus in this subsection we take the boundary term (3.90) and consider the action $I_{\text{JT-Max}}+I_{\text{Max,bdy}}$ which describes the solution with the fixed charge. When the Maxwell field satisfies the equation of motion

$$0=\nabla_\mu(\Phi_0F_0^{\mu\nu}),\ 0=\nabla_\mu(\Phi_0F^{\mu\nu}+\Phi(F_0)^{\mu\nu}) \tag{3.92}$$

we have the following equality

$$(\Phi_0+\Phi)F_0^2+2\Phi_0F_0^{\mu\nu}\tilde{F}_{\mu\nu}=2\nabla_\mu\left[(\Phi_0+\Phi)F_0^{\mu\nu}(A_0)_\nu+\Phi_0(F_0^{\mu\nu}\tilde{A}_\nu+\tilde{F}^{\mu\nu}(A_0)_\nu)\right]. \tag{3.93}$$

Then by the Stokes' theorem, we can convert the Maxwell boundary term into the bulk term as

$$\begin{aligned} I_{\text{Max,bdy}}|_{F_0,\tilde{F}:\text{on-shell}} &= -\frac{1}{2G_N}\int_{\mathcal{M}}d^2x\sqrt{g_E}\left[(\Phi_0+\Phi)F_0^2+2\Phi_0F_0^{\mu\nu}\tilde{F}_{\mu\nu}\right] \\ &= -\frac{1}{8\pi G_N}\int_{\mathcal{M}}d^2x\sqrt{g_E}(\Phi_0-\Phi)\left(\Lambda_2-\frac{1}{r_h^2}\right). \end{aligned} \tag{3.94}$$

Here we used the solutions for F_0 and $\tilde{F}$ in the second equality. Thus we can confirm the on-shell equivalence between the action of the JT model and the action $I_{\text{JT-Max}}$ with the Maxwell boundary term

$$I_{\text{JT-Max}}+I_{\text{Max,bdy}}|_{F_0,\tilde{F}:\text{on-shell}}=I_{\text{JT}}\,. \tag{3.95}$$

This implies that two theories are equivalent at least semi-classically $G_N\to 0$

$$\begin{aligned} Z_{\text{JT}}[g,\Phi] &= \int\mathcal{D}g_{\mu\nu}\mathcal{D}\Phi e^{-I^E_{\text{JT}}} \\ \approx\ Z^C_{\text{JT-Max}}[g,\Phi,A_0,A] &= \int\mathcal{D}g_{\mu\nu}\mathcal{D}\Phi\mathcal{D}A_0\mathcal{D}Ae^{-I^E_{\text{JT-Max}}-I^E_{\text{Max,bdy}}}\,, \end{aligned} \tag{3.96}$$

thus electromagnetic duality is indeed hidden in the two-dimensional actions while we no longer have the magnetic solutions since there are no spherical degrees of freedom.

For the later purpose, let us define the chemical potential associated with the Maxwell fields $(A_0)_\mu$ and $\tilde{A}_\mu$ in general case $\delta Q\neq 0$ as

$$\mu_0=\frac{1}{G_N}\lim_{r\to r_c}(A_0)_t\,,\ \tilde{\mu}=\frac{1}{G_N}\lim_{r\to r_c}\tilde{A}_t. \tag{3.97}$$

for gauge fields with a general $\delta Q\neq 0$

$$\begin{aligned} (F_0)_{\mu\nu}&=\frac{Q_{\text{ext}}}{\Phi_0}\epsilon_{\mu\nu}\,, & \tilde{F}_{\mu\nu}&=-\frac{Q_{\text{ext}}}{\Phi_0^2}\left(\tilde{\phi}_br'-\frac{1}{r_h^2\Lambda_2}\frac{\delta Q}{Q_{\text{ext}}}\Phi_0\right)\epsilon_{\mu\nu}\,, \\ (A_0)_t&=\frac{Q_{\text{ext}}}{\Phi_0}(r'-r'_+)\,, & \tilde{A}_t&=-\frac{Q_{\text{ext}}}{\Phi_0^2}\left(\frac{1}{2}\tilde{\phi}_b(r'^2-r'^2_+)-\frac{1}{r_h^2\Lambda_2}\frac{\delta Q}{Q_{\text{ext}}}\Phi_0(r'-r'_+)\right). \end{aligned} \tag{3.98}$$

The simple calculations lead to

$$I_{\text{Max,bdy}}=\beta(\mu_0Q+\tilde{\mu}Q_{\text{ext}}) \tag{3.99}$$

where we used the fact that the Euclidean time is periodic under $\tau \to \tau + \beta$ and Q is the "total charge" defined as $Q = Q_{\text{ext}} + \delta Q$. Since when we consider the linearized action, we are neglecting the terms $\mathcal{O}((\Phi/\Phi_0)^2)$ and we assumed $\delta Q/Q_{\text{ext}} \lesssim \mathcal{O}(\Phi/\Phi_0)$, we can rewrite the above relation as

$$I_{\text{Max,bdy}} = \beta\mu Q \tag{3.100}$$

up to $\mathcal{O}((\Phi/\Phi_0)^2)$ by defining the chemical potential for the total gauge potential $A_\mu = (A_0)_\mu + \tilde{A}_\mu$ as $\mu = \mu_0 + \tilde{\mu}$. We will use this expression in subsection 3.6.

3.5 Universality of the JT model

In this subsection, we will take the general form of the dimensionally reduced action which describes the AdS_2 spacetime and discuss the (non-)universality of the JT model both at the level of the equation of motion and the action. Similar arguments are found in [102]. It is known that a large number of situations we obtain the dimensionally reduced action which takes the form of

$$I = \frac{1}{4G_N}\int_{\mathcal{M}} d^2x\sqrt{-g}\left(\Psi^2 R + \lambda\left(\nabla\Psi\right)^2 - U(\Psi^2) - f(\Psi^2)F^2\right) . \tag{3.101}$$

First we consider the situation where we have $f(\Psi^2) = 0$. In this case, the action is simplified to

$$I = \frac{1}{4G_N}\int_{\mathcal{M}} d^2x\sqrt{-g}\left(\Psi^2 R + \lambda\left(\nabla\Psi\right)^2 - U(\Psi^2)\right) . \tag{3.102}$$

Such an action arises for example from the magnetically charged black holes described by the action (2.1) by identifying the parameter λ and the function $U(\Psi^2)$ as

$$\lambda = 2\,,\ U(\Psi) = -2 - 6\frac{\Psi^2}{L^2} + \frac{8\pi Q_m^2}{\Psi^2}\,. \tag{3.103}$$

In this subsection, we keep λ and $U(\Psi^2)$ in general. The equations of motion for the action (3.102) are given by

$$\begin{aligned} 0 &= R - \partial_{\Psi^2}U(\Psi^2) - \lambda\frac{\nabla^2\Psi}{\Psi}\,,\\ 0 &= \nabla_\mu\nabla_\nu\Psi^2 - \nabla^2\Psi^2 g_{\mu\nu} - \frac{1}{2}U(\Psi^2)g_{\mu\nu} - \lambda\nabla_\mu\Psi\nabla_\nu\Psi + g_{\mu\nu}\frac{\lambda(\nabla\Psi)^2}{2}\,. \end{aligned} \tag{3.104}$$

Motivated by the fact that the near horizon geometry of extremal black holes is AdS_2, we will demand that the action has a constant solution $4\pi\Psi^2 = \Phi_0$ which describes the AdS_2 spacetime $R = 2R_{\rm AdS}$ with a negative constant $R_{\rm AdS} < 0$. In that case, (3.104) reduces to

$$\begin{aligned} U(\Phi_0) &= 0\,,\\ \partial_{\Psi^2}U(\Phi_0) &= R_{\rm AdS} < 0\,. \end{aligned} \tag{3.105}$$

Now, we consider a small deviation from the constant solution (3.105) as

$$\Psi^2 = \frac{\Phi_0 + \Phi}{4\pi}\,, \tag{3.106}$$

such that $\Phi/\Phi_0 \ll 1$. This small expansion leads to the following bulk action [5]

$$I \approx \frac{\Phi_0}{16\pi G_N}\int_{\mathcal{M}} d^2x\sqrt{-g}R + \frac{1}{16\pi G_N}\int_{\mathcal{M}} d^2x\sqrt{-g}\Phi\left(R - R_{\rm AdS}\right) \tag{3.107}$$

[5] The contribution coming from the kinematic term is also neglected.

This allows us to see that an equation of the form (3.102) leads quite generally to the JT model by demanding (3.105). In the particular case where we come from the dimensional reduction of an extremal magnetically charged Reissner-Nordström black hole and we have (3.103), we can show that the constant solution is given by

$$\Phi_0 = 4\pi r_h^2 \tag{3.108}$$

where r_h is the position of the event horizon of the extremal black hole. In order to do this, notice that the charge parameter of the extremal black hole can be written in terms of r_h as

$$Q_{\text{ext}}^2 = 4\pi \left(r_h^2 + 3\frac{r_h^4}{L^2} \right) . \tag{3.109}$$

Hence, replacing (3.109) in the first equation of (3.105) we get that the constant solution is indeed (3.108). Moreover, using the second equation in (3.105), we find

$$R_{\text{AdS}} = -\frac{2}{L_2^2} = 2\Lambda_2 \,, \tag{3.110}$$

with

$$L_2^2 = \frac{L^2}{6 + L^2/r_h^2} \,. \tag{3.111}$$

With the Maxwell Field

Equivalence at the Level of Equations of Motion

We next consider more general case where the dimensionally reduced action has dynamical Maxwell field F in two dimension

$$I = \frac{1}{4G_N} \int_{\mathcal{M}} d^2x \sqrt{-g} \left(\Psi^2 R + \lambda \left(\nabla \Psi \right)^2 - U(\Psi^2) - 4\pi f(\Psi^2) F^2 \right) . \tag{3.112}$$

This situation arises when we derive the action from the electrically charged black hole with identifications

$$\lambda = 2 \,, \; U(\Psi^2) = -2 - 6\frac{\Psi^2}{L^2} \,, \; f(\Psi^2) = \Psi^2 \,. \tag{3.113}$$

The action (3.112) leads to the following equations of motion

$$0 = \partial_\mu \left(\sqrt{-g} f(\Psi^2) F^{\mu\nu} \right) \,, \tag{3.114}$$

$$\begin{aligned} 0 &= R - \partial_{\Psi^2} U(\Psi^2) - 4\pi \partial_{\Psi^2} f(\Psi^2) F^2 - \lambda \frac{\nabla^2 \Psi}{\Psi} = 0 \\ 0 &= \nabla_\mu \nabla_\nu \Psi^2 - \nabla^2 \Psi^2 g_{\mu\nu} - \frac{1}{2} U(\Psi^2) g_{\mu\nu} - 4\pi f(\Psi^2) \left(\frac{1}{2} F^2 g_{\mu\nu} + 2 F_{\mu\sigma} F_\nu^\sigma \right) \\ &\qquad - \lambda \nabla_\mu \Psi \nabla_\nu \Psi + g_{\mu\nu} \frac{\lambda (\nabla \Psi)^2}{2} \,. \end{aligned} \tag{3.115}$$

Solving for the gauge field assuming that $\sqrt{-g}$ =const. , yields

$$F^{\mu\nu} = \frac{Q\epsilon^{\mu\nu}}{4\pi f(\Psi^2)} \tag{3.116}$$

and inserting it back in (3.114) leads to

$$\begin{aligned} 0 &= R - \partial_{\Psi^2} U(\Psi^2) + 2\partial_{\Psi^2} f(\Psi^2)\frac{Q^2}{4\pi f(\Psi^2)^2} - \lambda\frac{\nabla^2\Psi}{\Psi}\,, \\ 0 &= \nabla_\mu\nabla_\nu\Psi^2 - \nabla^2\Psi^2 g_{\mu\nu} - \frac{1}{2}U(\Psi^2)g_{\mu\nu} - \frac{Q^2}{4\pi f(\Psi^2)} - \lambda\nabla_\mu\Psi\nabla_\nu\Psi + g_{\mu\nu}\frac{\lambda(\nabla\Psi)^2}{2}\,. \end{aligned} \tag{3.117}$$

We then see that equations (3.117) are the same as (3.104) if we redefine

$$U(\Psi^2) \to U(\Psi^2) + \frac{2Q^2}{4\pi f(\Psi^2)}\,. \tag{3.118}$$

Notice that, if we consider the specific case of the Reissner-Nordström black hole, this redefinition leads to a precise matching between (3.113) with (3.103) by idetifying $Q = Q_m$.

Difference at the Level of Action

Now that we see the equivalence of the equations of motions derived from the action (3.102) and (3.112), next let us consider the difference between them at the level of the off-shell action. We consider a constant solution $4\pi\Psi^2 = \Phi_0$ and $F^2 = \mathcal{F}_0^2$, leading to the equations of motion

$$\begin{aligned} U(\Phi_0) - 4\pi f(\Phi_0)\mathcal{F}_0^2 &= 0\,, \\ R_{\text{AdS}} - \partial_{\Psi^2}U(\Phi_0) - 4\pi\partial_{\Psi^2}f(\Phi_0)\mathcal{F}_0^2 &= 0\,. \end{aligned} \tag{3.119}$$

Inserting this information in (3.112) and considering a small deviation from the constant solution as

$$\begin{aligned} \Psi^2 &= \frac{\Phi_0 + \Phi}{4\pi}\,, \\ F_{\mu\nu} &= (F_0)_{\mu\nu} + \tilde{F}_{\mu\nu} \end{aligned} \tag{3.120}$$

such that $\Phi/\Phi_0 \ll 1, \tilde{F}/F_0 \ll 1$. We have

$$4\pi\Psi^2 R \approx (\Phi_0 + \Phi)\, R \tag{3.121}$$

$$U(\Psi^2) \approx U(\Phi_0) + \frac{\Phi}{4\pi}\,\partial_{\Psi^2}U(\Phi_0) = 4\pi f(\Phi_0)\mathcal{F}_0^2 + \frac{\Phi}{4\pi}\,\partial_{\Psi^2}U(\Phi_0)\,. \tag{3.122}$$

$$4\pi f(\Psi^2)F^2 \approx 4\pi f(\Phi_0)F_0^2 + \Phi\partial_{\Psi^2} f(\Phi_0)F_0^2 + 8\pi f(\Phi_0)F_0^{\mu\nu}\tilde{F}_{\mu\nu}\,. \tag{3.123}$$

Notice that joining two of the expression, we have

$$\begin{aligned} U(\Psi^2) + 4\pi f(\Psi^2)F^2 \approx R_{\text{AdS}}\frac{\Phi}{4\pi} &+ (4\pi f(\Phi_0) - \Phi\partial_{\Psi^2} f(\Phi_0))\mathcal{F}_0^2 \\ &+ (4\pi f(\Phi_0) + \Phi\partial_{\Psi^2} f(\Phi_0))F_0^2 + 8\pi f(\Phi_0)F_0^{\mu\nu}\tilde{F}_{\mu\nu}\,. \end{aligned} \tag{3.124}$$

Then we have the following bulk action

$$\begin{aligned} I \approx & I_{\text{JT}} - \frac{\mathcal{F}_0^2}{4G_N}\int_{\mathcal{M}} d^2x\sqrt{-g}(4\pi f(\Phi_0) - \Phi\partial_{\Psi^2} f(\Phi_0)) \\ & - \frac{1}{4G_N}\int_{\mathcal{M}} d^2x\sqrt{-g}\left[(4\pi f(\Phi_0) + \Phi\partial_{\Psi^2} f(\Phi_0))F_0^2 + 8\pi f(\Phi_0)F_0^{\mu\nu}\tilde{F}_{\mu\nu}\right]. \end{aligned} \tag{3.125}$$

Let us fix the function f by considering the one that comes from the dimensional reduction. In this case, assuming $\Phi_0 = 4\pi r_h^2$ as before, we can see that the first equation in (3.119) implies

$$4\pi\mathcal{F}_0^2 = -\frac{6}{L^2} - \frac{2}{r_h^2} = \Lambda_2 - \frac{1}{r_h^2}\,. \tag{3.126}$$

Again, the second equation in (3.119) implies (3.110). Moreover, considering the particular action that comes from the dimensional reduction, we see that it leads to

$$\begin{aligned} I \approx & I_{\text{JT}} - \frac{1}{16\pi G_N}\int_{\mathcal{M}} d^2x\sqrt{-g}(\Phi_0 + \Phi)\left(\Lambda_2 - \frac{1}{r_h^2}\right) \\ & - \frac{1}{4G_N}\int_{\mathcal{M}} d^2x\sqrt{-g}\left[(\Phi_0 + \Phi)F_0^2 + 2\Phi_0 F_0^{\mu\nu}\tilde{F}_{\mu\nu}\right]. \end{aligned} \tag{3.127}$$

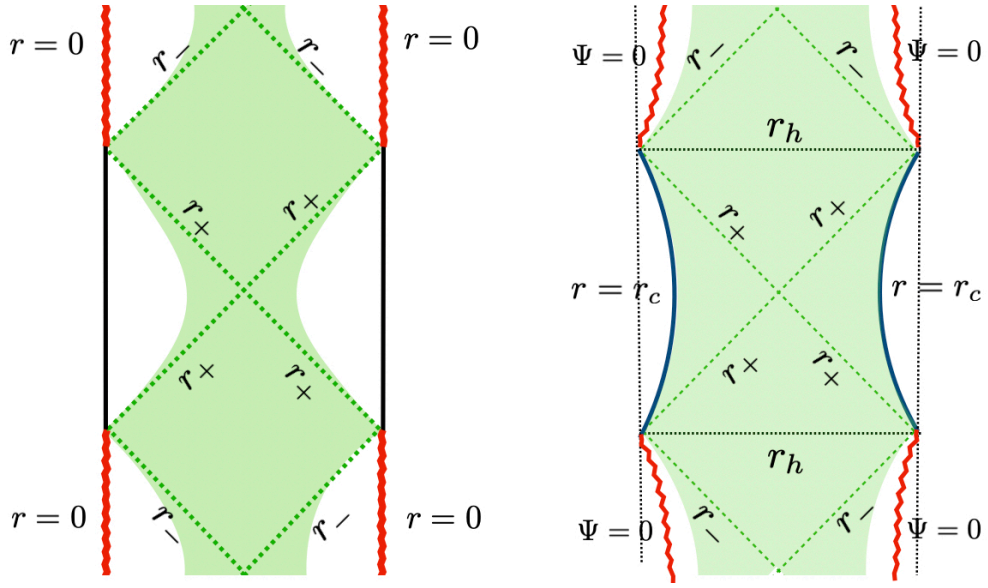

Figure 3: Left: The Penrose diagram of the Reissner-Nordström black hole solution of the Einstein-Maxwell theory (2.1) and its near horizon region, whose geometry is approximated to $\mathrm{AdS}_2 \times S^2$. Right: The AdS_2 solution of the two-dimensional dilaton gravity theories (3.128)(3.129) depicted in the global AdS coordinate. For both figures, the singularity is depicted with the zigzag lines colored in red. They share the common causal structure. If we let us remind ourselves that the theories (3.128)(3.129) are derived from the near horizon region of the four-dimensional Reissner-Nordström solution, we should also restrict AdS_2 geometry within the region (colored in green) which corresponds to the near horizon region in the four-dimensional black hole. This restriction introduces a finite radial cut-off of the AdS_2 geometry drawn with the blue curves.

3.6 Nearly AdS_2 Solution

In the previous subsections, we see that the sectors which only contain the metrics and the dilatons of the dimensionally reduced theories

$$I_{\mathrm{JT}} = \frac{\Phi_0}{16\pi G_N}\int_{\mathcal{M}} d^2x\sqrt{-g}R + \frac{1}{16\pi G_N}\int_{\mathcal{M}} d^2x\sqrt{-g}\Phi\left(R - 2\Lambda_2\right) \tag{3.128}$$

$$\begin{aligned} I_{\text{JT-Max}} = I_{\mathrm{JT}} &- \frac{1}{16\pi G_N}\int_{\mathcal{M}} d^2x\sqrt{-g}(\Phi_0 - \Phi)\left(\Lambda_2 - \frac{1}{r_h^2}\right) \\ &- \frac{1}{4G_N}\int_{\mathcal{M}} d^2x\sqrt{-g}\left[(\Phi_0 + \Phi)F_0^2 + 2\Phi_0 F_0^{\mu\nu}\tilde{F}_{\mu\nu}\right] \end{aligned} \tag{3.129}$$

are both described by the equations of motion in the JT model as

$$R - 2\Lambda_2 = 0\,, \tag{3.130}$$

$$\nabla_\mu\nabla_\nu\tilde{\Phi} - g_{\mu\nu}\nabla^2\tilde{\Phi} - g_{\mu\nu}\Lambda_2\tilde{\Phi} = 0\,. \tag{3.131}$$

while the actions depend on what type of charge and what kind of ensemble from which we derive the dimensionally reduced theories[6]. In this subsection, we describe the solution to these equations and implications for the thermodynamics of the solutions (for related arguments, see [39, 103]).

To make the variation principle well defined and obtain the equations of motion above, we should fix the boundary condition. We choose the Dirichlet boundary condition which fixes the boundary value of the metric and the dynamical dilation $\delta\Phi = \delta\gamma_{tt} = 0$. We write the values of them on the boundary $\partial\mathcal{M} : r = r_c$ as

$$\begin{aligned}\gamma_{tt}|_{\partial\mathcal{M}} &= -\frac{r_c^2}{L_2^2} \\ \tilde{\Phi}|_{\partial\mathcal{M}} &= \tilde{\Phi}_b = \tilde{\phi}_b r_c\,.\end{aligned} \tag{3.132}$$

with some positive constant $\tilde{\Phi}_b$ as we take $r_c \to \infty$. The first equation (3.130) implies that the theories describe the AdS_2 spacetime with a radius $L_2^2 = -1/\Lambda_2$. It turns out that the most general solution to the second equation (3.131) is given by

$$\tilde{\Phi} = Z \cdot X = Z_{-1}X^{-1} + Z_0 X^0 + Z_1 X^1 \tag{3.133}$$

where Z is an arbitrary vector in the embedding space and Y is a vector which represents a point in the AdS_2 spacetime $X = (X^{-1}, X^0, X^1)$. From this form of the solution, we can see that the dilaton is constant along the intersections of the embedded surface with a hypersurface which is normal to the vector Z. Notice that the AdS boundary is sitting at the spacelike infinity $X^1 \to \pm\infty$. If we take a spacelike vector Z, our boundary condition (3.132) contradicts with the behavior of the solution (3.133) since on one of the boundaries $X^1 \to \pm\infty$, the dilaton takes a large negative value. Therefore we take a timelike vector Z. Using the $SO(1,2)$ symmetry, we can take $Z_0 = Z_1$ without loss of generality. Thus we can take

$$\tilde{\Phi} = \frac{\tilde{\Phi}_h}{L_2} X^{-1}\,. \tag{3.134}$$

In the global coordinate (3.5), we can express it as

$$\tilde{\Phi} = \tilde{\Phi}_h \frac{\cos\tau}{\cos\eta} \tag{3.135}$$

[6]Notice that for the JT model, we have $\Phi_q = 0$, and thus $\tilde{\Phi}$ reduces to Φ.

and in the shifted Rindler (Reissner-Nordström-like) coordinate (3.7) as

$$\tilde{\Phi} = \frac{\tilde{\Phi}_h}{\sqrt{\mu}}(r - r_h)\,. \tag{3.136}$$

Notice that $\tilde{\Phi}_h$ denotes the value of the dynamical dilaton at the horizon $r = r_h + \sqrt{\mu}$. As depicted in Figure3, this solution represents the Reissner-Nordström like black hole spacetime with two horizons where the dilaton takes value $\tilde{\Phi} = \pm\tilde{\Phi}_h$. The horizon can be characterized by the condition $\partial_U\tilde{\Phi} = \partial_V\tilde{\Phi} = 0$ where (U, V) is the light-cone coordinate which is defined in the coordinate (3.7) as $U = t - r^*(r)$ and $V = t + r^*(r)$ with the tortoise coordinate r^*

$$r^* = -\int_r^\infty \frac{dr}{f(r)}\,. \tag{3.137}$$

In the four-dimensional black hole, a light ray moving inside the apparent horizon toward the future direction feels the area the sphere Ψ^2 shrinking and having a hunch that it will inevitably hit the singularity where the area of the sphere becomes zero. On the other hand, if it is traveling outside the horizon, it feels the area expanding as it moves in the future direction. Thus the apparent horizon can be characterized as the position where the area of the sphere is unchanged along the null direction. This condition reduces to $\partial_U\tilde{\Phi} = \partial_V\tilde{\Phi} = 0$ in two dimensions, and we can see that it actually coincides with the horizon of the coordinate (3.7). We could expect that the black hole singularity in this theory is sitting at the position of $\Psi^2 = 0$ i.e,

$$\tilde{\Phi} = \frac{\tilde{\Phi}_h}{\sqrt{\mu}}(r - r_h) = \tilde{\Phi}_h\frac{\cos\tau}{\cos\eta} = \Phi_q - \Phi_0\,, \tag{3.138}$$

and it can be spacelike when $T > \frac{\sqrt{\mu}}{2\pi L_2^2}\frac{\Phi_0-\Phi_q}{\tilde{\Phi}_h}$ and null when $T = \frac{\sqrt{\mu}}{2\pi L_2^2}\frac{\Phi_0-\Phi_q}{\tilde{\Phi}_h}$ and the timelike when $T < \frac{\sqrt{\mu}}{2\pi L_2^2}\frac{\Phi_0-\Phi_q}{\tilde{\Phi}_h}$ as depicted in Figure4.

Restriction to the Near-Horizon & Near-Extremal

Here let us remind ourselves that we study two-dimensional theories(3.128)(3.129) as dimensionally reduced theories derived from the near horizon limit of the near-extremal black holes. Under the assumption that we restrict ourselves in the near horizon region, we neglected higher order term in Φ/Φ_0. Therefore the spacetime region beyond $\Phi/\Phi_0 < 1$ is no longer precisely captured by the actions (3.128)(3.129). Thus we restrict the spacetime region which satisfies

$$\tilde{\Phi} = \frac{\tilde{\Phi}_h}{\sqrt{\mu}}(r - r_h) \ll \Phi_0 \tag{3.139}$$

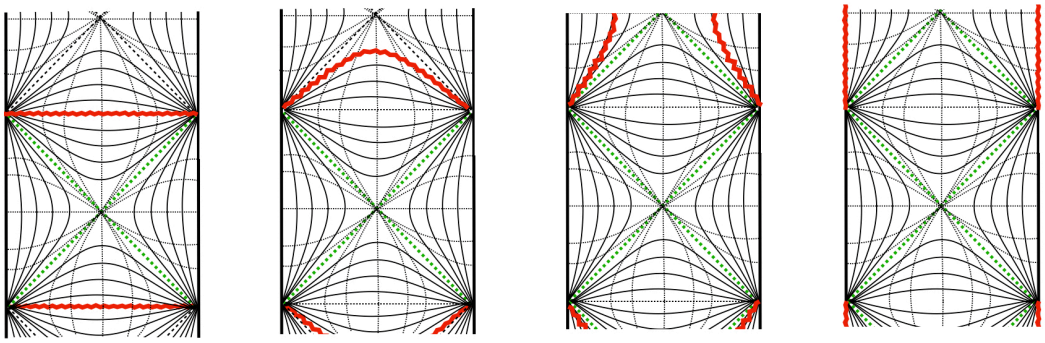

Figure 4: The positions of the black hole singularity depicted in the global AdS spacetime. It can be spacelike, null or timelike according to the black hole temperature. If we let us remind ourselves that the theories (3.128)(3.129) are derived from the near-extremal Reissner-Nordström black holes, the temperature is very small and the singularity would sit at a timelike curve (at least it is outside of the near horizon region depicted in Figure 3).

and moreover, to keep the near extremality we also demand

$$\tilde{\Phi}_h \ll \frac{\tilde{\Phi}_h}{\sqrt{\mu}} r_c \,. \tag{3.140}$$

Thus when we treat the theories (3.128)(3.129) as the dimensionally reduced theories which capture the near-horizon near-extremal physics in the four-dimensional black holes, we should restrict ourselves on the region

$$\tilde{\Phi}_h \ll \frac{\tilde{\Phi}_h}{\sqrt{\mu}} r_c \ll \Phi_0 \,. \tag{3.141}$$

This implies that we cannot send r_c to the infinity and we should cut off the spacetime at finite radial position $r = r_c$ before the $\tilde{\Phi}$ becomes too large as first pointed out in [40]. This one-dimensional cut-off surface plays a role of the physical boundary of the AdS_2 spacetime. This cutout spacetime only has $SL(2)$ symmetry as the asymptotic symmetry of AdS_2 while before we cut off we have full conformal (reparametrization) symmetry. As we explained in the introduction, on the one-dimensional boundary of AdS_2 the stress tensor has only one component, and if there is the full reparametrization symmetry on the boundary, we have the traceless condition on the stress tensor and it implies the theory has not finite excitations above the vacuum. On the other hand, the

spacetime cut-off reduces the symmetry to the subgroup $SL(2)$ of the full conformal symmetry and allows the theory to have finite energy excitations. This fact is also important in the SYK model and we will see that our actions (3.128) (3.129) reduce to the Schwarzian action which is invariant under $SL(2)$ and governs the low energy dynamics of the SYK model in the following section. This cutout AdS_2 spacetime is also called the nearly AdS_2 and sometimes written as $NAdS_2$ in short in the literature.

Notice that the black hole singularity placed at (3.138) is outside of the region (3.141) where the theory is reliable as the dimensionally reduced theory. Before one hits the singularity the higher order corrections in Φ will dominate over the leading order physics described by (3.128)(3.129), and the spacetime descriptions governed by the equations (3.130)(3.131) are no longer available.

Thermodynamics

Here we discuss the thermodynamic properties, namely, we aim to compute the temperature, the entropy and the mass of the black holes solutions described by the actions

$$I^E_{\rm JT} = -\frac{\Phi_0}{16\pi G_N}\int_{\mathcal{M}} d^2x\sqrt{g_E}R - \frac{1}{16\pi G_N}\int_{\mathcal{M}} d^2x\sqrt{g_E}\Phi\left(R-2\Lambda_2\right) \tag{3.142}$$

$$\begin{aligned} I^E_{\text{JT-Max}} = I^E_{\rm JT} &+ \frac{1}{16\pi G_N}\int_{\mathcal{M}} d^2x\sqrt{g_E}(\Phi_0-\Phi)\left(\Lambda_2-\frac{1}{r_h^2}\right) \\ &+ \frac{1}{4G_N}\int_{\mathcal{M}} d^2x\sqrt{g_E}\left[(\Phi_0+\Phi)F_0^2 + 2\Phi_0 F_0^{\mu\nu}\tilde{F}_{\mu\nu}\right]. \end{aligned} \tag{3.143}$$

which describe the AdS_2 geometry with the dilaton profile

$$\tilde{\Phi} = \Phi + \Phi_q = \tilde{\Phi}_b\frac{r'}{r'_c}. \tag{3.144}$$

Notice that here we should set $\Phi_q = 0$ for the JT model. In this subsection, we sloppily write $\tilde{\Phi}$ as Φ for both theories for simplicity. In subsection 3.4, we saw that the on-shell (Euclidean) action of $I_{\text{JT-Max}}$ is equivalent to the JT action by adding the Maxwell boundary term

$$I_{\text{Max,bdy}} = -\frac{1}{G_N}\int_{\partial\mathcal{M}} d\tau\sqrt{\gamma_{\tau\tau}}n_\mu\left[(\Phi_0+\Phi)F_0^{\mu\nu}(A_0)_\nu + \Phi_0(F_0^{\mu\nu}\tilde{A}_\nu + \tilde{F}^{\mu\nu}(A_0)_\nu)\right] \tag{3.145}$$

The temperature is proportional to the surface gravity $\kappa = \partial_r f(r_+)/2$ and expressed as

$$T = \frac{1}{4\pi}\partial_r f(r_+) = \frac{\sqrt{\mu}}{2\pi L_2^2}. \tag{3.146}$$

Identifying the parameter $\sqrt{\mu} = \delta r_h$, we can find that the solutions to the theories (3.142) (3.143) have the same temperature as the four-dimensional black hole (2.24) from which the theories are derived.

To derive other thermodynamic quantities, we need to evaluate the Euclidean on-shell actions I^E by wick rotating $\tau = it$. Let us remind that the action I^E_{JT} or (at least semi-classically) equivalently the action $I^E_{\text{JT-Max}} + I^E_{\text{Max,bdy}}$ describes the solutions in the canonical ensemble thus the partition function can be written in terms of the Helmholtz free energy F as

$$Z_{\text{C}} = e^{-\beta F} \,. \tag{3.147}$$

Since the partition function can be expressed as the Euclidean path-integral and semi-classically we can approximate it by the saddle point which is given by the Euclidean on-shell action evaluated on the black hole solution

$$\beta F \approx I^E_{\text{JT}}\big|_{\text{on-shell}} = (I^E_{\text{JT-Max}} + I^E_{\text{Max,bdy}})\big|_{\text{on-shell}} \,. \tag{3.148}$$

Let us remind that the Helmholtz free energy F can be written in terms of the mass, temperature and the entropy as

$$\beta F = \beta M - S \,. \tag{3.149}$$

On the other hand, the theory $I^E_{\text{JT-Max}}$describes the solutions in the grand canonical ensemble and its partition function is written by the Gibbs free energy G

$$Z_{\text{GC}} = e^{-\beta G} \,. \tag{3.150}$$

Using the same logic as above, semi-classically, the partition function is approximated by the exponential of the Euclidean on-shell action and we have

$$\beta G \approx I^E_{\text{JT-Max}}\big|_{\text{on-shell}} \,. \tag{3.151}$$

Notice that the Gibbs free energy G can be expressed as

$$\beta G = \beta M - S - \beta \mu Q \tag{3.152}$$

where μ is the chemical potential for the total gauge potential A_μ. Let us remind ourselves that we can rewrite the Maxwell boundary term as (3.100)

$$I^E_{\text{Max,bdy}} = \beta \mu Q \,, \tag{3.153}$$

Therefore we can confirm that the relation between the Helmholtz free energy F and the Gibbs free energy G

$$F = G + \mu Q \tag{3.154}$$

and the relation between I^E_{JT} and $I^E_{\text{JT-Max}}$

$$I^E_{\text{JT}} = I^E_{\text{JT-Max}} + I^E_{\text{Max,bdy}} \tag{3.155}$$

are consistent with each other. Since for both theories: I_{JT} and $I_{\text{JT-Max}}$, the entropy is given by

$$S = \beta^2 \frac{\partial F}{\partial \beta} = \beta^2 \frac{\partial G}{\partial \beta} = \beta^2 \frac{\partial}{\partial \beta} I^E_{\text{JT}}/\beta \,, \tag{3.156}$$

thus we will focus on evaluating the on-shell action of the JT model. Including the Gibbons-Hawking-York boundary term, the Euclidean action of the JT model can be written as

$$\begin{aligned} I^E_{\text{JT}} = &-\frac{\Phi_0}{16\pi G_N}\left[\int_{\mathcal{M}} d^2x\sqrt{g_E}R + 2\int_{\partial\mathcal{M}} K\right] \\ &-\frac{1}{16\pi G_N}\left[\int_{\mathcal{M}} d^2x\sqrt{g_E}\Phi\left(R - 2\Lambda_2\right) + 2\int_{\partial\mathcal{M}} \Phi K\right] \end{aligned} \tag{3.157}$$

The extrinsic curvature K is computed via

$$K = \nabla_\alpha n^\alpha \,, \tag{3.158}$$

where n^α is the outward directed normal vector to the boundary. The term in the first line is purely topological I^E_{top} and we can evaluate it as

$$I^E_{\text{top}} = -\frac{\Phi_0}{16\pi G_N}\left[\int_{\mathcal{M}} d^2x\sqrt{g_E}R + 2\int_{\partial\mathcal{M}} K\right] = -\frac{\Phi_0}{4G_N} \tag{3.159}$$

The bulk term in the second line of (3.157) is zero by putting the solution of the equation $R = 2\Lambda_2$, thus as a result we obtain

$$I^E_{\text{JT}}\big|_{\text{on-shell}} = -\frac{\Phi_0}{4G_N} - \frac{1}{8\pi G_N}\int_{\partial\mathcal{M}} \Phi K \,. \tag{3.160}$$

Using the definition of the extrinsic curvature (3.158), we can evaluate the on-shell JT action as

$$I^E_{\text{JT}}\big|_{\text{on-shell}} = -\frac{\Phi_0}{4G_N} - \frac{\Phi_b \beta}{8\pi G_N L_2^2}(r_c - r_h) \,, \tag{3.161}$$

where we write the boundary value of the dynamical dilaton $\Phi_b \equiv \Phi|_{\partial\mathcal{M}}$. To subtract the divergent part appeared as we send $r_c \to \infty$, we introduce the boundary counter term

$$\begin{aligned} I_{\rm ct} &= \frac{1}{8\pi G_N L_2}\int_{\partial\mathcal{M}} \sqrt{\gamma_{\tau\tau}}\Phi_b \\ &= \frac{\Phi_b \beta\sqrt{f(r_c)}}{8\pi G_N L_2}\,. \end{aligned} \tag{3.162}$$

This prescription for subtracting the divergence when $r_c \to \infty$ is common in the context of the AdS/CFT correspondence [104]. Since we can evaluate the divergent factor $\sqrt{f(r_c)}$ as

$$\sqrt{f(r_c)} \approx \frac{r_c - r_h}{L_2}\left(1 - \frac{\mu}{2(r_c - r_h)^2}\right)\,, \tag{3.163}$$

thus we obtain

$$(I^E_{\rm JT} + I_{\rm ct})\big|_{\text{on-shell}} = -\frac{\Phi_0}{4G_N} - \frac{\Phi_b\sqrt{\mu}}{8G_N r_c'}\,. \tag{3.164}$$

up to higher order in μ. We can compute the entropy of the two-dimensional system as[7]

$$\begin{aligned} S &= -\frac{\partial}{\partial T} T\,(I^E_{\rm JT} + I_{\rm ct})\big|_{\text{on-shell}} \\ &= \frac{1}{4G_N}(\Phi_0 + \Phi_h)\,, \end{aligned} \tag{3.165}$$

where we used $\Phi_h = \phi_b\sqrt{\mu}$. Here $S_0 = \Phi_0/4G_N$ is the extremal entropy associated to the grand state of the black hole and $S = \Phi_h/4G_N$ is the entropy associated to Φ, i.e, the small deviations from the extremality. Notice that the sum of Φ_0 and Φ_h gives the area of the black hole in four dimensions, thus it reproduces the Hawking-Bekenstein formula for the black hole entropy. The mass is computed via $M = (I^E_{\rm JT} + I_{\rm ct} + S)/\beta$ and the result can be expressed as

$$M = \frac{\Phi_b \mu}{16\pi G_N L_2^2 r_c'}\,. \tag{3.166}$$

One can see that the mass in the dimensionally reduced theories in two dimensions corresponds to the deviation of the mass (2.27) away from extremality in the four-dimensional Reissner-Nordström black hole with an identification of a parameter $\Phi_b/r_c' = 8\pi r_h$.

[7] In the case of the theory $I_{\text{JT-Max}}$, Φ_h in the expression of the entropy should be replaced by $\Phi_h + \Phi_q$.

4 Relation to the Sachdev-Ye-Kitaev model

4.1 The Sachdev-Ye-Kitaev model

We investigate the relation between the two-dimensional dilaton gravity theories analyzed in the previous section and the so-called Sachdev-Ye-Kitaev (SYK) model [42–45]. The SYK model is the one-dimensional quantum mechanical model of Majorana fermions. It is extensively studied recently since it is solvable in the strong coupling and large N limit. Since it shows the chaotic behavior, it is also expected to capture the black hole physics in two dimensions holographically. We review the SYK model in this subsection [36, 45] and we will see the relation to the dimensionally reduced theories in the next subsection. The Hamiltonian of the SYK model is written as

$$H = i^{q/2} \sum_{1\leq q_1 \leq \cdots \leq i_q \leq N} J_{i_1 \cdots i_q} \psi_{i_1} \cdots \psi_{i_q} \,, \tag{4.1}$$

where ψ is the Majorana fermion and $J_{i_1 \cdots i_q}$ is a random coupling chosen from the Gaussian distribution with zero mean and variance

$$\langle J^2_{i_1 \cdots i_q} \rangle = \frac{J^2 (q-1)!}{N^{q-1}} \,. \tag{4.2}$$

Originally, this model was proposed in the case $q = 4$ by Kitaev [42, 43] and it was generalized to an arbitrary number of q by Maldacena et. al in [45]. We first derive the master equation of the bi-local fields G and Σ which governs the large N dynamics of the SYK model. We will work on the Euclidean signature. We define the sum of the time ordered two-point functions

$$G(\tau) = \frac{1}{N} \sum_i G_{ij}(\tau) \,, \tag{4.3}$$

where G_{ij} is defined as

$$G_{ij} \equiv \langle T \psi_i(\tau) \psi_j(0) \rangle = \theta(\tau) \langle \psi_i(\tau) \psi_j(0) \rangle - \theta(-\tau) \langle \psi_i(0) \psi_j(\tau) \rangle \,. \tag{4.4}$$

In the free theory limit $J = 0$, we have

$$G^{\text{free}}_{ij}(\tau) = \frac{1}{2} \delta_{ij} \text{sgn}\tau \,, \; G^{\text{free}}_{ij}(\omega) = \int d\tau e^{i\omega\tau} G^{\text{free}}_{ij}(\tau) = -\frac{1}{i\omega} \delta_{ij} \,, \tag{4.5}$$

where we also wrote the Fourier transformed version of G^{free}_{ij} . Now let us compute the two-point function using this free propagator, The corrections come from the taking into account of the interaction of the Hamiltonian (represented in real lines) and the averaging with respect to the disorder (represented in dashed lines) as Figure 5.

Each diagram is called a melon diagram. Notice that each link corresponding to the disorder average scales like J^2.

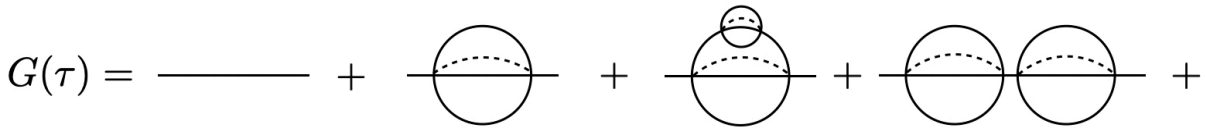

Figure 5: Diagrams which compute the corrections to the two-point function. The two-point function in the free limit is depicted with the solid line. Dashed lines represent the averaging over disorder. We write this in the case of $q = 4$,

We can summarize these simple diagrams in the following self-consistency equations

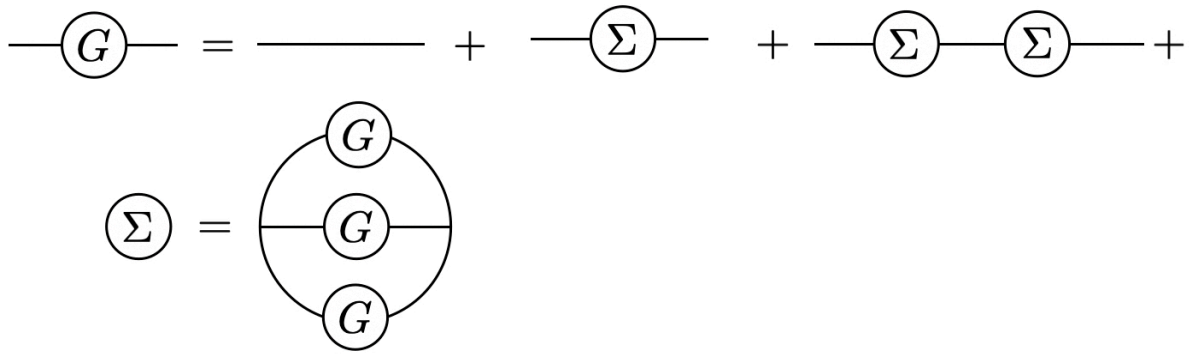

Figure 6: Diagrams which represent the self-consistency condition between the full two-point function G and the one particle irreducible contributions Σ in the $q = 4$ case.

where $\Sigma(\tau, \tau')$ is a self-energy, which includes all the one particle irreducible contributions to the propagator. We can write these self-consistency equations as

$$\frac{1}{G} = \partial_\tau - \Sigma\,,\ \Sigma(\tau,\tau') = J^2 G(\tau,\tau')^{q-1}\,. \tag{4.6}$$

We can derive the above equations as the classical equations of motion derived from the saddle point of path-integral with respect to an action of the bi-local fields G and Σ in the large N limit. The original Euclidean path-integral of the SYK model can be

written as

$$Z_{\rm SYK} = \int dJ_{ijkl} \exp\left[-\frac{N^3}{2\cdot 3! J^2}\sum_{ijkl} J_{ijkl}^2\right] \int \mathcal{D}\psi_i \exp\left[-\int d\tau \left(\frac{1}{2}\sum_i \psi_i \partial_\tau \psi_i + \sum_{ijkl} J_{ijkl}\psi_i\psi_j\psi_k\psi_l\right)\right]. \tag{4.7}$$

The Gaussian integration over the random coupling J_{ijkl} can be easily performed and as a result, we have the path-integral of the following form

$$\begin{aligned} Z_{\rm SYK} &= \int \mathcal{D}\psi_i \exp\left[-\frac{1}{2}\int d\tau \sum_i \psi_i\partial_\tau\psi_i + \sum_{ijkl}\frac{3J^2}{N^3}\int\int d\tau d\tau' (\psi_i\psi_j\psi_k\psi_l)(\tau)(\psi_i\psi_j\psi_k\psi_l)(\tau')\right] \\ &= \int \mathcal{D}\psi_i \exp\left[-\frac{1}{2}\int d\tau \sum_i \psi_i\partial_\tau\psi_i + \sum_{ijkl}\frac{3J^2}{4!N^3}\int\int d\tau d\tau' (\sum_i \psi_i(\tau)\psi_i(\tau'))^4\right], \end{aligned} \tag{4.8}$$

where in the second line we used the property $\psi_i^2(\tau) = 0$.

We insert the following expression of "1"

$$\begin{aligned} 1 &= \int \mathcal{D}G\,\delta(NG(\tau,\tau') - \sum_i \psi_i(\tau)\psi_i(\tau')) \\ &= \int \mathcal{D}G\mathcal{D}\Sigma \exp\left[-\frac{N}{2}\int\int d\tau d\tau' \Sigma\left(G - \frac{1}{N}\sum_i \psi_i\psi_i\right)\right] \end{aligned} \tag{4.9}$$

in the path-integral. Here we regard G and Σ as dynamical fields to be path-integrated. Then we obtain the following expression for the partition function

$$Z_{\rm SYK} = \int \mathcal{D}\psi_i \mathcal{D}G\mathcal{D}\Sigma \exp\left[-\frac{1}{2}\int d\tau \sum_i \psi_i\partial_\tau\psi_i + \int\int d\tau d\tau' \left(\frac{J^2N}{8}G^4 - \frac{1}{2}N\Sigma\left(G - \frac{1}{N}\sum_i \psi_i\psi_i\right)\right)\right].$$

Performing the fermion path-integral leads to the determinant $(\det(\partial_\tau - \Sigma))^{N/2}$, then we finally obtain the partition function expressed by the path-integral over the bi-local fields G and Σ as

$$Z_{\rm SYK} = \int \mathcal{D}\psi_i \mathcal{D}G\mathcal{D}\Sigma e^{-NI[G,\Sigma]} \tag{4.10}$$

with the action of G and Σ of the following form

$$I[G,\Sigma] = -\frac{1}{2}\log\det(\partial_\tau - \Sigma) + \frac{1}{2}\int\int d\tau d\tau' (\Sigma G - \frac{1}{4}J^2G^4). \tag{4.11}$$

Here N plays a role of $\hbar^{-1}$ and the in the large N limit, the saddle point approximation is valid. As a result, we obtain the set of equations (4.6) as the equations of motion for the action (4.11).

First we compute the two-point functions by solving the equations (4.6) in the IR limit. Since J has the dimension of the energy, in the IR limit we can discard the low frequencies compared to J. This corresponding to discarding ∂_τ in the equations (4.6) in the coordinate space. Then we have a set of equations

$$\int d\tau'' G(\tau,\tau'')\Sigma(\tau'',\tau') = -\delta(\tau-\tau')\,,\ \Sigma(\tau,\tau') = J^2 G(\tau,\tau')^{q-1}\,. \tag{4.12}$$

in the IR limit. Notice that these equations are invariant under the reparametrizations $\tau \to f(\tau)$ provided the fields transforms as

$$G(\tau,\tau') \to [f'(\tau)f'(\tau')]^{\Delta} G(f(\tau),f(\tau'))\,,\ \Sigma(\tau,\tau') \to [f'(\tau)f'(\tau')]^{\Delta(q-1)}\Sigma(\tau,\tau') \tag{4.13}$$

with $\Delta = 1/q$. Therefore these two fields both transforms like the conformal two-point functions with $\Delta = 1/q$. Then we obtain the solution to the equations (4.12) of the same form as the two-point function in the conformal theory in a line as

$$G_c(\tau) = \frac{b}{|\tau|^{2\Delta}}\mathrm{sgn}(\tau)\,, \tag{4.14}$$

where the constant b can be calculated as

$$b^q = \frac{1}{\pi J^2}\left(\frac{1}{2}-\frac{1}{q}\right)\tan\frac{\pi}{q}\,. \tag{4.15}$$

Notice that this reparametrization (two-dimensional conformal) symmetry, which maps solutions to solutions is emergent symmetry in the IR obtained by discarding the derivative term ∂_τ in the equations (4.6). The symmetry is explicitly broken by the existence of the derivative term. This is the expression in the Euclidean Poincaré coordinate, and if we perform a reparametrization as $f(\tau) = \tan\frac{\pi\tau}{\beta}$, we can obtain the expression in the Euclidean Rindler coordinate

$$G_c(\tau) = b\left[\frac{\pi}{\beta\sin\frac{\pi\tau}{\beta}}\right]^{2\Delta}\mathrm{sgn}(\tau)\,. \tag{4.16}$$

where the solution looks thermal, i.e, it is periodic under $\tau \to \tau+\beta$. The reparametrizations of the solution above are also other solutions. The $SL(2,\mathbb{R})$ transformation

$$\tau \to \frac{a\tau+b}{c\tau+d}\,,\ ad-bc=1 \tag{4.17}$$

keep the form of the solution (4.14) invariant. Therefore, the reparametrization symmetry is also spontaneously broken to $SL(2,\mathbb{R})$. This is similar to the situation where in two-dimensional conformal field theory which has the full Virasoro symmetry, since the vacuum breaks a part of the symmetry and it is only invariant under its $SL(2,\mathbb{R})$ subgroup, thus two-point functions on the vacuum is also invariant under the $SL(2,\mathbb{R})$ symmetry. If we are away from the strict IR point, we will see the violation of the reparametrization symmetry suppressed by $1/\beta J$.

Schwarzian Action

The SYK model has the emergent reparametrization symmetry in the IR limit, which also corresponds to the strong coupling limit $\beta J \to \infty$. Therefore there are directions of the path integration where the pre-factor of the action is lowered by $1/\beta J$ and which describes the dynamics of the reparametrization modes $f(\tau)$. We will find the action which governs such dynamics. Since in the action (4.11) we have a reparametrization invariant part

$$\frac{1}{2}\int\int d\tau d\tau'(\Sigma G - \frac{1}{4}J^2G^4) \subset I[G,\Sigma]\,, \tag{4.18}$$

thus we can consider the effective action which takes in the effect of the reparametrization of the following form

$$I_{\text{eff}}[f] = -\frac{1}{2}\log\det\left(\partial_\tau - \Sigma_*^f\right) + \frac{1}{2}\log\det(\partial_\tau - \Sigma_*) \tag{4.19}$$

where Σ_* denotes the true saddle point and Σ_*^f is its reparametrization.

Now we formally expand the effective action with respect to ∂_τ, then we obtain

$$\begin{aligned} I_{\text{eff}}[f] &\approx \frac{1}{2}(\text{Tr}[\partial_\tau(\Sigma_*^f)^{-1}]) - \text{Tr}[\partial_\tau(\Sigma_*)^{-1}]) \\ &= \frac{1}{2}(\text{Tr}[\partial_\tau G_*^f]) - \text{Tr}[\partial_\tau G]) \\ &= -\frac{1}{2}\int d\tau d\tau' \partial_{\tau'}\delta(\tau-\tau')(\partial_\tau G_*^f(\tau,\tau') - \partial_\tau G(\tau,\tau')) \end{aligned} \tag{4.20}$$

where in the second line we used $(\Sigma_*^f)^{-1} = G_*^f + \mathcal{O}(\partial_\tau)$ and $(\Sigma_*)^{-1} = G_* + \mathcal{O}(\partial_\tau)$. More precisely, in order to avoid divergences, we have to replace the delta function $\delta(x)$ by a smooth function $\delta_\epsilon(x)$ which approaches to the delta function in the limit $\epsilon \to 0$ [36]. At the same time, we have to smoothen all the derivatives of the theory as we did above and use the solution $G_{*\epsilon}$ of such an alternative theory instead of the original one G_*,

but here we neglect such subtleties. Since we have

$$G^f_*(\tau,\tau') - G_*(\tau,\tau') = \left[\frac{f'(\tau)f'(\tau')}{(f(\tau)-f(\tau'))^2}\right]^{1/q}\mathrm{sgn}(\tau-\tau') - \frac{1}{|\tau-\tau'|^{2/q}}\mathrm{sgn}(\tau-\tau')$$
$$\approx |\tau-\tau'|^{2-2/q}\left[\frac{1}{12q}\mathrm{Sch}(f,\tau)+\mathcal{O}(\tau-\tau')\right] \tag{4.21}$$

with the Schwarzian derivative $\mathrm{Sch}(f,\tau)$ defined by

$$\mathrm{Sch}(f,\tau) = -\frac{1}{2}\frac{f''^2}{f'^2} + \left(\frac{f''}{f'}\right)', \tag{4.22}$$

we finally obtain the so-called Schwarzian action

$$I_{\text{eff}}[f] \propto \frac{1}{J}\int d\tau \mathrm{Sch}(f,\tau)\,. \tag{4.23}$$

The $1/J$ suppression means that these modes are easily excited in the region $1 \ll \beta J \ll N$. Therefore the pattern of the conformal symmetry breaking of the SYK model near the IR limit is governed by the Schwarzian action. We will see in the next subsection that the Schwarzian action can be also obtained from the dimensionally reduced theories we derived in section 3 in the bulk side Thus SYK model shares the same mechanism of the conformal symmetry breaking as the AdS_2 geometry. The interpretation of the conformal symmetry breaking in the AdS side will be explained in subsection 4.2.

Thermodynamics

Finally we will make a brief comment on the thermodynamics of the SYK model to compare with the AdS_2 black holes. At the large N limit, the free energy F is calculated by the saddle point approximation

$$\beta F/N = -\log Z_{\text{SYK}}/N \approx -\frac{1}{2}\log\det(\partial_\tau - \Sigma_*) + \frac{1}{2}\int\int d\tau d\tau'(\Sigma_* G_* - \frac{1}{q}J^2 G^q)\,,$$

where we generalized the action (4.11) to an arbitrary even integer q. We have an exact solution in the large q limit [45]

$$G = \frac{1}{2}\mathrm{sgn}(\tau)e^{\frac{g(\tau)}{q-1}} \text{ with } e^{g(\tau)/2} = \frac{\cos\frac{\pi v}{2}}{\cos[\frac{\pi v}{2}(1-\frac{2\tau}{\beta})]}\,,\ \beta\mathcal{J} = \frac{\pi v}{\cos\frac{\pi v}{2}}\,, \tag{4.24}$$

where $\mathcal{J} = \sqrt{q}J/2^{\frac{q-1}{2}}$. Using this solution, we can evaluate the free energy as [36, 45]

$$-\beta F = -\beta E + S \tag{4.25}$$

where the energy E and the entropy S is given by

$$E = -\frac{N\mathcal{J}}{q^2}\sin\frac{\pi v}{2}\,,\ S = N\left(\frac{1}{2}\log 2 - \frac{\pi^2 v^2}{4q^2}\right)\,. \tag{4.26}$$

Since we can expand v in $1/\beta\mathcal{J}$ as

$$v = 1 - \frac{2}{\beta\mathcal{J}} + \frac{4}{(\beta\mathcal{J})^2} - \frac{(24+\pi^2)}{3(\beta\mathcal{J})^3} + \cdots, \tag{4.27}$$

thus the ground state energy and entropy, and the first order corrections of them are given by

$$E_0 = -\frac{N\mathcal{J}}{q^2}\,,\ \delta E = \frac{N\pi^2}{2q^2\mathcal{J}\beta^2}\,,\ S_0 = N\left(\frac{1}{2}\log 2 - \frac{\pi^2}{4q^2}\right)\,,\ \delta S = \frac{N\pi^2}{2q^2\mathcal{J}\beta} \tag{4.28}$$

The most interesting feature here is that we have ground state (zero temperature) entropy S_0 of the order N. The leading contribution $\frac{N}{2}\log 2$ can also be explained as follows. In the large q limit, theory essentially approaches a free theory $J = 0$ which is seen from the expansion of (4.24) in $1/q$: $G = \frac{1}{2}\mathrm{sgn}(\tau)(1 + g(\tau)/q + \cdots)$ and the corresponding quantity in the free limit (4.5). When $J = 0$, the Hamiltonian vanishes $H = 0$ and all the states in the Hilbert space whose dimension is $2^{N/2}$ is degenerate at the ground state, thus the ground state entropy becomes $\frac{N}{2}\log 2$. One might think that the ground state degeneracy is an unusual thing, but is necessary for the SYK model to describe the black hole microstates quantum mechanically. The ground state $\beta = \infty$ corresponds to the extremal black hole. Thus the ground state degeneracy explains how the SYK model can describe quantum black holes which have the microstates of the extremal black hole in the classical limit. It might be interesting to compare these results with the corresponding quantities in the bulk two-dimensional dilaton gravity theories which describe the black holes in the nearly AdS_2 spacetime.

$$\delta M = \frac{\phi_b \pi L_2^2}{2G_N\beta^2}\,,\ S_0 = \frac{\Phi_0}{4G_N}\,,\ \delta S = \frac{\phi_b\pi L_2^2}{2G_N\beta}\,. \tag{4.29}$$

Since we expect to have the relation $N \sim L_2^2/G_N$, we can see the interesting coincidence in the thermodynamic quantities between the SYK model and the gravitational theories except for the lack of the ground state energy in the bulk side, which we neglected because of divergences.

To summarize this subsection, the SYK model shares the same thermodynamic behavior with the bulk gravitational theories and as another important property, it has emergent reparametrization symmetry at the strict IR limit. As we saw, the reparametrization symmetry is spontaneously broken by the vacuum and also explicitly

broken away from the IR point by that the reparametrization modes acquires the action, so-called the Schwarzian action. The breaking patterns of the reparametrizations are governed by the action.

In the next subsection, we will see how the Schwarzian action appears the gravity side and how we can interpret the breaking of the reparametrization symmetry in the gravitational picture.

4.2 Bulk Dynamics of the Schwarzian Action

In order to find the relation between the dimensionally reduced theories and the Schwarzian action which describes IR dynamics of the SYK model, let us remind ourselves the following action of the JT model

$$\begin{aligned} I_{\rm JT} = &\frac{\Phi_0}{16\pi G_N}\left[\int_{\mathcal{M}} d^2x\sqrt{-g}R + 2\int_{\partial\mathcal{M}} K\right] \\ &+ \frac{1}{16\pi G_N}\left[\int_{\mathcal{M}} d^2x\sqrt{-g}\Phi\left(R-2\Lambda_2\right) + 2\int_{\partial\mathcal{M}}\Phi(K-1)\right], \end{aligned} \tag{4.30}$$

where we subtracted "-1" from the extrinsic curvature by adding the boundary counter term (3.162). The linearized theory derived from the dimensional reduction from the electric solutions in the grand canonical ensemble is given by the following action

$$\begin{aligned} I_{\text{JT-Max}} = I_{\rm JT} &- \frac{1}{16\pi G_N}\int_{\mathcal{M}} d^2x\sqrt{-g}(\Phi_0-\Phi)\left(\Lambda_2 - \frac{1}{r_h^2}\right) \\ &- \frac{1}{4G_N}\int_{\mathcal{M}} d^2x\sqrt{-g}\left[(\Phi_0+\Phi)F_0^2 + 2\Phi_0 F_0^{\mu\nu}\tilde{F}_{\mu\nu}\right]. \end{aligned} \tag{4.31}$$

First let us consider the topological part of the JT model

$$I_{\rm JT}^{\rm top} = \frac{\Phi_0}{16\pi G_N}\left[\int_{\mathcal{M}} d^2x\sqrt{-g}R + 2\int_{\partial\mathcal{M}} K\right]. \tag{4.32}$$

It gives the same number as long as we consider the same topology of the manifold. We have a large amount of symmetry generated by zero modes of this action. In order to see that more explicitly, we choose the Poincaré coordinate

$$ds^2 = L_2^2\frac{-d\tilde{t}^2 + dz^2}{z^2}. \tag{4.33}$$

We write the proper time on the boundary $z=\epsilon$ as u and parametrize the boundary trajectory by u

$$(\tilde{t}(u), z(u)). \tag{4.34}$$

As we did in subsection 3.6 in the Rindler coordinate, we choose the Dirichlet boundary condition which fixes the boundary value of the metric and the dynamical dilation $\delta\Phi = \delta\gamma_{\tilde{t}\tilde{t}} = 0$. We write the values of them on the boundary $\partial\mathcal{M} : z=\epsilon$ as

$$\begin{aligned} \gamma_{uu}|_{\partial\mathcal{M}} &= -\frac{L_2^2}{\epsilon^2} \\ \Phi|_{\partial\mathcal{M}} &= \frac{\phi_b}{\epsilon}. \end{aligned} \tag{4.35}$$

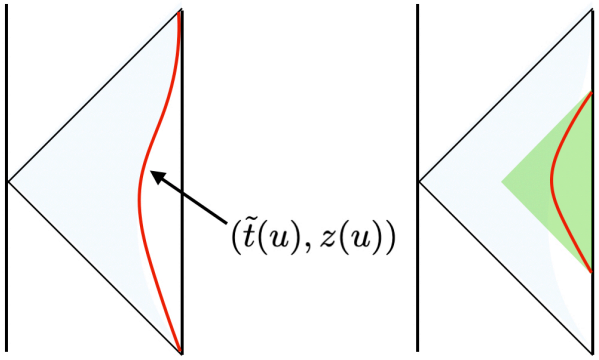

Figure 7: The gravitational dynamics in the two-dimensional dilaton gravity theories reduces to the dynamics of the boundary trajectory which is governed by the Schwarzian action (left picture). The solution of the Schwarzian action nicely fits a finite radial cut-off $r = r_c$ in the Rindler coordinate (right picture). We can obtain the thermal solution of AdS_2 purely from the boundary dynamics.

with some positive constant ϕ_b and we take ϵ to be very small. The Dirichlet boundary condition (4.35) relates time coordinate $\tilde{t}$ and radial coordinate z on the boundary as

$$z \approx \epsilon \tilde{t}' + \mathcal{O}(\epsilon^3)\,, \tag{4.36}$$

thus the boundary position is determined a single function $\tilde{t}(u)$. We can regard this function as the dynamical mode of the gravitational system (4.30) and (4.31). The topological part of the JT model is invariant under the choice of $\tilde{t}(u)$. It can be regarded as a symmetry under the reparametrizations $\tilde{t}(u) \to f(u)$. While some of the reparametrizations fix the boundary curve, most of them map a given boundary trajectory to a different one. Since the isometry of the AdS_2 is $SL(2,\mathbb{R})$, thus the $SL(2,\mathbb{R})$ subgroup

$$t(u) \to \frac{at(u)+b}{ct(u)+d}\,,\ ad-bc=1 \tag{4.37}$$

of all reparametrization fixes the shape of the boundary curve.

The dynamical part of the JT action

$$I_{\rm JT}^{\rm dyn} = \frac{1}{16\pi G_N}\left[\int_{\mathcal{M}} d^2x\sqrt{-g}\Phi\,(R-2\Lambda_2) + 2\int_{\partial\mathcal{M}}\Phi(K-1)\right] \tag{4.38}$$

plays a role of breaking the reparametrization symmetry down to $SL(2,\mathbb{R})$. Notice that in both actions the dynamical dilaton Φ appears linearly, thus it is essentially Lagrange

multiplier. Performing the path-integral over Φ gives a constraint on the metric

$$R = 2\Lambda_2\,, \tag{4.39}$$

for the JT model. Thus the metric is forced to be AdS_2. For the model $I^E_{\text{JT-Max}}$, we consider the situation where the gauge coupling g of the Maxwell field is very small while keeping the Newton constant G_N to be an arbitrary value for simplicity. In this case, we can use the classical solution for F_0 and performing the path-integral over Φ also gives a constraint on the metric (4.39). Thus now we focus on the AdS geometry and ignore the degrees of freedom of the Maxwell field.

Therefore the dynamical gravitational part of each action reduces to the Gibbons-Hawking-York boundary term

$$I^{\text{dyn}}_{\text{GHY}} = \frac{1}{8\pi G_N}\int_{\partial\mathcal{M}} \Phi(K-1)\,. \tag{4.40}$$

Using the boundary condition (4.35) and the proper time u, one can express the boundary term as

$$I^{\text{dyn}}_{\text{GHY}} = \frac{\phi_b L_2}{8\pi G_N}\int_{\partial\mathcal{M}} \frac{du}{\epsilon^2}(K-1)\,. \tag{4.41}$$

The most important observation here is that in the Poincaré coordinate, one can evaluate the extrinsic curvature and express it in terms of the Schwarzian derivative which appears in the SYK model as well [40]!

$$\begin{aligned} K &= \frac{\tilde{t}'(\tilde{t}'^2 - z'^2 - z'z'') + zz'\tilde{t}''}{(\tilde{t}'^2 - z'^2)^{3/2}} \\ &= 1 - \epsilon^2 \text{Sch}(\tilde{t}, u) + \mathcal{O}(\epsilon^4) \end{aligned} \tag{4.42}$$

Here $\text{Sch}(\tilde{t}, u)$ is the Schwarzian derivative defined by

$$\text{Sch}(\tilde{t}, u) = -\frac{1}{2}\frac{\tilde{t}''^2}{\tilde{t}'^2} + \left(\frac{\tilde{t}''}{\tilde{t}'}\right)'\,. \tag{4.43}$$

Thus the JT action also reduces to the Schwarzian action

$$I^{\text{dyn}}_{\text{GHY}} \propto -\frac{1}{8\pi G_N}\int_{\partial\mathcal{M}} du\,\text{Sch}(\tilde{t}, u). \tag{4.44}$$

Notice that the Schwarzian action is invariant under the $SL(2,\mathbb{R})$ transformations

$$\text{Sch}(\tilde{t}, u) \to \text{Sch}\left(\frac{at(u)+b}{ct(u)+d}, u\right)\,,\ ad - bc = 1 \tag{4.45}$$

then we can see that the full reparametrization symmetry breaks down to the subgroup $SL(2,\mathbb{R})$ and the pattern of conformal symmetry breaking is governed by the Schwarzian action.

Now we try to find the boundary curve which is the solution of the Schwarzian action. The equation of motion becomes

$$\frac{\left[\mathrm{Sch}(\tilde{t},u)\right]'}{t'}=0\,, \tag{4.46}$$

then we should find the solution $\tilde{t}'\neq 0$ with a constant Schwarzian. To find a solution, we move from the Poincaré coordinate to the Rindler coordinate via the map

$$\tilde{t}=\tanh\frac{\pi}{\beta}t\,, \tag{4.47}$$

where $1/\beta=\sqrt{\mu}/2\pi L_2^2$. Schwarzian action can be written in terms of the Rindler time $t(u)$ as

$$\begin{aligned} I_{\mathrm{GHY}}^{\mathrm{dyn}} &\propto -\frac{1}{8\pi G_N}\int_{\partial\mathcal{M}} du\mathrm{Sch}(\tilde{t},u) \\ &= -\frac{1}{8\pi G_N}\int_{\partial\mathcal{M}} du\left[\mathrm{Sch}(t,u)+\frac{t'^2}{2}\right]\,. \end{aligned} \tag{4.48}$$

We see that when $t'=0$, we have $\mathrm{Sch}(\tilde{t},u)=\mathrm{Sch}(t,u)$, then the Schwarzian is constant and we have a solution. The solution is expressed

$$t=u \tag{4.49}$$

then for this solution the boundary sits along the flow of the Rindler time, i.e, the constant $r=r_c$ slice. Since the Euclidean Rindler time is periodic with period β, this solution describes the thermal (black hole) solution which we discussed in subsection 3.6.

We can summarize arguments in this section as follows. First we found that the divergent behavior of the dilaton forces us to move the AdS boundary into the bulk and as a result, the full reparametrization symmetry is broken. In the boundary theory perspective, it corresponds to the situation where we move a little bit away from the conformal fixed point by introducing the source term which corresponds to the dilaton in the bulk, and which is the case for the SYK model as we saw. In the bulk side, the gravitational dynamics reduces to the dynamics of the boundary trajectory in the fixed AdS geometry. This is not surprising since dilaton gravity theories in two dimensions have no propagating degrees of freedom. Both in the bulk and the boundary

side, the symmetry is broken to $SL(2,\mathbb{R})$ and the patterns of the symmetry breaking are governed by the Schwarzian action. In the bulk side, different breaking patterns correspond to the different boundary trajectories. In this way, we found a complete match in the descriptions between the bulk dilaton gravity theory and the SYK model.

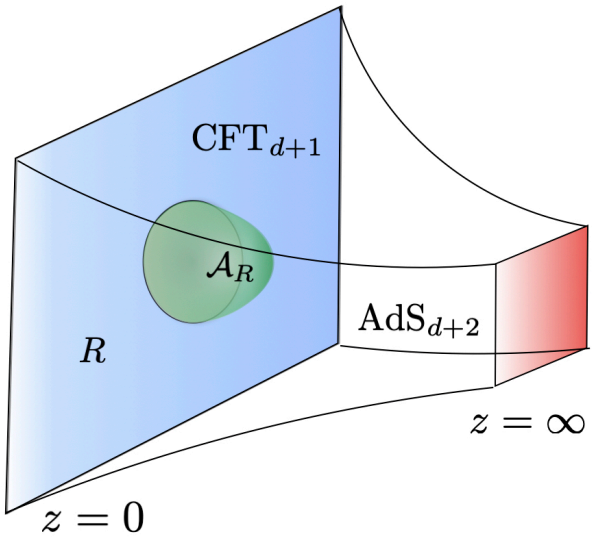

Figure 8: Ryu-Takayanagi surface in the Poincaré coordinate in the AdS which calculates the entanglement entropy in the CFT.

5 Holographic Complexity of NAdS$_2$

In the last few years, a deep connection between spacetime geometry and quantum information theoretic properties of the dual field theory has been found in the context of the AdS/ CFT correspondence. The most famous example is the so-called Ryu-Takayanagi formula [27] for the entanglement entropy which relates the spacetime connectivity to the entanglement in the CFT by the following equality

$$S_E(R) = \min_{\partial\mathcal{A}=\partial R} \frac{\mathcal{A}_R}{4G_N} \,. \tag{5.1}$$

Here $S_E(R)$ in the left hand side represents the entanglement entropy for the region R in the CFT$_d$ and $\mathcal{A}_R$ in the right hand side is the area of the co-dimension two spacelike surface in the $d+1$-dimensional asymptotically AdS spacetime which is anchored on the boundary of the region R. It is known that the entanglement entropy in the holographic CFT can capture many interesting semi-classical gravitational properties.

It is natural to ask whether the entanglement in the CFT can explain all the properties of the spacetime geometry in AdS. Let us consider the eternal black hole which is described by the thermofield double state on the CFT

$$|\mathrm{TFD}\rangle = \frac{1}{\sqrt{Z}} \sum_E e^{-\beta E/2} |E\rangle_L |E\rangle_R \,. \tag{5.2}$$

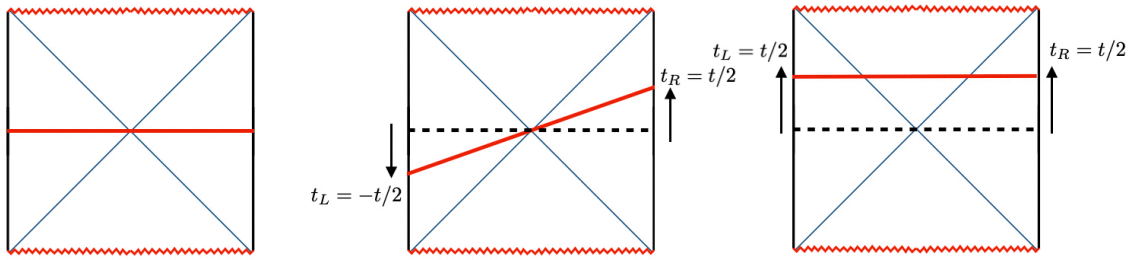

Figure 9: Left:The bulk picture corresponding to the thermofield double state in the CFT. It is dual to the eternal black hole geometry in the AdS. We can consider two ways of the time evolution generated by $H^{\rm tot}$ or $\tilde{H}^{\rm tot}$. Each evolution corresponds to the middle or the right picture in the bulk side. As seen from the picture, the $H^{\rm tot}$ is the symmetry of the state while $\tilde{H}^{\rm tot}$ is not.

Here $|E\rangle_{L,R}$ are energy eigenstates in the left/right CFT and β is the inverse temperature and Z is the partition function of the system. A seen above, the thermofield double state is expressed as an entangled state between the two CFTs. In the bulk, it is dual to a wormhole spacetime with two asymptotically AdS regions connected by the Einstein-Rosen bridge. The entanglement of the CFT state (5.2) is represented as spacetime connectivity in the AdS side. This state has a time translation symmetry which is generated by the sum of the Hamiltonian in the left and the right CFTs $H^{\rm tot} = H_L - H_R$

$$(H_L - H_R)|\mathrm{TFD}\rangle = 0. \tag{5.3}$$

In the bulk picture: Figure 9, this generator moves time "backward" on the left and forwards on the right. Therefore the thermofield state is an "eternal" or static state with respect to the total Hamiltonian $H^{\rm tot}$. On the other hand, we can also think the time evolution with respect to the Hamiltonian $\tilde{H}^{\rm tot} = H_L + H_R$. It moves time forwards both on the left and right as the right picture in Figure 9. Under this generator, the thermofield double state is no longer invariant and time evolved state is expressed as

$$|\mathrm{TFD}(t_L, t_R)\rangle = \frac{1}{\sqrt{Z}} \sum_E e^{-\beta E/2} e^{-iE(t_L+t_R)} |E\rangle_L |E\rangle_R \,. \tag{5.4}$$

If the system evolves in time, it reaches the thermal equilibrium after some time. Thermalization time is estimated by a polynomial of the number of the degrees of the system. After the system is thermalized, many physical quantities, including the entanglement entropy, saturates at their equilibrium values. In the bulk side, the saturation of the

entanglement entropy can be explained as follows [105]. Let us consider taking region R to be a sum of finite strips with width L on left and right sides and consider the minimal surface which extends from ∂R to the bulk which gives the entanglement entropy via Ryu-Takayanagi formula. At early times the minimal surface extends to across the black hole interior from one asymptotic region to the other, then it captures the time evolution of the size of the black hole interior. After t becomes compatible with the size of the region R, the minimal surface consists of two disconnected pieces and each piece stays on each exterior region. Thus the entanglement entropy stops to probe the evolution of the size of the black hole interior and saturates at some value. Even after the entanglement entropy stops growing, the black hole interior is expected to continue to grow forever at least classically as seen from the Figure 9. Thus it is natural to ask whether there is a CFT quantity which can probe the time evolution of the size of the black hole interior even after the thermalization.

Very recently, Susskind proposed that the eternal growth of the black hole interior reflects the growth of the computational complexity of the quantum state in the CFT rather than entanglement of the state [28, 29]. Computational Complexity is a notion in the quantum information theory and it measures how difficult it is to transform a simple reference state $|\Psi_0\rangle$ to some other state $|\Psi\rangle$. The complexity of the state $|\Psi\rangle$ is roughly defined as the number of the elementary operations which one need to apply to the reference state $|\Psi_0\rangle$ to get the state $|\Psi\rangle$. Though a satisfactory definition of the complexity for generic CFTs is not known yet, several interesting approaches have been considered [75–88]. As a general property of the complexity, it is expected to continue growing linearly in time for a very long time even after the thermalization. Therefore it is expected to be holographic dual to the eternal growth of the black hole interior. Conversely, for this reason, the size of the black hole interior in this context is called "holographic complexity" in the literature.

Susskind and Brown et al. gave two different proposals for the holographic complexity. One is called "Complexity=Volume" [28, 52](or CV in short) and the size of the black hole interior at a time $t = t_0$ is measured by the maximal volume of the spacelike slice anchored at the boundary at a time t_0

$$\mathcal{C}_{\mathcal{V}} \equiv \frac{1}{G_N L} \max_{\Sigma=\partial\mathcal{B}} \mathcal{V}(\mathcal{B}) \tag{5.5}$$

where L is an arbitrary length scale which we often take it to be the AdS scale and the $\mathcal{V}$ is the volume of the slice Σ connecting two boundaries of the eternal black hole which is anchored at $t = t_0$ slice $\mathcal{B}$ on the boundary. Since we expect that the complexity is proportional to the number of the degrees of freedom in the system, thus it is proportional to the Newton's constant G_N in the bulk side. Moreover, it

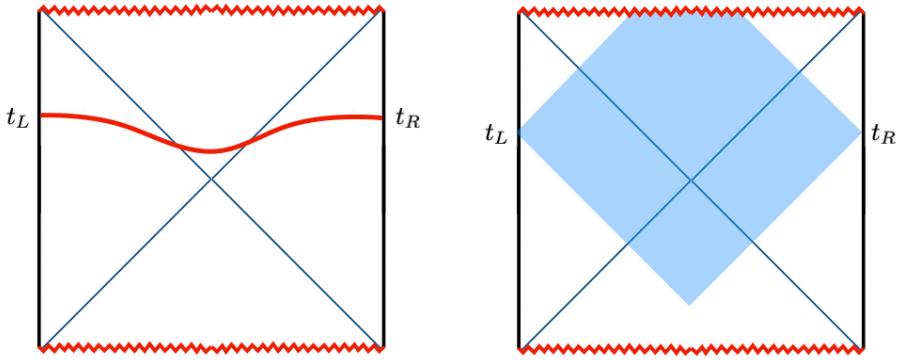

Figure 10: Complexity=Volume proposal (left) and the Complexity= Action proposal (right). The red line in the left panel represents the maximal volume slice and the blue region in the right panel represents the WDW patch.

should be a dimensionless quantity thus we should divide it by some length L. The Complexity=Volume proposal has at least two shortcomings. One is that we have to introduce an arbitrary length scale L in its definition. Another is that we don't have any particular reason why we should choose the maximal volume slice out of other different spacelike slices.

The other proposal is "Complexity=Action" proposal [53, 54](or CA in short) that the holographic complexity is given by the gravitational action $I_{\rm WDW}$ evaluated on a region of the spacetime called "Wheeler-DeWitt patch" (WDW patch), which corresponds to the causal development of any of the bulk surfaces $\mathcal{B}$, it is written explicitly as[8]

$$\mathcal{C}_{\mathcal{A}} \equiv I_{\rm WDW}/\hbar\,. \tag{5.6}$$

In this proposal, we don't need to introduce a length scale L and we don't have to choose a special spacelike slice to compute the complexity either. Since we don't have an appropriate definition of the complexity in CFT side, it is not known yet which proposal correctly leads to the behavior of the complexity of CFT or whether each proposal leads to a different definition or interpretation of the complexity. However there have been several checks which imply both of these definitions can be good candidates [28, 29, 53–73] .

Compared with simple qubit systems where the suitable definition of complexity is already known, the generic quantum field theories is so complicated that we still cannot

[8]In the literature, the Complexity=Action is defined as $\frac{I_{\rm WDW}}{\pi\hbar}$ and it differs from our definition by a factor π.

find a good way to define it. Recently it was found that the so-called SYK model can capture the gravitational physics in AdS_2 holographically, and certain aspects of the SYK models such as IR physics, $1/N$ corrections, and its generalizations and modifications e.t.c. have been extensively studied in the literature. The SYK model is a simple quantum mechanical model of Majorana fermions, thus it can be considered as the most appropriate model to start with when we consider the definition of the complexity in the holographic context. We expect that to know about the complexity of the SYK model becomes a starting point to look for a suitable definition of complexity in higher dimensional CFTs and it will also shed light on the fundamental role of the complexity in AdS/CFT.

In previous sections, we studied the dimensional reduction of the four-dimensional electrically and magnetically charged black hole solutions and we derived two different linearized two-dimensional actions: One for the magnetic solutions in the canonical ensemble

$$I_{\rm JT}^{\rm bulk} = \frac{\Phi_0}{16\pi G_N}\int_{\mathcal{M}} d^2x\sqrt{-g}R + \frac{1}{16\pi G_N}\int_{\mathcal{M}} d^2x\sqrt{-g}\Phi\left(R-2\Lambda_2\right)\,, \tag{5.7}$$

and the other for electric solutions in the grand canonical ensemble

$$\begin{aligned} I_{\rm JT\text{-}Max}^{\rm bulk} = I_{\rm JT}^{\rm bulk} &- \frac{1}{16\pi G_N}\int_{\mathcal{M}} d^2x\sqrt{-g}(\Phi_0-\Phi)\left(\Lambda_2-\frac{1}{r_h^2}\right) \\ &- \frac{1}{4G_N}\int_{\mathcal{M}} d^2x\sqrt{-g}\left[(\Phi_0+\Phi)F_0^2 + 2\Phi_0 F_0^{\mu\nu}\tilde{F}_{\mu\nu}\right]\,. \end{aligned} \tag{5.8}$$

We also found that both actions lead to the so-called Schwarzian action which describes the IR physics of the SYK model. In this sense, it can be thought that both theories are describing certain gravitational aspects of the SYK model holographically. Therefore it is very important to know about the behavior of the holographic complexity of these models in order to obtain information on the complexity of the SYK model. In this section, we will compute the holographic complexity of the models (5.7)(5.8) both in the CA and CV proposal.

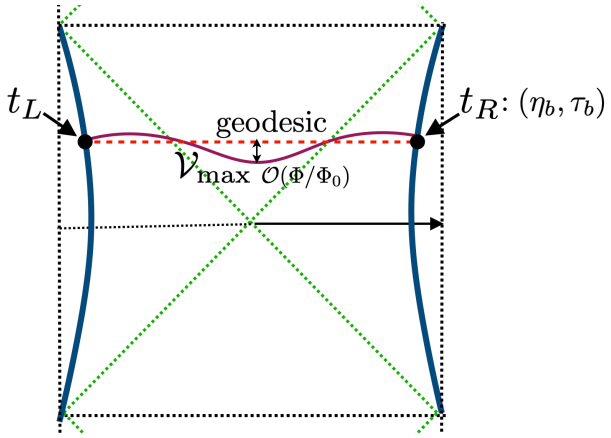

Figure 11: We compute the maximal volume which anchored at $t_R = t_L = t/2$ on the boundary. The boundary point (t_R, r_c) corresponds to (η_b, τ_b) in the global coordinate. The curve which gives maximal volume can be approximated to the geodesic up to the order $\mathcal{O}(\Phi/\Phi_0)$.

5.1 Complexity= Volume

In this section, we compute the holographic complexity of the JT model $I_{\rm JT}$ and the linearized theory $I_{\text{JT-Max}}$ derived from electric solution in the grand canonical ensemble in the CV proposal

$$\mathcal{C}_{\mathcal{V}} \equiv \frac{1}{G_N L} \max_{\Sigma=\partial\mathcal{B}} \mathcal{V}(\mathcal{B})\,, \tag{5.9}$$

i.e, using the volume of the maximal surface that goes through the wormhole. We found that both theories lead to the (nearly) AdS$_2$ solution

$$\begin{aligned} \Phi &= \phi_b (r - r_h) \\ ds^2 &= -\frac{(r-r_+)(r-r_-)}{L_2^2} dt^2 + \frac{L_2^2}{(r-r_+)(r-r_-)} dr^2\,, \end{aligned} \tag{5.10}$$

in the Reissner-Nordstrom like coordinate and

$$\begin{aligned} \Phi &= \phi_b \sqrt{\mu} \frac{\cos\tau}{\cos\eta} \\ ds^2 &= L_2^2 \frac{-d\tau^2 + d\eta^2}{\cos^2\eta} \end{aligned} \tag{5.11}$$

in the global coordinate. Therefore we should evaluate the maximal volume in the AdS$_2$ background. We consider the maximal volume which is anchored at the time on the

right boundary t_R and the left boundary t_L respectively. In this section, we focus on the symmetric case where we vary $t \equiv t_L + t_R$ while fixing $t_L = t_R$ for simplicity. Since the volume of the co-dimension one surface becomes the length of the one-dimensional curve, naively, one could just compute the volume of the maximal slice in this geometry

$$\mathcal{V} = \int d\lambda \sqrt{-h}\,, \tag{5.12}$$

where h is the induced metric on the curve of which we compute the length. Clearly, this is just given by the length of the geodesic in AdS$_2$. However, since we want our result to replicate one in the higher dimensional black hole, the most natural thing to do is to consider the two-dimensional quantity which corresponds to the volume in the higher dimensional spacetime. The volume in the four-dimensional spacetime can be expressed as

$$\mathcal{V} = \int d\lambda d^2\Omega_2 \sqrt{-h'} = 4\pi \int d\lambda \sqrt{-h}\Psi^2\,, \tag{5.13}$$

where h' is the induced metric on the three-dimensional surface of which we compute the volume and h is again the induced metric on the curve. Thus we want to find the curve that extremizes this integral and the compute the volume complexity via

$$\mathcal{C}_{\mathcal{V}} = \frac{1}{G_N L_2} \max_{\gamma} \int_{\gamma} d\lambda \sqrt{-h}(\Phi_0 + \Phi)\,. \tag{5.14}$$

To compute the volume in the AdS$_2$ geometry, it is convenient to use the global coordinate (3.6). We parametrize the curve in term of η as $(\eta, \tau(\eta))$, then the volume (5.13) can be expressed as

$$\int_{\gamma} d\lambda \sqrt{-h}(\Phi_0 + \Phi) = L_2 \int_{-\eta_c}^{\eta_c} \frac{d\eta}{\cos\eta} \sqrt{1 - \dot{\tau}^2}[\Phi_0 + \Phi(\eta, \tau(\eta))]\,, \tag{5.15}$$

where we write $\dot{\tau} \equiv \frac{d\tau}{d\eta}$.

In order to consider the variation of the integral (5.15) to look for the extremal curve, we define the following Lagrangian

$$\mathcal{L}(\eta, \tau, \dot{\tau}) = \frac{\sqrt{1 - \dot{\tau}^2}}{\cos\eta}[\Phi_0 + \Phi(\eta, \tau(\eta))] \tag{5.16}$$

This Lagrangian yields the following Euler-Lagrange equation

$$\dot{\tau} = -\dot{\tau}\left(\frac{\Phi}{\Phi_0} + \cot\eta \frac{d}{d\eta}\left(\frac{\Phi}{\Phi_0}\right)\right) + (\dot{\tau}^2 - 1)\cot\eta \frac{\partial}{\partial\tau}\left(\frac{\Phi}{\Phi_0}\right)\,. \tag{5.17}$$

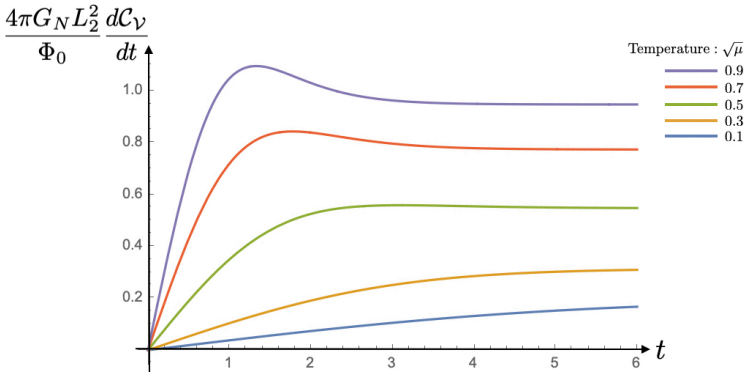

Figure 12: The growth rate of the volume complexity in the Jackiw-Teitelboim model. It shows the linear growth at late times as expected. The growth rate approaches a finite value which is proportional to the temperature of the system. Here, we set $\Phi_0 = \Phi_b = L_2 = 1$.

Therefore, we can see that the solution $\tau(\eta)$ should satisfy

$$\dot{\tau} = 0 \tag{5.18}$$

up to $\mathcal{O}(\Phi/\Phi_0)$, i.e, the solution is given by the geodesic at the leading order and the corrections come from the order Φ/Φ_0. Plugging this solution into (5.19), we have

$$\begin{aligned}\mathcal{C}_\mathcal{V} &= \frac{1}{G_N L_2}\max_\gamma \int_\gamma d\lambda\sqrt{-h}[\Phi_0 + \Phi(\eta,\tau(\eta))]\,. \\ &= \frac{1}{G_N}\int_{-\eta_c}^{\eta_c}\frac{d\eta}{\cos^2\eta}[\Phi_0 + \Phi(\eta,\tau_b)] + \mathcal{O}((\Phi/\Phi_0)^2)\,.\end{aligned} \tag{5.19}$$

This shows that volume $\mathcal{V}$ can be written as the integral over the geodesic

$$\max_\gamma \int_\gamma d\lambda\sqrt{-h}[\Phi_0+\Phi] = \int_{\text{geodesic}} d\lambda\sqrt{-h}[\Phi_0+\Phi] + \mathcal{O}((\Phi/\Phi_0)^2)\,, \tag{5.20}$$

then it coincides with our naive definition of the volume in two dimensions (5.12). Then one can easily compute the maximal volume anchored at a point (η_b, τ_b) on the boundary as

$$\mathcal{C}_\mathcal{V} = \frac{\Phi_0}{G_N}\log\left(\frac{1+\sin\eta_b}{1-\sin\eta_b}\right) + \frac{2\phi_b\sqrt{\mu}}{G_N}\cos\tau_b\tan\eta_b + \mathcal{O}(\mu)\,. \tag{5.21}$$

Using the relation between two coordinate systems (3.9) and (3.6), we can see that the first term grows linearly in t as $\Phi_0\sqrt{\mu}t/G_N L_2^2$ while the second term approaches

some finite value when $t \to \infty$. Thus at late times, the contribution from the extremal degrees of freedom are the most relevant for the complexification. The growth of the complexity approaches

$$\lim_{t\to\infty} \frac{d\mathcal{C}_{\mathcal{V}}}{dt} = 2S_0 T \tag{5.22}$$

as we take $t \to \infty$. This result reproduces the higher dimensional result. Since we neglect terms proportional to T^2 in our near-extremal approximation, thus the result above reproduces the expected rate of the linear growth of complexity $d\mathcal{C}/dt = 2ST$.

Proper Time on the Boundary

Above, we took the time derivative with respect to the coordinate time t, but more generally we can consider the situation where the boundary does not sit on the line $r = r_c$ in the coordinate (3.9), for example, see [40, 90, 106]. For the generic boundary trajectory, we can use the proper time as the time on the boundary. In our case, the only effect of doing this is a constant redshift factor

$$\frac{d\mathcal{C}_{\mathcal{A}}}{du} = \frac{1}{\sqrt{f(r_c)}} \frac{d\mathcal{C}_{\mathcal{A}}}{dt} , \tag{5.23}$$

where u is the proper time.

5.2 Complexity= Action

In this section, we study the growth of the holographic complexity for the JT model using the Complexity=Action conjecture

$$\mathcal{C}_{\mathcal{A}} \equiv \frac{I_{\text{WDW}}}{\hbar} . \tag{5.24}$$

Since the WDW patch is enclosed by the null boundaries, thus we especially need to be careful about the boundary terms. First let us remind ourselves the prescription of the CA proposal in four dimensions.

Dimensional Reduction Including Null Boundaries

In four dimensions, the most general form of the gravitational part of the action when the boundary of the region of interest contains the null segment can be written as

$$I_{\text{tot}} = I_{\text{bulk}} + I_{\text{surf}} + I_{\text{ct}} . \tag{5.25}$$

Here I_{bulk} is the bulk term which will be evaluated in the WDW patch. The next term I_{surf} contains various surface terms needed to make the variational principle well-defined

for the metric,

$$\begin{aligned} I_{\text{surf}} = &\frac{1}{8\pi G_N}\int_{\mathcal{B}} d^3x\sqrt{|h|}K + \frac{1}{8\pi G_N}\int_{\Sigma} d^2x\sqrt{\sigma}\eta \\ &+ \frac{1}{8\pi G_N}\int_{\mathcal{B}'} d\lambda\, d^2\theta\sqrt{\gamma}\kappa + \frac{1}{8\pi G_N}\int_{\Sigma'} d^2x\sqrt{\sigma}a\,, \end{aligned} \tag{5.26}$$

This contains the usual Gibbons-Hawking-York term [91, 92] for time-like and space-like boundary segments, the Hayward terms [107, 108] for intersections of these segments in the first line. We also have the GHY and joint terms introduced in [57] for null boundary segments in the left part of the second line[9]. The coordinates θ^A label the null hypersurface and λ is a parameter along each generator. γ is the cross-sectional metric of a bundle of the null generators. κ is a constant defined by the equation

$$k^\rho\nabla_\rho k^\mu = \kappa k^\mu\,,\ \ k^\mu \equiv \frac{dx^\mu}{d\lambda} \tag{5.27}$$

where k is the future directed tangent vector on the null hypersurface. It measures the failure of λ to be an affine parameter on the null generators. The last term in (5.64) is the joint terms whose contributions come from the intersections of the null boundaries. σ is the determinant of the metric induced at the intersection and a is defined as

$$a = \epsilon\log|k_i\cdot k_j|\,, \tag{5.28}$$

where k_i, k_j are the future directed tangent vectors associated with the hypersurfaces i and j respectively. we take $\epsilon = 1$ for the future and past corners and $\epsilon = -1$ for the left and the right corners. We also introduce the boundary counterterm

$$I_{\text{ct}} = \frac{1}{8\pi G_N}\int_{\mathcal{B}'} d\lambda\, d^2\theta\sqrt{\gamma}\,\Theta\,\log\left(\ell_{\text{ct}}\Theta\right)\,, \tag{5.29}$$

which is not needed for the variational principle, but it was introduced in [57] to ensure reparametrization invariance on the null boundaries. Here ℓ_{ct} is an arbitrary constant length scale and Θ is the expansion of the null boundary generators, which measures the rate of change of the cross-sectional area $\sqrt{\gamma}d^2\theta$ of a bundle of the null generators.

$$\Theta = \partial_\lambda\log\sqrt{\gamma}\,. \tag{5.30}$$

In order to consider the counterparts of them in two dimensions, we will consider the dimensional reduction of these terms. Generally, the bulk term reduces to

$$\begin{aligned} I^{\text{bulk}} = &\frac{1}{4G_N}\int_{\mathcal{M}} d^2x\sqrt{-g}\left(\Psi^2 R + \lambda\left(\nabla\Psi\right)^2 - U(\Psi^2) - f(\Psi^2)F^2\right) \\ &- \frac{1}{2G_N}\int_{\partial\mathcal{M}} dx\sqrt{-\gamma}n^\mu\nabla_\mu\Psi^2\,. \end{aligned} \tag{5.31}$$

[9] see [57] for a complete discussion.

Notice that here we have a boundary term in the second line which arises from the bulk action in four dimensions while we neglected this piece in the previous sections. The GHY term gives rise to

$$I_{\rm GHY} = \frac{1}{2G_N}\int_{\partial\mathcal{M}} dx\sqrt{-\gamma}n^\mu\nabla_\mu\Psi^2 + \frac{1}{2G_N}\int_{\partial\mathcal{M}}\sqrt{-h}\Psi^2 K\,, \tag{5.32}$$

where the first term could cancel the boundary term that arises from the bulk action. Even though the boundary term in (5.31) is canceled for spacelike and timelike boundaries, it survives for the WDW patch which is enclosed only by the null boundaries. We can simplify this boundary term by turning it into a corner contribution

$$\begin{aligned} I_{\rm lap} &= -\frac{1}{2G_N}\int_{\partial\mathcal{M}} dx\sqrt{-\gamma}n^\mu\nabla_\mu\Psi^2 \\ &= \frac{1}{4\pi G_N}(\Phi_0+\Phi)\Big|_l^f + \frac{1}{4\pi G_N}(\Phi_0+\Phi)\Big|_r^p\,, \end{aligned} \tag{5.33}$$

where f, p, l and r label the value of Φ on the future, past, left and the right corners of the WDW patch respectively. The GHY term for the null boundaries are given by

$$\begin{aligned} I_{\text{GHY-null}} &= \frac{1}{8\pi G_N}\int_{\mathcal{B}'} d\lambda\, d^2\theta\sqrt{\gamma}\kappa \\ &= \frac{1}{8\pi G_N}\int_{\mathcal{B}'}(\Phi_0+\Phi)\kappa \end{aligned} \tag{5.34}$$

and the joint terms for the corners arising from the intersection of null boundaries are

$$\begin{aligned} I_{\rm joint} &= \frac{1}{8\pi G_N}\int_{\Sigma'} d^{d-1}x\sqrt{\sigma}a \\ &= \frac{1}{8\pi G_N}\Big[(\Phi_0+\Phi)|_f\log|k_1\cdot k_2| + (\Phi_0+\Phi)|_p\log|k_3\cdot k_4|\Big] \\ &- \frac{1}{8\pi G_N}\Big[(\Phi_0+\Phi)|_r\log|k_2\cdot k_3| + (\Phi_0+\Phi)|_l\log|k_4\cdot k_1|\Big]\,, \end{aligned} \tag{5.35}$$

where k_i, k_j are the future directed tangent vectors associated to the null line i and j respectively (Figure 13). Finally, the boundary counterterm is calculated as

$$\begin{aligned} I_{\rm ct} &= \frac{1}{8\pi G_N}\int_{\mathcal{B}'} d\lambda\, d^2\theta\sqrt{\gamma}\,\Theta\,\log\left(\ell_{\rm ct}\Theta\right) \\ &= \frac{1}{8\pi G_N}\int_{\mathcal{B}'} d\lambda\,(\Phi_0+\Phi)\,\Theta\,\log\left(\ell_{\rm ct}\Theta\right)\,. \end{aligned} \tag{5.36}$$

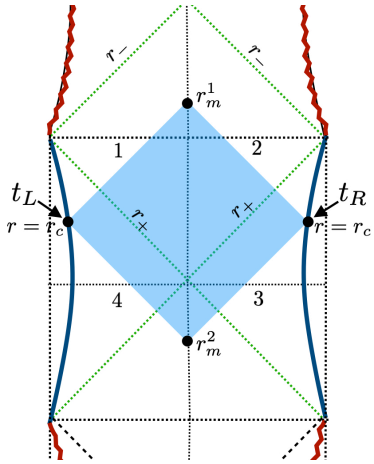

Figure 13: The WDW patch anchored at $t_R = t_L$ on the boundary. The outer and inner horizons appear at $r = r_\pm$.

where the expansion of the null generators are expressed in terms of the two-dimensional quantities as

$$\Theta = \partial_\lambda \log(\Phi_0 + \Phi)\,. \tag{5.37}$$

Complexity=Action in the Jackiw-Teitelboim Model $I_{\rm JT}$

Now we evaluate the Complexity=Action $\mathcal{C}_\mathcal{A}$ for the JT model. The JT model admits the nearly AdS$_2$ solution

$$\begin{aligned} \Phi &= \phi_b(r - r_h) \\ ds^2 &= -\frac{(r-r_+)(r-r_-)}{L_2^2}dt^2 + \frac{L_2^2}{(r-r_+)(r-r_-)}dr^2\,, \end{aligned} \tag{5.38}$$

then we evaluate the action in the WDW patch on this background. We take the WDW patch which is anchored on boundary $r = r_c$ at a time $t = t_L/2 = t_R/2$ as depicted in Figure 13. We can see that the future edge will approach the inner horizon of the black hole at late times and never touches the singularity while it does for the black hole which has the spacelike singularity in higher dimensions. It is possible to show that the equations for the meeting points in the interior are given by

$$\begin{aligned} \frac{t}{2} + r^*(r_c) - r^*(r_m^1) &= 0\,, \\ \frac{t}{2} + r^*(r_c) - r^*(r_m^1) &= 0\,. \end{aligned} \tag{5.39}$$

Using the definition of the tortoise coordinate, these equations imply

$$\begin{aligned}\frac{dr_m^1}{dt} &= \frac{f(r_m^1)}{2}\,,\\ \frac{dr_m^2}{dt} &= -\frac{f(r_m^2)}{2}\,.\end{aligned} \tag{5.40}$$

The action of the JT model in the WDW patch is given by

$$I = I_{\text{bulk}}^{\text{JT}} + I_{\text{GHY}-\text{null}} + I_{\text{lap}} + I_{\text{joint}} + I_{\text{ct}}\,, \tag{5.41}$$

where the bulk term is expressed as

$$I_{\text{bulk}}^{\text{JT}} = \frac{\Phi}{16\pi G_N}\int_{\text{WDW}} d^2x\sqrt{-g}R + \frac{1}{16\pi G_N}\int_{\text{WDW}} d^2x\sqrt{-g}\Phi\left(R-2\Lambda_2\right)\,, \tag{5.42}$$

and we also have the GHY term for the null boundaries of the WDW patch of the form

$$I_{\text{GHY-null}} = \frac{1}{8\pi G_N}\int_{\partial\text{WDW}}(\Phi_0+\Phi)\kappa \tag{5.43}$$

which is evaluated on the WDW patch and the joint term contributions and the boundary counter term

$$\begin{aligned}I_{\text{lap}} + I_{\text{joint}} + I_{\text{ct}} =\ & \frac{1}{4\pi G_N}(\Phi_0+\Phi)\Big|_l^f + \frac{1}{4\pi G_N}(\Phi_0+\Phi)\Big|_r^p\\ &+ \frac{1}{8\pi G_N}\left[(\Phi_0+\Phi)\big|_f\log|k_1\cdot k_2| + (\Phi_0+\Phi)\big|_p\log|k_3\cdot k_4|\right]\\ &- \frac{1}{8\pi G_N}\left[(\Phi_0+\Phi)\big|_r\log|k_2\cdot k_3| + (\Phi_0+\Phi)\big|_l\log|k_4\cdot k_1|\right]\\ &+ \frac{1}{8\pi G_N}\int_{\partial\text{WDW}} d\lambda\,(\Phi_0+\Phi)\,\Theta\,\log\left(\ell_{\text{ct}}\Theta\right)\,,\end{aligned} \tag{5.44}$$

evaluated at the edges and corners of the WDW patch. Using the reparametrization invariance, we can choose an affine parametrization of null vectors such that $\kappa = 0$ with which we can throw all boundary contributions to the corners, then we have

$$I_{\text{GHY-null}} = 0\,. \tag{5.45}$$

For simplicity, this is what we will always do below. Again due to the reparametrization invariance, we can also impose the following condition on the null vectors

$$k\cdot\hat{t} = c \tag{5.46}$$

for simplicity, where c is some constant and $\hat{t}$ is the vector associated with the time in the coordinate (3.9). More explicitly, the future directed tangent null vectors are given by

$$\begin{aligned} 1:\ k^\mu\partial_\mu &= \alpha\left(\frac{\partial_t}{f(r)}-\partial_r\right), \qquad 2: k^\mu\partial_\mu = \alpha\left(\frac{\partial_t}{f(r)}-\partial_r\right), \\ 3:\ k^\mu\partial_\mu &= \alpha\left(\frac{\partial_t}{f(r)}+\partial_r\right), \qquad 4: k^\mu\partial_\mu = \alpha\left(\frac{\partial_t}{f(r)}+\partial_r\right), \end{aligned} \tag{5.47}$$

for each null line where we are using the same normalization constant α for every vector for simplicity. Using this parametrization, contributions from the joint terms and the boundary counterterm can be computed as

$$\begin{aligned} I_{\rm lap}+I_{\rm joint}+I_{\rm ct} =& -\frac{1}{8\pi G_N}\left[(\Phi_0+\Phi)\log\left(\frac{\ell_{\rm ct}^2\Phi_b^2|f(r)|}{\Phi_0^2}\right)-2\Phi\right]_{r_c}^{r_m^1} \\ & -\frac{1}{8\pi G_N}\left[(\Phi_0+\Phi)\log\left(\frac{\ell_{\rm ct}^2\Phi_b^2|f(r)|}{\Phi_0^2}\right)-2\Phi\right]_{r_c}^{r_m^2}. \end{aligned} \tag{5.48}$$

As expected, the α dependence disappears in the final expression thanks to the existence of the boundary counterterm. On the other hand, the bulk action can be simplified if we put the on-shell value of the metric which satisfies $R=2\Lambda_2$ as

$$I_{\rm bulk}^{\rm JT}=\frac{1}{16\pi G_N}\int_{\rm WDW}d^2x\sqrt{-g}R=\frac{\Lambda_2}{8\pi G_N}\int_{\rm WDW}d^2x\sqrt{-g}\,. \tag{5.49}$$

This can be calculated easily and it is expressed as

$$I_{\rm bulk}^{\rm JT}=\left[\frac{\Phi_0}{16\pi G_N}\log|f(r)|\right]_{r_c}^{r_m^1}+\left[\frac{\Phi_0}{16\pi G_N}\log|f(r)|\right]_{r_c}^{r_m^1}. \tag{5.50}$$

Notice that the most dominant contributions to the complexity at late times which are proportional to $\Phi_0\log|f(r)|$ are exactly canceled between the bulk term and the other terms. This cancelation can be explained more generally by the fact that the topological term in the JT action always gives zero contribution to the action

$$\begin{aligned} I_{\rm top}^{\rm JT} &= \frac{1}{16\pi G_N}\int_{\rm WDW}d^2x\sqrt{-g}R-\frac{1}{8\pi G_N}\left[\log|f(r)|\right]_{r_c}^{r_m^1}-\frac{1}{8\pi G_N}\left[\log|f(r)|\right]_{r_c}^{r_m^2} \\ &= 0\,, \end{aligned} \tag{5.51}$$

irrespectively of the shape of the WDW patch. Furthermore, even when the metric deviates from the AdS$_2$, the statement explained above still holds. We prove this in

Appendix C. The time derivative can be determined by the dynamics of the future and past boundaries of the WDW patch r_m^1 and r_m^2 via the relation (5.40), and we can evaluate the growth rate of the complexity as

$$\frac{d\mathcal{C}_{\mathcal{A}}}{dt} = -\frac{\Phi_b}{16\pi^2 G_N}\left[f(r)\log\left(\frac{\ell_{ct}^2\Phi_b^2|f(r)|}{\Phi_0^2}\right)\right]_{r_m^2}^{r_m^1}. \tag{5.52}$$

At late times, points r_m^1 and r_m^2 approach $r_m^1 \to r_-$ and $r_m^2 \to r_+$ respectively, and thus it is easy to see that this leads to

$$\lim_{t\to\infty}\frac{d\mathcal{C}_{\mathcal{A}}}{dt} = 0\,. \tag{5.53}$$

Surprisingly, we see that the JT action leads to a puzzling vanishing complexity growth rate at late times. This is particularly surprising when we consider that the JT model is supposed to capture the low energy dynamics of the SYK model, which is maximally chaotic and hence expected to have non-trivial complexity growth for long times. Next we will see whether we have the same behavior of the complexity growth for the dimensionally reduced theory $I_{\text{JT-Max}}$ in the CA proposal.

Complexity=Action in the Linearized Model $I_{\text{JT-Max}}$

We discuss complexity=action for the dimensionally reduced theory derived from the grand canonical ensemble. We evaluate the on-shell action The action of the JT model in the WDW patch is given by

$$I = I_{\text{bulk}}^{\text{JT-Max}} + I_{\text{GHY}-\text{null}} + I_{\text{lap}} + I_{\text{joint}} + I_{\text{ct}}\,, \tag{5.54}$$

where only the difference from the case of the JT model comes from the bulk term

$$\begin{aligned} I_{\text{JT-Max}}^{\text{bulk}} = I_{\text{JT}}^{\text{bulk}} &- \frac{1}{16\pi G_N}\int_{\text{WDW}} d^2x\sqrt{-g}(\Phi_0-\Phi)(\Lambda_2 - 1/r_h^2) \\ &- \frac{1}{4G_N}\int_{\text{WDW}} d^2x\sqrt{-g}\left[(\Phi_0+\Phi)F_0^2 + 2\Phi_0 F_0^{\mu\nu}\tilde{F}_{\mu\nu}\right]. \end{aligned} \tag{5.55}$$

Putting it on-shell, it gives

$$I_{\text{bulk}}^{\text{JT-Max}} = I_{\text{JT}}^{\text{bulk}} - \frac{\Phi_0}{8\pi G_N}\int_{\text{WDW}} d^2x\sqrt{-g}\left[1 - \frac{\Phi}{\Phi_0} + \frac{\delta Q}{Q_{\text{ext}}}\right]\left(\Lambda_2 - \frac{1}{r_h^2}\right) \tag{5.56}$$

We found that the late-time growth rate of the holographic complexity vanished for the JT model, and so in the theory $I^{\text{JT-Max}}$, the late-time growth rate will come entirely

from the time derivative of this term,

$$
\begin{aligned}
&-\frac{\Phi_0}{8\pi G_N}\frac{d}{dt}\int_{\rm WDW} d^2x\sqrt{-g}\left[1-\frac{\Phi}{\Phi_0}+\frac{\delta Q}{Q_{\rm ext}}\right]\left(\Lambda_2-\frac{1}{r_h^2}\right)\\
&=-\frac{\Phi_0}{8\pi G_N}\left[\left(1+\frac{1}{\Lambda_2 r_h^2}\frac{\delta Q}{Q_{\rm ext}}\right)r-\frac{\phi_b r^2}{2\Phi_0}\right]_{r_m^1}^{r_m^2}\left(\Lambda_2-\frac{1}{r_h^2}\right)\,.
\end{aligned}
\tag{5.57}
$$

At late times, points r_m^1 and r_m^2 again approach $r_m^1\to r_-$ and $r_m^2\to r_+$ respectively, but this time there remains a finite contribution as

$$
\lim_{t\to\infty}\frac{d\mathcal{C}_{\mathcal{A}}^{\text{JT-Max}}}{dt}=\frac{\Phi_0\sqrt{\mu}}{4\pi G_N}\left(1+\frac{1}{r_h^2\Lambda_2}\frac{\delta Q}{Q_{\rm ext}}\right)\left(\Lambda_2-\frac{1}{r_h^2}\right),
\tag{5.58}
$$

This result nicely match the higher dimensional result (5.82) at the leading order, i.e, to the order $\mathcal{O}(\sqrt{\mu})$ and $\mathcal{O}(\delta Q/Q_{\rm ext})$ while $\mathcal{O}(\sqrt{\mu}\delta Q/Q_{\rm ext})$ terms disagree.

Only keeping the leading order of the near-extremal and the large black hole limit, this reduces to

$$
\begin{aligned}
\lim_{t\to\infty}\frac{d\mathcal{C}_{\mathcal{A}}^{\text{JT-Max}}}{dt}&\simeq\frac{\Phi_0\sqrt{\mu}}{4\pi G_N L_2^2}\\
&=2S_0T\,.
\end{aligned}
\tag{5.59}
$$

This result is equivalent to the late time growth in the Complexity=Volume proposal. This result is natural since the result should reflect how the dual SYK model is complexified by the time evolution, and it should be proportional to the entropy and the temperature of the system. It might be intriguing to rewrite the late time behavior of the complexity (5.59) defining the chemical potential defined at the inner and outer horizon

$$
\begin{aligned}
\mu_-&=\frac{1}{G_N}\lim_{r\to r_-}\left((A_0)_t+\tilde{A}_t\right)=\frac{Q_{\rm ext}}{\Phi_0 G_N}\left(1+\frac{1}{r_h^2\Lambda_2}\frac{\delta Q}{Q_{\rm ext}}\right)\left(r'_--r'_+\right),\\
\mu_+&=\frac{1}{G_N}\lim_{r\to r_+}\left((A_0)_t+\tilde{A}_t\right)=0\,,
\end{aligned}
\tag{5.60}
$$

then we obtain the expression

$$
\lim_{t\to\infty}\frac{d\mathcal{C}_{\mathcal{A}}^{\text{JT-Max}}}{dt}=\mu_-Q_{\rm ext}-\mu_+Q_{\rm ext}\,.
\tag{5.61}
$$

It is intriguing to compare this expression with the corresponding higher dimensional one (5.87).

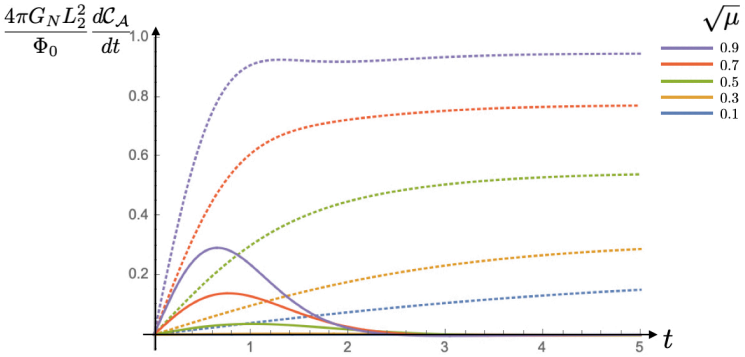

Figure 14: The growth rate of the action complexity in the dimensionally reduced theories. The solid lines correspond to the JT model $I_{\rm JT}$ and the dotted lines correspond to $I_{\text{JT-Max}}$. As seen from the plots, the complexity of the JT model stops growing at late times while for $I_{\text{JT-Max}}$ the complexity grows linearly and it growth rate approaches a finite value which s proportional to the temperature. Here, we set $\Phi_0 = \Phi_b = 1$, $L_2 = 1, \ell_{\rm ct} = \sqrt{10}$ and $r_c = 3$.

5.3 Comparison with Higher Dimensional Black Holes

In this section, we compare the results we show above with results in higher dimensional Reissner-Nordström black holes in AdS. As we explained in the previous section, we divide the action for four-dimensional Einstein-Maxwell theory in terms of the usual Einstein-Hilbert and Maxwell actions, as well as various possible surface terms

$$I_{\rm tot} = I_{\rm EH} + I_{\rm Max} + I_{\rm surf} + I_{\rm ct} + I_{\mu \rm Q}\,, \tag{5.62}$$

where the first two terms are integrated over the bulk of the manifold of interest

$$\begin{aligned} I_{\rm EH} &= \frac{1}{16\pi G_N}\int_{\mathcal{M}} d^4x\,\sqrt{-g}\left(\hat{R} + \frac{6}{L^2}\right)\,, \\ I_{\rm Max} &= -\frac{1}{4G_N}\int_{\mathcal{M}} d^4x\,\sqrt{-g}\,F_{\mu\nu}F^{\mu\nu}\,. \end{aligned} \tag{5.63}$$

The next term $I_{\rm surf}$ contains various surface terms needed to make the variational principle well-defined for the metric,

$$\begin{aligned} I_{\rm surf} = &\frac{1}{8\pi G_N}\int_{\mathcal{B}} d^3x\sqrt{-\gamma}K + \frac{1}{8\pi G_N}\int_{\Sigma} d^2x\sqrt{\sigma}\eta \\ &+ \frac{1}{8\pi G_N}\int_{\mathcal{B}'} d\lambda\, d^2\theta\sqrt{\gamma}\kappa + \frac{1}{8\pi G_N}\int_{\Sigma'} d^2x\sqrt{\sigma}a\,, \end{aligned} \tag{5.64}$$

The null surface counter term which is necessary to ensure reparametrization invariance on the null boundaries is defined as

$$I_{\rm ct} = \frac{1}{8\pi G_N}\int_{\mathcal{B}'} d\lambda\, d^2\theta\sqrt{\gamma}\,\Theta\,\log\left(\ell_{\rm ct}\Theta\right)\,. \tag{5.65}$$

The final contribution in (5.62) is a boundary term for the Maxwell field

$$I_{\mu\rm Q} = \frac{\gamma}{G_N}\int_{\partial\mathcal{M}} d\Sigma_\mu\, F^{\mu\nu}\,A_\nu \tag{5.66}$$

which changes the boundary conditions that must be imposed for consistency of the variational principle.

For the calculations which are immediately following, we will drop the Maxwell boundary term (5.66) by setting the parameter $\gamma = 0$. That is, we examine the holographic complexity working with the action

$$I_0 = I_{\rm tot}(\gamma = 0)\,. \tag{5.67}$$

With this action, we apply the CA proposal to study the holographic complexity for a spherically symmetric *dyonic* Reissner-Nordstrom-AdS black hole whose metric is given by

$$\begin{aligned} ds^2 &= -f(r)dt^2 + \frac{dr^2}{f(r)} + r^2\left(d\theta^2 + \sin^2\theta d\phi^2\right) \\ \text{with}\qquad f(r) &= 1 - \frac{2G_N M}{r} + \frac{Q_e^2+Q_m^2}{4\pi r^2} + \frac{r^2}{L^2}\,. \end{aligned} \tag{5.68}$$

As indicated above, the black hole carries both electric and magnetic charges. The corresponding Maxwell field strength and vector potential can be written as

$$\begin{aligned} A &= \frac{Q_m}{4\pi}(1-\cos\theta)\,d\phi + \left(\frac{Q_e}{4\pi r_+} - \frac{Q_e}{4\pi r}\right)dt\,, \\ F &= \frac{Q_e}{4\pi r^2}\,dr\wedge dt + \frac{Q_m}{4\pi}\sin\theta\,d\phi\wedge d\theta\,. \end{aligned} \tag{5.69}$$

where Q_e and Q_m denote the electric and magnetic charges.

Following the conventions of [60], we write the tortoise coordinates for the black hole spacetime (5.68), as

$$r^*(r) = -\int_r^\infty \frac{d\tilde{r}}{f(\tilde{r})}\,. \tag{5.70}$$

The Eddington-Finkelstein coordinates, v and u, for ingoing and outgoing rays (from the right boundary), respectively, are given by

$$v = t + r^*(r)\,, \qquad\qquad u = t - r^*(r)\,. \tag{5.71}$$

Complexity Growth

Next, we evaluate the growth rate of the holographic complexity for the dyonic black hole (5.68). We anchor the WDW patch symmetrically on the left and right asymptotic boundaries with $t_L = t_R = t/2$. The time evolution of the WDW patch can be encoded in the time dependence of points where the null boundaries intersect in the bulk, *i.e.,* the future boundaries meet at $r = r_m^1$ (and $t = 0$) while the past boundaries, at $r = r_m^2$ (and $t = 0$). The position of these meeting points is determined by [60]

$$\frac{t}{2} - r^*(r_m^1) = 0\,, \qquad\qquad \frac{t}{2} + r^*(r_m^2) = 0\,, \tag{5.72}$$

and then the rate at which these positions change is simply given by

$$\frac{dr_m^1}{dt} = \frac{f(r_m^1)}{2}\,, \qquad\qquad \frac{dr_m^2}{dt} = -\frac{f_(r_m^2)}{2}\,. \tag{5.73}$$

Bulk contribution

We start by evaluating the time derivative of the two bulk terms in (5.63). With the Reissner-Nordstrom geometry (5.68) and the Maxwell field (5.69), these terms yield

$$I_{\text{bulk}} = I_{\text{EH}} + I_{\text{Max}} = \frac{1}{4G_N}\int_{\text{WDW}} dr\, dt\, r^2 \left(-\frac{6}{L^2} + \frac{2\,(Q_e^2 - Q_m^2)}{4\pi r^4}\right)\,, \tag{5.74}$$

where we have used the trace of Einstein equations: $\hat{R} = -\frac{12}{L^2}$. Notice that in the Maxwell contribution (*i.e.,* the second term in the integrand), the electric and magnetic charges appear with opposite signs as we saw in the dimensionally reduced theories. This fact is directly related to the vanishing of the late time rate of complexity for magnetic black holes, as we will see below. Following [60, 63], the time derivative of the bulk action reduces to the difference of terms evaluated at the future and past meeting points,

$$\frac{dI_{\text{bulk}}}{dt} = \frac{1}{2G_N}\left[\frac{r^3}{L^2} + \frac{Q_e^2 - Q_m^2}{4\pi r}\right]_{r_m^2}^{r_m^1}\,. \tag{5.75}$$

Joint contributions

To avoid the divergences, the WDW patch should be cut off by a UV regulator surface at some large $r = r_{\text{max}}$. However, the boundary contributions coming from this time-like surface segment and the corresponding joints yield a fixed constant, *i.e.,* they do not contribute to the time derivative of the action. Further, with affinely-parametrized null normals (for which $\kappa = 0$), the null surface term in (5.64) vanishes. This leaves

only the joint terms at the meeting points, $r = r_m^1$ and r_m^2. The final result for these joint contributions is given by [60]

$$I_{\text{joint}} = -\frac{1}{2\,G_N}\left[(r_m^1)^2 \log\left[\frac{|f(r_m^1)|}{\xi^2}\right] + (r_m^2)^2 \log\left[\frac{|f(r_m^2)|}{\xi^2}\right]\right], \tag{5.76}$$

where ξ is the normalization constant appearing in the null normals, *i.e.*, $k\cdot\partial_t|_{r\to\infty} = \pm\xi$. In a moment, the addition of the counterterm (5.65) will eliminate the ξ dependence of the action. Using (5.72), the time derivative of (5.76) becomes

$$\frac{dI_{\text{joint}}}{dt} = -\frac{1}{4G_N}\left[2rf_(r)\log\frac{|f(r)|}{\xi^2} + r^2\partial_r f(r)\right]_{r_m^2}^{r_m^1}. \tag{5.77}$$

Note that at late times, $r_m^{1,2}$ approach the horizons and so the first term above vanishes. Hence only the second term contributes to the late-time growth rate.

Counterterm contribution

The boundary counterterm (5.65) requires evaluating the expansion scalar $\Theta = \partial_\lambda \log\sqrt{\gamma}$ in the null boundaries of the WDW patch and the final result is given by

$$\begin{aligned} I_{\text{ct}} &= \frac{r_{\max}^2}{G_N}\left[\log\left(\frac{4\xi^2\ell_{\text{ct}}^2}{r_{\max}^2}\right)+1\right] \\ &- \frac{(r_m^1)^2}{2G_N}\left[\log\left(\frac{4\xi^2\ell_{\text{ct}}^2}{(r_m^1)^2}\right)+1\right] - \frac{(r_m^2)^2}{2G_N}\left[\log\left(\frac{4\xi^2\ell_{\text{ct}}^2}{(r_m^2)^2}\right)+1\right]. \end{aligned} \tag{5.78}$$

The term in the first line comes from the UV regulator surface and again only contributes a fixed constant. Hence the time dependence comes only from the terms evaluated at the meeting points in the second line. The time derivative of (5.78) has a compact form,

$$\frac{dI_{\text{ct}}}{dt} = -\left[\frac{rf(r)}{2G_N}\log\left(\frac{4\xi^2\ell_{\text{ct}}^2}{r^2}\right)\right]_{r_m^2}^{r_m^1}. \tag{5.79}$$

Again at late times, this contribution vanishes and so it only changes the transient behavior in the growth rate at early times. It is useful to combine (5.77) and (5.3) to explicitly see that the ξ dependence is eliminated,

$$\begin{aligned} \frac{d}{dt}\left(I_{\text{joint}}+I_{\text{ct}}\right) &= -\frac{1}{4G_N}\left[2rf(r)\log\left[\frac{|f(r)|4\ell_{\text{ct}}^2}{r^2}\right] + r^2\partial_r f(r)\right]_{r_m^2}^{r_m^1} \\ &= -\frac{1}{4G_N}\left[2rf(r)\log\left[\frac{|f(r)|4\ell_{\text{ct}}^2}{r^2}\right] + 2\frac{r^3}{L^2} - \frac{2(Q_e^2+Q_m^2)}{4\pi r}\right]_{r_m^2}^{r_m^1}. \end{aligned} \tag{5.80}$$

Note that in contrast to (5.75), the electric and magnetic charges contribute with the same sign above.

Total growth rate

The growth rate of the holographic complexity is then given by the sum of eqs. (5.75) and (5.80), which yields

$$\frac{d\mathcal{C}_A}{dt} = \frac{d}{dt}\left(I_{\text{bulk}} + I_{\text{joint}} + I_{\text{ct}}\right) = \frac{Q_e^2}{4\pi G_N r}\bigg|_{r_m^2}^{r_m^1} - \frac{r\,f(r)}{2\pi G_N}\log\left[\frac{|f(r)|4\ell_{\text{ct}}^2}{r^2}\right]_{r_m^2}^{r_m^1}. \tag{5.81}$$

At late times, the past and future meeting points meet the outer and inner horizons, respectively, and so the second term vanishes. This leaves the surprising result

$$\lim_{t\to\infty}\frac{d\mathcal{C}_A}{dt} = \frac{Q_e^2}{4\pi G_N\, r}\bigg|_{r_+}^{r_-}. \tag{5.82}$$

Hence if we consider a purely magnetic black hole with $Q_e = 0$, the growth rate vanishes! More generally, we might introduce (5.82) as

$$Q_T^2 \equiv Q_e^2 + Q_m^2 \qquad \text{and} \qquad \chi \equiv \frac{Q_e}{Q_m}, \tag{5.83}$$

which allows us to re-express (5.82) as

$$\lim_{t\to\infty}\frac{d\mathcal{C}_A}{dt} = \frac{\chi^2}{1+\chi^2}\,\frac{Q_T^2}{4\pi G_N\, r}\bigg|_{r_+}^{r_-}. \tag{5.84}$$

Now fixing Q_T, which fixes the spacetime geometry (*e.g.,* $r_\pm$), this expression reveals a nontrivial dependence of this growth rate on χ, the ratio of the electric and magnetic charges. In particular, we see that as we put more of the charge Q_T into the magnetic monopole with $\chi \to 0$, the late-time growth rate shrinks to zero.

Figure 15 illustrates the full time-dependence of the growth rate, as we change the ratio of the electric and magnetic charges while keeping the spacetime geometry fixed.

To compare with the dimensionally reduced theory $I_{\text{JT-Max}}$, we consider the pure electric case $Q_m = 0$ and the consider the near-extremal black hole with extremal charge $Q_e = Q_{\text{ext}}$,

$$\lim_{t\to\infty}\frac{d\mathcal{C}_A}{dt} \simeq 2S_0 T, \tag{5.85}$$

which is agrees with the result (5.59). Moreover if we defined the chemical potential

$$\mu_\pm = \frac{Q_e}{4\pi r_\pm}, \tag{5.86}$$

we can rewrite the result

$$\lim_{t\to\infty}\frac{d\mathcal{C}_A}{dt} = \mu_- Q_e - \mu_+ Q_e. \tag{5.87}$$

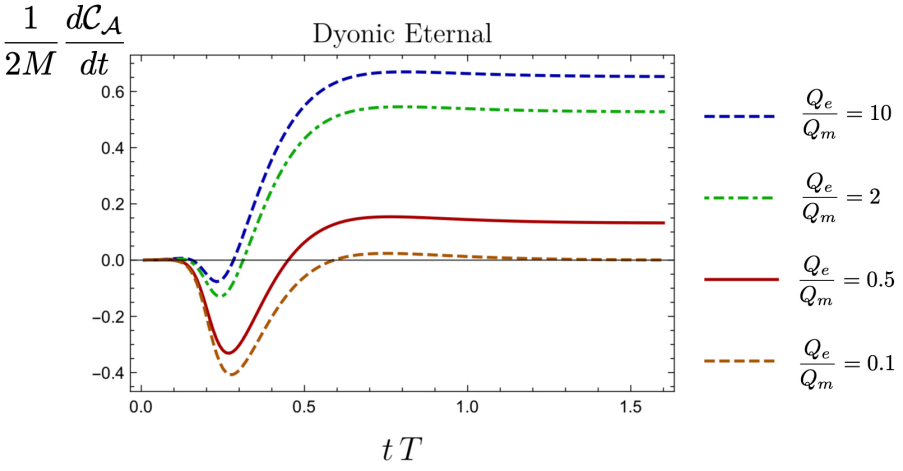

Figure 15: The rate of change of complexity for the dyonic black hole given by (5.68), with $r_- = 0.3\,r_+$, $L = 0.5\,r_+$ and $\ell_{\rm ct} = L$. We fix the parameters that determine the geometry, but vary the ratio between electric and magnetic charges. As predicted by (5.82), when the charge is mostly magnetic, the growth rate of complexity approaches zero at late times. The limit $Q_m \to 0$ essentially matches the top curve for $\chi = 10$. Similarly the $Q_e \to 0$ and the $\chi = 0.1$ curves are indistinguishable on this scale.

The results presented here correctly reproduce the complexity growth of the dimensionally reduced theories $I_{\rm JT}$ and $I_{\text{JT-Max}}$.

Maxwell Boundary Term

In the following, we will argue how the Maxwell boundary term changes the behavior of the complexity growth

$$I_{\mu\rm Q} = \frac{\gamma}{G_N}\int_{\partial\mathcal{M}} d\Sigma_\mu\, F^{\mu\nu}\, A_\nu\,. \tag{5.88}$$

Let us remind ourselves that we use the Maxwell equations $\nabla_\mu F^{\mu\nu} = 0$, then the boundary term (5.88) can be converted into a bulk term via Stokes' theorem as

$$I_{\mu\rm Q}\big|_{\text{on shell}} = \frac{\gamma}{2G_N}\int_{\mathcal{M}} d^4x\sqrt{-g}\, F^{\mu\nu}F_{\mu\nu}\,, \tag{5.89}$$

Thus combining (5.89) with $I_{\rm Max}$ yields

$$I_{\rm Max} + I_{\mu\rm Q}\big|_{\text{on-shell}} = \frac{2\gamma-1}{4G_N}\int_{\mathcal{M}} d^4x\sqrt{-g}\, F^{\mu\nu}F_{\mu\nu}\,. \tag{5.90}$$

Hence in evaluating the WDW action for the general action $I_{\rm tot}(\gamma)$, *i.e.,* including the contribution of the Maxwell boundary term in (5.62), the only change that has to be

made to the previous calculation is to change the overall coefficient of the Maxwell contribution in (5.74). As a result, (5.75) is replaced by

$$\frac{d}{dt}\left(I_{\text{bulk}}+I_{\mu\text{Q}}\right)=\frac{1}{2G_N}\left[\frac{r^3}{L^2}-(2\gamma-1)\,\frac{Q_e^2-Q_m^2}{4\pi r}\right]_{r_m^2}^{r_m^1}. \tag{5.91}$$

Subsequently, the final result for the late-time growth rate for the complexity becomes

$$\lim_{t\to\infty}\frac{d\mathcal{C}_A}{dt}=\left.\frac{\left((1-\gamma)\,Q_e^2+\gamma\,Q_m^2\right)}{4\pi G_N r}\right|_{r_+}^{r_-}. \tag{5.92}$$

Therefore if we set $\gamma = 1$, the dependence on the electric charge drops out of the numerator and the late-time growth rate is primarily sensitive to the magnetic charge. In particular then, with this choice of γ, the late-time growth rate drops to zero for an electrically charged black hole at late times.

6 Summary and Future Directions

In this thesis we performed a comprehensive study of the dimensional reductions of the four-dimensional Reissner-Nordström black holes and investigate various properties of the reduced theories. We mainly chose two types of the black holes: the magnetically charged black holes in the canonical ensemble and the electrically charged black holes in the grand canonical ensemble. Each black hole leads to a certain two-dimensional dilaton gravity theory. We considered the near-extremal and the near-horizon limit of the Reissner-Nordström black holes where the dynamical dilaton in the dimensionally reduced theories takes very small values. Under this limit, we constructed the linearized actions with respect to the dynamical dilaton from the full dimensionally reduced actions. For the magnetic case, we obtained the so-called Jackiw-Teitelboim model. For the electric case, we instead obtained a different dilaton gravity theory coupled to the two-dimensional Maxwell field. While their off-shell actions take the completely different form, they both lead to the same equations of motion with respect to the metric and the dynamical dilaton. We investigated the nearly-AdS_2 solutions of the two theories and computed thermodynamical quantities.

In four dimensions, it is known that electromagnetic duality holds semi-classically between the electric solutions and the magnetic solutions. We also considered how the four-dimensional duality is hidden in the two-dimensional dilaton gravity theories.

We also argued on the relation between our dilaton gravity theories and the so-called SYK model, which is a quantum mechanical model of Majorana fermions. We found that they share various common features. One of the most important features is that in both sides, the reparametrization symmetry is broken to $SL(2,\mathbb{R})$ and the pattern of the symmetry breaking is governed by the so-called Schwarzian action.

To see the difference between the two theories, we also computed a gravitational quantity which is called "holographic complexity". In the Complexity=Volume proposal, both theories give the same answer. This is because the volume only captures the information about background geometry which is common to the two theories. We also computed the complexity in the Complexity=Action proposal. While both theories lead to the same geometry, the behavior of the complexity is completely distinct between them since their on-shell actions are different. For the JT model we see the vanishing growth of the complexity at late times. For the theory derived from the electric solution, the Complexity=Action gives the same late time behavior as the Complexity=Volume proposal. To see the origin of the difference, we also computed the Complexity=Action in the four-dimensional Reissner-Nordström black holes. We found a complete match in the late time behavior of the complexity with the two-dimensional theories.

Future Directions

Permeable Boundary of the JT Model

In this thesis, we analyzed the role of the Maxwell boundary term both in the four-dimensional Einstein-Maxwell theory and the dimensionally reduced theories. In the literature, people mainly have analyzed it for the electric case and stayed away from the magnetic solutions, thus we additionally gave the arguments on the Maxwell boundary term for the magnetic solutions in subsection 2.2. A subtlety comes from the existence of the Dirac monopole. We found a correct prescription which reproduces the electromagnetic duality. We saw that the JT model is derived from the magnetic solution in the canonical ensemble described by the Einstein-Maxwell action without the Maxwell boundary term. We naively expect that adding a dimensionally reduced Maxwell boundary term to the JT model leads to making the boundary of the JT model permeable to the "magnetic charge". However, we didn't give fully satisfactory arguments in this direction in this thesis. The difficulty comes from the fact that we don't know how to treat the Maxwell term for "Dirac monopole" in two dimensions. Moreover the magnetic charge in four dimensions is "absorbed" by the cosmological constant of the two-dimensional AdS spacetime and it is no longer a charge associated to the Maxwell field in two dimensions. These difficulties prevent us from making the permeable boundary of the JT model. What we can do at most in the related direction is to add the on-shell bulk action which is derived from the dimensional reduction of (2.69), but this is an unusual thing to do. We want to explore this direction to obtain a better understanding of the pearmeable boundary for the JT model. This will also help us to give a fully satisfactory explanation on how the electromagnetic duality in four dimensions is encoded in the two-dimensional theories.

Complexity of the JT Model

In this thesis, we computed a quantity which is called "holographic complexity" in the two-dimensional models derived by the dimensional reduction from the four dimensions. We obtained a favorable result for the theory derived from the electric solution since the growth rate at late times approaches a finite value which is commonly expected for the chaotic systems. On the other hand, for the JT model we have the vanishing growth rate at late times. We saw that both models can describe the IR physics of the SYK model by the Schwarzian action. Therefore both theories can be candidates for the holographic duals of (a sub-sector of) the SYK model. (Notice that even if the theory derived from the electric solution could be dual to the SYK model, it would describe some kind of the generalization of the SYK model such as the"charged SYK model" rather than the SYK model itself.) It will be intriguing to see which theory is more favorable from the viewpoint of the complexity behavior as a dual to the SYK

model by defining and computing the complexity of the SYK model itself. While higher dimensional strongly coupled CFTs are so complicated that we cannot have a fully satisfactory definition of complexity (though there are some proposals), but since the SYK model is just the quantum mechanical model of Majorana fermions, we may be able to work on it more easily. Such arguments will also become a starting point to look for a suitable definition of complexity in higher dimensional CFTs and may be able to shed light on the fundamental role of the complexity in AdS/CFT.

Wheeler DeWitt Wave Functions and the Brown-Teitelboim Mechanism
In this thesis, we focused on the semi-classical analyses of the two-dimensional models. It will be interesting to construct Wheeler DeWitt (WDW) wave functions of these models to perform the full quantum gravity analyses. For the JT model, some people already discussed the WDW wave function for the JT model [74, 103, 109]. In [74], they argued the complexity of the JT model using the WDW wave function. It will interesting to compare their approach with ours and the proposal given by [79]. In [79], they proposed a definition of complexity for the wave function the CFT state and holographically reproduced the Complexity=Action proposal using their definition. It is interesting to see how the Complexity=Action proposal can be derived from the WDW wave function of the bulk theory.

In this thesis, we found two-dimensional theories (3.56), (3.76) where the dynamical dilaton and the two-dimensional Maxwell field are coupled with each other. Constructing the WDW wave function of such theories, we will be able to argue about the so-called Brown-Teitelboim mechanism [110, 111] in AdS/CFT context. Brown-Teitelboim mechanism is the model which describes the dynamical change of the cosmological constant of the universe by introducing the d-form flux in the d-dimensional Einstein's gravity. In this mechanism, the value of cosmological constant varies due to the existence of the d-form field source. We want to argue about how the Brown-Teitelboim mechanism works for the two-dimensional dilaton gravity theory. It might be possible to describe the situation where the cosmological constant of the spacetime flows from the negative one (=AdS_2 spacetime) to the zero or positive one. Therefore it will give us the insight into the generalizations of AdS/CFT to the gravity theories with dynamical cosmological constant as well as the holography for the de-Sitter spacetimes.

Relation to the $T\bar{T}$ Deformation of AdS_3/CFT_2
We saw that in order for the JT model or the SYK model to describe the AdS_2 spacetime, it is important to break conformal symmetry by cutting off the IR part of the AdS geometry. Holography at a finite radial cut-off is also extensively argued recently in the context of the AdS_3/CFT_2 correspondence. This can be achieved by deforming

the CFT_2 with the irrelevant operator $T\bar{T}$ and moving it away from the CFT fixed point[112–117]. This mechanism might be related to the mechanism of the conformal symmetry breaking in AdS_2/CFT_1 described by the JT model, thus it is interesting to compare them into details. In the holography of AdS_2/CFT_1, in some sense, the appropriate coordinate system is chosen dynamically. As we saw in the subsection 4.2, the dynamics of the boundary trajectory is governed by the Schwarzian action. If two independent $NCFTs$ (=the SYK models) or Schwarzian actions describe the AdS geometry, the Rindler coordinate is the most natural choice since the boundary trajectory sits along the fixed radial position $r = r_c$ in the Rindler coordinate. As a result, the system describes the thermal (black hole) state. On the other hand, if we consider the situation where the two SYKs or two Schwarzian actions are coupled with each other, it describes the global AdS spacetime since now the boundary trajectory sit at a finite radial position $\eta = \eta_c$ in the global coordinate [118]. In this case, two disconnected boundaries are causality related with each other[10]. Such a dynamical mechanism of choosing the coordinate system has not be considered in the higher dimensional AdS/CFT since the boundary of the AdS is always put at infinity $r = \infty$ and the dual field theory defined on the boundary has the exact conformal symmetry. It is interesting to see whether the same mechanism can be considered in two-dimensional CFTs by deforming the CFT with irrelevant operators such as $T\bar{T}$ operator. This mechanism might give us insight into the resolution of the black hole paradoxes explained in the introduction because the choice of the coordinate system is deeply related to the nature of the gravity and the black hole paradoxes such as Hawking's information problem and the firewall problem are related to the problem about how we can consistently consider the general coordinate covariance in quantum gravity [119–121] (One of the most famous arguments related to that is the black hole complementarity proposal given in [120, 121]). Some difficulties are known in understanding the physics when we impose the Dirichlet boundary condition at a finite radial cut-off of the AdS spacetime [114, 122–124]. Such boundary condition induces the negative image mass on "the other side" of the boundary cut-off and they screen the gravitational force. This might lead to the violation of the causality in the bulk and lack of the UV-completion of the dual field theory. On the other hand, it seems that we do not have similar difficulties in the $NAdS_2/NCFT_1$ correspondence. We want to understand these issues better by comparing the higher dimensional case with the mechanism of the conformal symmetry breaking in the JT model and the SYK model.

[10]This explains one of the strangeness of AdS_2/CFT_1, that is, the fact that two disconnected boundaries of AdS_2 can communicate causality with each other through the bulk spacetime

A More on the linearized theory

In this section, we investigate the "linearized" reduced action (3.53)

$$I_{\text{JT-Max}} = I_{\text{JT}} - \frac{1}{16\pi G_N}\int_{\mathcal{M}} d^2x\sqrt{-g}(\Phi_0-\Phi)\left(\Lambda_2 - \frac{1}{r_h^2}\right) - \frac{1}{4G_N}\int_{\mathcal{M}} d^2x\sqrt{-g}(\Phi_0+\Phi)F^2\,. \tag{A.1}$$

This action seems to only contains the linear terms in Φ, however it is not "self-consistently" truncated while the JT model is. That is, as we will see, plugging the solution of the equations of motion derived from this theory back into the original action, higher order terms show up, and the on-shell action is no longer linearized. This is because the solution of the field strength above contains the dynamical dilaton Φ in the denominator and if we expand it round Φ_0, it contains infinite higher terms. For this reason, in subsection 3.3, we also consider the small deviation of the field strength $\tilde{F}_{\mu\nu}$ from its extremal value $F_0^2 = (\Lambda_2 - 1/r_h^2)/4\pi$ and truncated higher order terms than the linear order with respect both to Φ and $\tilde{F}_{\mu\nu}$. As a result, we obtained the self-consistent truncated theory (3.56). In this section, we stick to the action (A.1) and derive the equations of motion.

The action (A.1) yields the following equations of motion

$$0 = \partial_\mu(\sqrt{-g}(\Phi_0+\Phi)F^{\mu\nu}) \tag{A.2}$$

$$0 = R - 2\Lambda_2 - \left(4\pi F^2 - \Lambda_2 + \frac{1}{r_h^2}\right) \tag{A.3}$$

$$\begin{aligned} 0 = {}& \nabla_\mu\nabla_\nu\Phi - g_{\mu\nu}\nabla^2\Phi - \Lambda_2 g_{\mu\nu}\Phi - \frac{1}{2}\left(\Lambda_2 - \frac{1}{r_h^2}\right)g_{\mu\nu}(\Phi_0-\Phi) \\ & + 2\pi(\Phi_0+\Phi)\left(4F_{\mu\sigma}F_\nu{}^\sigma - g_{\mu\nu}F^2\right). \end{aligned} \tag{A.4}$$

We assume that the solution of the metric take form (3.43) and solve the equation of motion for $F_{\mu\nu}$ as

$$\begin{aligned} F_{\mu\nu} &= \frac{Q}{(\Phi_0+\Phi)}\epsilon_{\mu\nu} = \frac{Q}{\Phi_0}\epsilon_{\mu\nu}\left(1-\frac{\Phi}{\Phi_0}\right) + \mathcal{O}((\Phi(/\Phi_0)^2)\,, \\ F^2 &= -\frac{2Q^2}{(\Phi_0+\Phi)^2} = -\frac{2Q^2}{\Phi_0^2}\left(1-\frac{2\Phi}{\Phi_0}\right) + \mathcal{O}((\Phi/\Phi_0)^2)\,. \end{aligned} \tag{A.5}$$

We choose a constant Φ_0 as

$$\Phi_0 = 4\pi r_h^2\,. \tag{A.6}$$

Since we can approximately compute the following terms using the solution for $F_{\mu\nu}$ (A.5)

$$2\pi(\Phi_0+\Phi)\left(4F_{\mu\sigma}F_\nu{}^\sigma - g_{\mu\nu}F^2\right) = \frac{1}{2}\Phi_0 g_{\mu\nu}\left(\Lambda_2 - \frac{1}{r_h^2}\right)\left(1+\frac{2\delta Q}{Q_{\rm ext}} - \frac{\Phi}{\Phi_0}\right) + \mathcal{O}(\Phi^2/\Phi_0)\,,$$
$$4\pi F^2 - \Lambda_2 + \frac{1}{r_h^2} = \left(\Lambda_2 - \frac{1}{r_h^2}\right)\left(-2\frac{\Phi}{\Phi_0} + 2\frac{\delta Q}{Q_{\rm ext}}\right) + \mathcal{O}(\Phi^2/\Phi_0)\,, \quad \text{(A.7)}$$

then the equations (A.3)(A.4) reduce to

$$0 = R - 2\Lambda_2 + 2\left(\Lambda_2 - \frac{1}{r_h^2}\right)\left[\frac{\tilde{\Phi}}{\Phi_0} - \frac{1}{r_h^2\Lambda_2}\frac{\delta Q}{Q_{\rm ext}}\right] + \mathcal{O}((\Phi/\Phi_0)^2) \quad \text{(A.8)}$$
$$0 = \nabla_\mu\nabla_\nu\tilde{\Phi} - g_{\mu\nu}\nabla^2\tilde{\Phi} - g_{\mu\nu}\Lambda_2\tilde{\Phi} + \mathcal{O}(\Phi^2/\Phi_0), \quad \text{(A.9)}$$

where we shifted the dynamical dilaton $\tilde{\Phi} = \Phi + \Phi_q$. If we only keep the leading order terms both in the equations, it reduces the equations for the JT model. We can see that these equations contain higher order terms $\mathcal{O}(\Phi^2)$, and even if we truncated them, once we plug the solutions back into the original action, the on-shell action inevitably contains higher order terms. Let us compare the result with the equations (3.48) which are obtained from the full action by performing the near-horizon approximations at the level of the equation. The only difference $-\nabla^2\Phi/\Phi$ in the first line of (3.48) comes from the absence of the kinetic term of Ψ in action (3.38). Therefore the "linearized" action (A.1) cannot lead to the correct equations even at the linear order of Φ, then in this sense (A.1) is not a good truncation of the full theory.

B Dimensional Reduction From Higher Dimensional Theories

In this section, we give general arguments on the dimensional reduction of a Reissner-Nördstrom black hole in $d+1$ dimensions. We start with the action

$$I = \frac{1}{16\pi G_N}\int_{\mathcal{M}} d^{d+1}x\sqrt{-\hat{g}}\left(\hat{R} - 2\Lambda\right) + \frac{1}{8\pi G_N}\int_{\mathcal{B}} d^dx\sqrt{-\hat{\gamma}}K$$
$$- \frac{1}{4g^2}\int_{\mathcal{M}} d^{d+1}x\sqrt{-\hat{g}}F_{\mu_1\cdots\mu_{d-1}}F^{\mu_1\cdots\mu_{d-1}}$$

The first line contains the standard Einstein-Maxwell action, including the Ricci scalar $\hat{R}$, the cosmological constant $\Lambda = -d(d-1)/(2L^2)$ with the Gibbons-Hawking-York (GHY) surface term. In the second line, we have the $(d-1)-$form field strength F. The equations of motion and the Bianchi identity for F read

$$\nabla_\mu F^{\mu\nu_1\ldots\nu_{d-2}} = 0\,,\ \nabla_{[\mu}F_{\nu_1\ldots\nu_{d-1}]} = 0\,. \quad \text{(B.1)}$$

The energy momentum tensor is given by

$$T_{\mu\nu} = \frac{d-1}{2g^2}\left(F_{\mu\nu_1\ldots\nu_{d-2}}F_{\nu}{}^{\nu_1\ldots\nu_{d-2}} - \frac{1}{2(d-1)}g_{\mu\nu}F^2\right), \tag{B.2}$$

thus we should solve a pair of the equations of motion

$$R_{\mu\nu} - \frac{1}{2}g_{\mu\nu}R + \Lambda g_{\mu\nu} = 8\pi T_{\mu\nu} \tag{B.3}$$

with (B.1). This system has the charged black hole solution

$$ds^2 = -f(r)dt^2 + \frac{dr^2}{f(r)} + r^2 d\Omega_{d-1}^2\,, \tag{B.4}$$

with the blackening factor

$$f(r) = \frac{r^2}{L^2} + 1 - \frac{\omega^{d-2}}{r^{d-2}} + \frac{q^2}{r^{2(d-2)}}\,. \tag{B.5}$$

and the background magnetic $(d-1)$-form

$$F = g\sqrt{\frac{(d-1)(d-2)}{4\pi G_N (d-1)!}}q d\Omega_{k,d-1}\,. \tag{B.6}$$

The blackening factor (B.5) has two real roots, r_+ and r_- (where $r_+ \geq r_-$) corresponding to the outer and inner horizons respectively. The parameters ω and q are constants which are related to the mass and the charge of the solution, respectively. The F^2 term can be calculated as

$$F_{\mu_1\ldots\mu_{d-1}}F^{\mu_1\ldots\mu_{d-1}} = \frac{g^2(d-1)(d-2)}{4\pi G_N}\frac{q^2}{r^{2(d-1)}}\,. \tag{B.7}$$

The Near Horizon Region

We will now explore the properties of the near horizon region of (near)-extremal black holes in a fixed charge ensemble. At extremality, we find

$$\omega_{ext}^{d-2} = 2\left(\frac{d-1}{(d-2)L^2} + \frac{1}{r_h^2}\right)r_h^d\,, \tag{B.8}$$

$$q_{ext}^2 = r_h^{2d-4}\left(1 + \frac{dr_h^2}{(d-2)L^2}\right), \tag{B.9}$$

where r_h is the position of the horizon of the extremal black hole. The two equations (B.8) and (B.9) come from solving for $f(r_h) = 0$, which determines the position of the horizon, and $\partial_r f(r_h) = 0$ which sets the temperature of the black hole to zero. Inserting

(B.9) and (B.8) in (B.5), in the near-horizon region $r - r_h \ll r_h$, we find that at leading order the metric (B.4) becomes

$$ds^2 = -\frac{(r-r_h)^2}{L_2^2}dt^2 + \frac{L_2^2}{(r-r_h)^2}dr^2 + r_h^2 d\Omega_{d-1}^2\,, \tag{B.10}$$

with

$$L_2^2 = \frac{L^2}{d\,(d-1) + (d-2)^2\,\frac{L^2}{r_h^2}}\,. \tag{B.11}$$

This corresponds to an $AdS_2 \times \Omega_{d-1}$ spacetime, where AdS_2 has curvature scale L_2 and the sphere Ω_{d-1} has curvature scale r_h. This is a feature of extremal black holes, but our interest lies in near-extremal ones. We will now consider a small deviation from extremality by taking the horizons to be

$$r_\pm = r_h \pm \delta r_h\,. \tag{B.12}$$

In this case, at leading order in the parameters that give the deviation from extremality and from the horizon, we have

$$f(r) = \frac{(r-r_h)^2}{L_2^2} + (...)\delta r_h^2\,. \tag{B.13}$$

If we are very close to the horizon, the difference between the extremal and near-extremal geometries is relevant and therefore $AdS_2 \times \Omega_{d-1}$ is not the geometry of the near-horizon region of a near-extremal black hole. However, there is a region given by

$$r_h \gg r - r_h \gg \delta r_h\,, \tag{B.14}$$

where, to leading order, the near-extremal geometry is well approximated by the extremal one (B.10).

The temperature and the entropy of the near-extremal black hole are given, at leading order, by

$$T = \frac{\partial_r f(r_+)}{4\pi} \approx \frac{\delta r_h}{2\pi L_2^2}\,, \tag{B.15}$$

$$\begin{aligned} S = \frac{\Omega_{d-1} r_+^{d-1}}{4G_N} &\approx \frac{\Omega_{d-1} r_h^{d-1}}{4G_N} + \frac{(d-1)\Omega_{k,d-1}\delta r_h r_h^{d-2}}{4G_N} \\ &= \frac{\Omega_{d-1} r_h^{d-1}}{4G_N} + \frac{(d-1)\Omega_{d-1}\pi L_2^2 r_h^{d-2} T}{2G_N}\,. \end{aligned} \tag{B.16}$$

Moreover, if we are considering a near-extremal black hole, it means that we need to slightly deviate from the parameters of the extremal black hole. We choose to work

in an ensemble of fixed charge, hence what changes with respect to extremality is the mass

$$M = M_{ext} + \delta M \,, \tag{B.17}$$

where

$$\delta M = \frac{(d-1)\Omega_{d-1} r_h^{d-2} \delta r_h^2}{16\pi G_N L_2^2} = \frac{(d-1)\Omega_{d-1}\pi}{4G_N} r_h^{d-2} T^2 L_2^2 \tag{B.18}$$

and M_{ext} is the mass of the extremal black hole with mass parameter (B.8).

Dimensional Reduction

We now consider dimensionally reducing the action (B.1). In general, consider a warped product geometry given by

$$ds^2 = ds^2_{(1)} + e^{2\tau\left(x_{(1)}\right)} ds^2_{(2)} \,. \tag{B.19}$$

Then, we have

$$\hat{R} = R_{(1)} + e^{-2\tau} R_{(2)} - 2D\nabla^2_{(1)}\tau - D(D+1) g^{ab}_{(1)} \partial_a \tau \partial_b \tau \tag{B.20}$$

Inserting (B.7) and (B.20) in the bulk action of (B.1) and integrating out the transverse degrees of freedom in the bulk part leads to the following contribution

$$\begin{aligned} I_{\text{bulk}} = & \frac{\Omega_{d-1}}{16\pi G_N} \int_{\mathcal{M}} d^2x\sqrt{-g} \left(\Psi^2 \left(R - 2\Lambda\right) + (\Psi^2)^{\frac{d-3}{d-1}} (d-1)(d-2) + 4\frac{(d-2)}{(d-1)} \left(\nabla\Psi\right)^2 \right) \\ & - \frac{\Omega_{d-1}(d-1)(d-2)q^2}{16\pi G_N} \int_{\mathcal{M}} d^2x\sqrt{-g} \frac{1}{\Psi^2} \\ & - \frac{\Omega_{d-1}}{8\pi G_N} \int_{\partial\mathcal{M}} d\Sigma^\alpha \partial_\alpha (\Psi^2) \,, \end{aligned} \tag{B.21}$$

where the first line comes from the dimensional reduction of the Einstein-Hilbert action, the second line arises from the Maxwell action and the third line is a boundary term which appears due to integration by parts. In (B.21), $\Psi^2 = r^{d-1}$ and R and g refer to the two-dimensional metric that remains after the dimensional reduction of the transverse directions of the higher dimensional metric. We still need to dimensionally reduce the boundary terms present in the action (B.1). The GHY term gives rise to

$$I_{\text{GHY}} = \frac{\Omega_{d-1}}{8\pi G_N} \int_{\partial\mathcal{M}} d\Sigma^\alpha \partial_\alpha \left(\Psi^2\right) + \frac{\Omega_{d-1}}{8\pi G_N} \int_{\partial\mathcal{M}} \sqrt{-\gamma} \Psi^2 K \,, \tag{B.22}$$

where the first term cancels the boundary term that arises from the bulk action in (B.21).

After doing the full dimensional reduction of (B.1), the action reads

$$I = \frac{\Omega_{d-1}}{16\pi G_N}\int_{\mathcal{M}} d^2x\sqrt{-g}\left(\Psi^2 R + \lambda\left(\nabla\Psi\right)^2 - U(\Psi)\right) + \frac{\Omega_{d-1}}{8\pi G_N}\int_{\mathcal{B}}\sqrt{-\gamma}\Psi^2 K \tag{B.23}$$

with

$$\lambda = 4\frac{(d-2)}{(d-1)}\,, \tag{B.24}$$

$$U(\Psi^2) = -(\Psi^2)^{\frac{d-3}{d-1}}(d-1)(d-2) + 2\Psi^2\Lambda + \frac{(d-1)(d-2)q^2}{\Psi^2}\,. \tag{B.25}$$

The bulk part of the action (B.23) is able to capture a wide range of dimensional reductions of higher dimensional spacetimes with different choices of λ and $U(\Psi^2)$. These have been studied in the literature recently [39]. Let us check that the bulk part of this action captures the near horizon region of the extremal Reissner-Nördstrom black hole. In order to write the equations of motion coming from this action, let's work in a gauge where the two-dimensional metric takes the following form

$$ds^2 = -e^{2\omega}dt^2 + e^{-2\omega}dr^2\,. \tag{B.26}$$

We know that the higher dimensional metric is supposed to take the form $AdS_2\times\Omega_{(d-1)}$ in the near horizon region, so we want to look for solutions where the dilaton is a constant $\Psi^2 = \Psi_h^2$ representing the length scale of the manifold $\Omega_{(d-1)}$. In this case, we find the following equations of motion for the action (B.23)

$$U(\Psi_h) = 0 \tag{B.27}$$

$$4(\omega')^2 + 2\omega'' + e^{-2\omega}\partial_{\Psi^2}U(\Psi_h) = 0 \tag{B.28}$$

From the first equation, we get that

$$\Psi_h = r_h^{\frac{d-1}{2}}\,, \tag{B.29}$$

where r_h is the location of the event horizon of the extremal black hole with charge parameter q_{ext}. One can also check that AdS_2 is a solution to the second equation of motion. Considering a metric of the form

$$ds^2 = -\frac{(r-r_h)^2}{L_2^2}dt^2 + \frac{L_2^2}{(r-r_h)^2}dr^2\,, \tag{B.30}$$

we have

$$\omega = \log\frac{r-r_h}{L_2}\,, \tag{B.31}$$

One can check that this is a solution of (B.28) when

$$L_2^2 = \frac{L^2}{d\,(d-1) + k\,(d-2)^2\,\frac{L^2}{r_h^2}}\,, \tag{B.32}$$

which matches (B.10) and (B.11).

Deriving the Jackiw-Teitelboim Model

Starting with the action (B.23), assuming that we have an AdS_2 solution for constant dilaton $\Psi = \Psi_h$ leads to

$$U(\Psi_h) = 0\,, \tag{B.33}$$

$$\partial_{\Psi^2} U(\Psi_h) + \frac{2}{L_2^2} = 0\,. \tag{B.34}$$

In order to deviate from extremality, we will now add a small perturbation to the constant solution r_h

$$r = r_h(1+\psi)\,, \tag{B.35}$$

where

$$\psi = \frac{r - r_h}{r_h} \tag{B.36}$$

is a small parameter. This leads to

$$\Psi = r_h^{\frac{d-1}{2}} \left(1 + \frac{d-1}{2}\psi\right)\,. \tag{B.37}$$

This small perturbation is encoding the deviation from extremality around the near-horizon region of the black hole. We can now expand the potential $U(\Psi^2)$ in a series

$$U(\Psi^2) \approx \partial_{\Psi^2} U(\Psi_h^2)\left((d-1) r_h^{d-1}\psi\right) = -(d-1) r_h^{d-1}\psi \frac{2}{L_2^2}\,. \tag{B.38}$$

Moreover, assuming that we are working with an AdS geometry, we can show that the kinetic term $(\nabla\Psi)^2$ is subleading with respect to the rest. Notice that using (B.30) and (B.37), we have asymptotically

$$(\nabla\Psi)^2 = g^{\mu\nu}\partial_\mu\Psi\partial_\nu\Psi \propto \psi^2\,. \tag{B.39}$$

but we will be working to linear order in ψ and so this term is negligible. Our assumption that we have an AdS geometry is reasonable because, as we commented before, there is a region of the near-extremal black hole where $AdS_2 \times \Omega_{d-1}$ is a good approximation and that is the place where we are going to introduce the boundary of the model. Even though the geometry of the black hole deviates from AdS at linear

order in ψ, this correction would be negligible in computing the above derivative. The dimensionally reduced action (B.23) then leads to

$$\begin{aligned} I \approx & \frac{\Omega_{d-1} r_h^{d-1}}{16\pi G_N} \left(\int_{\mathcal{M}} d^2x \sqrt{-g} \mathcal{R} + 2 \int_{\mathcal{B}} \sqrt{-\gamma} K \right) \\ & + \frac{(d-1)\Omega_{d-1} r_h^{d-1}}{16\pi G_N} \left(\int_{\mathcal{M}} d^2x \sqrt{-g} \psi \left(\mathcal{R} + \frac{2}{L_2^2} \right) + 2 \int_{\mathcal{B}} \sqrt{-\gamma} \psi K \right) \end{aligned} \tag{B.40}$$

If we make the following definitions

$$\Phi_0 \equiv \Omega_{d-1} r_h^{d-1} , \tag{B.41}$$

$$\Phi \equiv (d-1)\Omega_{d-1} r_h^{d-2} (r - r_h) , \tag{B.42}$$

we can rewrite the action (B.40) as

$$\begin{aligned} I = & \frac{\Phi_0}{16\pi G_N} \left(\int_{\mathcal{M}} d^2x \sqrt{-g} R + 2 \int_{\mathcal{B}} \sqrt{-\gamma} K \right) \\ & + \frac{1}{16\pi G_N} \left(\int_{\mathcal{M}} d^2x \sqrt{-g} \Phi \left(R + \frac{2}{L_2^2} \right) + 2 \int_{\mathcal{B}} \sqrt{-\gamma} \Phi K \right) . \end{aligned} \tag{B.43}$$

This is the action of the Jackiw-Teitelboim model.

We see that Φ_0 corresponds to the area of the sphere Ω_{d-1} that appears in the near horizon region of the extremal black hole and Φ is a dynamical dilaton which gives deviations from this area which capture the near-extremal regime. We emphasize that although we have in the back of our mind that this model is arising from the charged black hole, the action (B.43) arises generally from a small expansion of the action (B.23) with different choices of $U(\Psi)$ and λ.

In getting this model, it was assumed that

$$\frac{\Phi}{\Phi_0} \ll 1 . \tag{B.44}$$

Notice that working to linear order in ψ means, indeed, linear order in the ratio $\frac{\Phi}{\Phi_0}$. Besides that, we will also take

$$\frac{\Phi^h}{\Phi^b} \ll 1 , \tag{B.45}$$

where h and b label the values of Φ at the horizon and at the boundary, respectively. In short, we must cut the spacetime in a place where Φ is large but still much smaller than Φ_0. If we did not introduce this cut-off boundary, Φ would grow indefinitely and become bigger than Φ_0 as can be seen from (B.42). Our full condition on the dilaton then reads

$$1 \gg \frac{\Phi^b}{\Phi_0} \gg \frac{\Phi^h}{\Phi_0} . \tag{B.46}$$

Explicitly for the model arising from the charged black hole, we have from (B.42)

$$\Phi^h = (d-1)\Omega_{d-1} r_h^{d-2} \delta r_h \,, \tag{B.47}$$

$$\Phi^b = (d-1)\Omega_{d-1} r_h^{d-2} (r_b - r_h) \,, \tag{B.48}$$

where r_b is the location of the boundary. We then see that the condition (B.46) we are imposing in the dilaton is equivalent to the condition (B.14) which tells us the region in the near-extremal black hole where $AdS_2 \times \Omega_{d-1}$ is a good approximation. This allows for identification of the boundary of the two-dimensional model with a timelike slice in the black hole spacetime that satisfies (B.14). However, we should keep in mind that the geometry of the near-extremal black hole deviates from AdS in linear order in ψ at the boundary, so the geometries of both cases are not precisely the same. Moreover, close to the horizon, there are additional corrections proportional to δr_h^2.

We emphasize that in deriving the JT model, we assumed that we were working in an ensemble of fixed charge by using the action (B.1). For this reason, we can only expect the JT model to capture the properties of black holes with fixed charge but not with fixed chemical potential.

C Topological Part of the Jackiw-Teitelboim Action

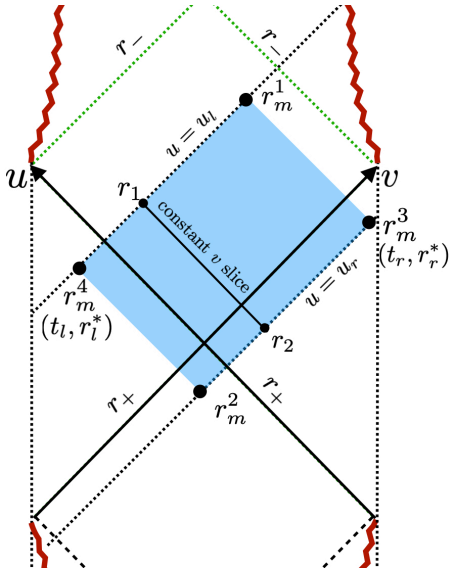

Figure 16: The generic region for the WDW patch.

In this section, we consider the topological term in the JT model

$$I^{top} = \frac{\Phi_0}{4G_N}\left[\int_{\mathcal{M}} d^2x\sqrt{-g}R - 2\log|f(r)||_{r_m^4}^{r_m^1} - 2\log|f(r)||_{r_m^3}^{r_m^2}\right], \tag{C.1}$$

where r_m^3 and r_m^4 are the values of r at the right and the left corner of the WDW patch respectively, and explicitly check that this action is indeed independent of the metrics and the regions $\mathcal{M}$ for WDW patches under the assumption that the metric of the following form

$$ds^2 = -f(r)dt^2 + \frac{1}{f(r)}dr^2\,. \tag{C.2}$$

The scalar curvature of the metric (C.2) is calculated as

$$R = -f''(r)\,. \tag{C.3}$$

We take the WDW patch, which is anchored at the left corner (t_l, r_l^*) and the right corner (t_r, r_r^*), where r^* is the tortoise coordinate defined by

$$r^* = \int^r \frac{dr}{f(r)}\,. \tag{C.4}$$

We also define light cone coordinates u and v as

$$u = t - r^*\,,\ v = t + r^*\,. \tag{C.5}$$

We can express the integral

$$\int_{\mathcal{M}} d^2x\sqrt{-g}R \tag{C.6}$$

in terms of integration variable r and v. First we consider the constant v slice of the WDW patch and perform the r integration. Let us assume that the constant v slice intersects with the line $u = u_l = t_l - r_l^*$ at a point $(u_l, r_1(v))$ and with the line $u = u_r = t_r - r_r^*$ at a point $(u_r, r_2(v))$. Then the integral can be calculated as

$$\int_{\mathcal{M}} dudrR = -\int dv(f'(r_2(v)) - f'(r_1(v)))\,. \tag{C.7}$$

Next we consider the v integral. We can see that the integration should be performed along the $u = u_r$ line and the $u = u_l$ line respectively. Since $v = u + 2\int^r \frac{dr}{f(r)}$, we can parametrize v on the $u = u_l$ line in terms of r_1 and on the $u = u_r$ line in terms of r_2 as

$$v|_{u=u_l} = u_l + 2\int^{r_1} \frac{dr}{f(r)}\,,\ v|_{u=u_r} = u_r + 2\int^{r_2} \frac{dr}{f(r)}\,. \tag{C.8}$$

Therefore, the v integral can be evaluated as

$$\begin{aligned}\int_{\mathcal{M}} d^2x\sqrt{-g}R &= 2\int_{r_m^4}^{r_m^1} dr_1 \frac{f'(r_1)}{f(r_1)} - 2\int_{r_m^2}^{r_m^3} dr_2 \frac{f'(r_2)}{f(r_2)} \\ &= 2\log|f(r)||_{r_m^4}^{r_m^1} + 2\log|f(r)||_{r_m^3}^{r_m^2}. \end{aligned} \tag{C.9}$$

Thus the topological term is always zero

$$I^{top} = 0 \tag{C.10}$$

independently of the choices of $f(r)$ and the regions $\mathcal{M}$. From this fact, we can see that the topological term doesn't contribute to the holographic complexity $\mathcal{C}_{\mathcal{A}}$ even when we take into account of the deviation of the metric from AdS_2 as (3.33) (3.52).

D Free massive particles in AdS

We analyze the motion of a free scalar particle in AdS whose Lagrangian is expressed as

$$S = m\int d\tau = m\int dt\sqrt{g_{\mu\nu}(X(t))\frac{dX^\mu}{dt}\frac{dX^\mu}{dt}} \tag{D.1}$$

Introducing the Lagrange multiplier α, we get

$$S = \int dt\left(\frac{1}{2\alpha}g_{\mu\nu}(X(t))\frac{dX^\mu}{dt}\frac{dX^\mu}{dt} + \frac{\alpha}{2}m^2\right) \tag{D.2}$$

In the case of AdS_2, we can take $X^\mu(t) = (t, \eta(t))$, thus we obtain

$$S = m\int \frac{dt}{\cos\eta}\sqrt{1-\dot{\eta}^2}. \tag{D.3}$$

The canonical momentum conjugate to η is

$$P_\eta = \frac{\partial L}{\partial\dot{\eta}} = -\frac{m\dot{\eta}}{\cos\eta\sqrt{1-\dot{\eta}^2}} \tag{D.4}$$

Using this momentum, we can construct the Hamiltonian

$$H \equiv P_\eta\dot{\eta} - L = \sqrt{\frac{m^2}{\cos^2\eta} - P_\eta^2} \tag{D.5}$$

The smartest way to consider the equations of motions of a free particle is to consider a particle motion in $\mathbb{R}^{2,1}$ constrained to move on the hypersurface $Y_a Y^a = Y_{-1}^2 + (Y^0)^2 - (Y^1)^2 = 1$

$$S = \int ds \left(\frac{1}{2\alpha} \dot{Y}_a \dot{Y}^a + \lambda(1 - Y_a Y^a) + \frac{\alpha}{2} m^2 \right). \tag{D.6}$$

where

$$\alpha = \frac{1}{m} \sqrt{\dot{Y}_a \dot{Y}^a}. \tag{D.7}$$

Equation of motion becomes

$$\ddot{Y}^a = -\lambda Y^a \tag{D.8}$$

along with the constraint equation

$$Y_a Y^a = 1. \tag{D.9}$$

We effectively have three choices: $\lambda = 1, 0, \text{or} -1$. These three choices correspond to timelike, null, or spacelike trajectories in AdS. We focus on the massive particles whose trajectories are timelike $\lambda = 1$. The momentum conjugate to Y^a is given by

$$P_a = \frac{\partial L}{\partial \dot{X}^a} = \frac{1}{\alpha} \dot{Y}_a = \frac{m \dot{Y}_a}{\sqrt{\dot{Y}_a \dot{Y}^a}} = m \dot{Y}_a \tag{D.10}$$

where we used

$$\dot{Y}_a \dot{Y}^a = -\ddot{Y}_a Y^a = \lambda Y_a Y^a = \lambda = 1. \tag{D.11}$$

Using these momenta, we can construct $SL(2)$ generators (angular momentum or boost generators) as

$$L_a = m \epsilon_{abc} Y^b \partial_s Y^c. \tag{D.12}$$

These generators are perpendicular to the geodesic since

$$L \cdot Y = L_a Y^a = m \epsilon_{abc} Y^a Y^b \partial_s Y^c = 0 \tag{D.13}$$

and constant along the geodesic

$$\partial_s L_a = m \epsilon_{abc} Y^b \partial_s^2 Y^c = -m \epsilon_{abc} Y^b Y^c = 0. \tag{D.14}$$

Thus we can associate conserved $SL(2)$ charges to each particle trajectory. Note that the length of the vector L_a is given by the mass of the particle

$$L^2 = m^2. \tag{D.15}$$

From the arguments above we can see that a geodesic is lying on the plane perpendicular to a fixed vector L_a. Thus we get a geodesic trajectory as an intersection between the hypersurface $Y_a Y^a = Y_{-1}^2 + (Y^0)^2 - (Y^1)^2 = 1$ and a plane perpendicular to L_a and contains the origin $Y = (0, 0, 0)$ of $\mathbb{R}^{2,1}$.

The most simple geodesic is given by an intersection between the hypersurface and $Y^1 = 0$

$$\begin{aligned} Y^{-1} &= \cos s \\ Y^0 &= \sin s \\ Y^1 &= 0. \end{aligned} \tag{D.16}$$

This represents a particle sit at $\eta = 0$. In this case, the proper time s is naturally associated with the global time τ(since the global coordinate is coordinate naturally associated with the static observer at $\eta = 0$). For this particle, one can associate a $SL(2)$ charge as

$$\begin{aligned} L_{-1} &= 0 \\ L_0 &= 0 \\ L_1 &= m. \end{aligned} \tag{D.17}$$

A more general solution is given by

$$\begin{aligned} Y^{-1} &= \frac{\cos s}{\cos \eta_*} \\ Y^0 &= \sin s \\ Y^1 &= \tan \eta_* \cos s. \end{aligned} \tag{D.18}$$

which represents the particle is oscillating back and forth between $\eta = \pm\eta_*$. In this case, one can associate a $SL(2)$ charge as

$$\begin{aligned} L_{-1} &= -m \tan \eta_* \\ L_0 &= 0 \\ L_1 &= \frac{m}{\cos \eta_*}. \end{aligned} \tag{D.19}$$

Notice that the Hamiltonian takes constant value $H = |\vec{L}| = m$ along the geodesic of a free scalar particle.

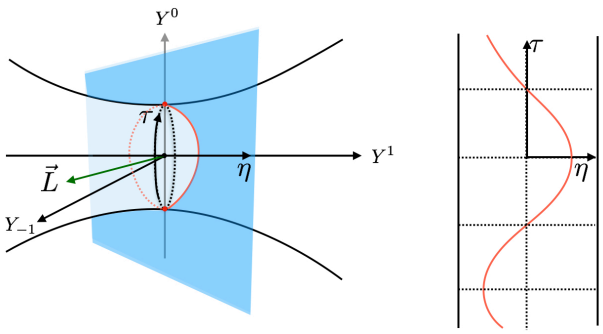

Figure 17: A geodesic of a free massive particle as an intersection between the hypersurface and a plane which is perpendicular to $\vec{L}$ and contains the origin $\vec{Y} = 0$.

E Massive charged particles in AdS

Next we consider the motion of a charged particle in AdS whose trajectory is along $\rho_r = \rho_0$ curve. Due to the curvature of AdS, these trajectory needs an extra electric field which overcomes the gravitational attraction. The Lagrangian for a charged particle is expressed as

$$S = \int ds \left(\frac{1}{2\alpha} \dot{Y}_a \dot{Y}^a + \lambda(1 - Y_a Y^a) + \frac{\alpha}{2} m^2 + q \dot{Y}_a A^a(Y(s)) \right). \tag{E.1}$$

Equation of motion becomes

$$m(\ddot{Y}^a + Y^a) + q F^{ab} \dot{Y}_b = 0 \tag{E.2}$$

along with the constraint equation

$$Y_a Y^a = 1, \tag{E.3}$$

where we take s as a proper time of the particle $\dot{Y}_a \dot{Y}^a = 1$ and $\lambda = m$. We consider the electric field which takes a form

$$F^a_b = \epsilon^a_{bc} Y^c. \tag{E.4}$$

In this case, the equation of motion reduces to

$$m(\ddot{Y}^a + Y^a) + q \epsilon^a_{bc} Y^b \dot{Y}^c = 0. \tag{E.5}$$

This particle trajectory can be obtained by an intersection of the hyperbolic and a plane which is perpendicular to $SL(2)$ vector Q_a

$$Q_a = m \epsilon_{abc} Y^b \partial_s Y^c - q Y_a. \tag{E.6}$$

and contains a point $Y^a = Q^a$. Actually,

$$Q_a Y^a = -q \tag{E.7}$$

and

$$\begin{aligned}\dot{Q}_a &= m\epsilon_{abc}Y^b\partial_s^2 Y^c - q\partial_s Y_a \\ &= \epsilon_{abc}Y^b(-q\epsilon^c_{de}Y^d\dot{Y}^e) - q\partial_s Y_a \\ &= -qY^b(\delta_{ad}\delta_{be} - \delta_{ae}\delta_{bd})Y^d\dot{Y}^e - q\partial_s Y_a \\ &= -qY^aY^b\dot{Y}_b = 0\end{aligned} \tag{E.8}$$

implies that the $SL(2)$ charge is conserved along the particle trajectory.

References

[1] A. Einstein and M. Grossman, "Kovarianzeigenschaften der Feldgleichungen der auf die verallgemeinerte Relativitätstheorie gegründeten Gravitationstheorie," Zeitschrift für Mathematik und Physik, **63**, 215-225 1914.

[2] A. Einstein, "Grundgedanken der allgemeinen Relativitätstheorie und Anwendung dieser Theorie in der Astronomie," Preussische Akademie der Wissenschaften, Sitzungsberichte, **1915 (part 1)**, 315,

[3] A. Einstein, "Zur allgemeinen Relativitätstheorie," Preussische Akademie der Wissenschaften, Sitzungsberichte, **1915 (part 2)**, 778-786, 799-801

[4] A. Einstein, "Erklärung der Perihelbewegung des Merkur aus der allgemeinen Relativitätstheorie," Preussische Akademie der Wissenschaften, Sitzungsberichte, **1915 (part 2)**, 831-839,

[5] A. Einstein, "Feldgleichungen der Gravitation," Preussische Akademie der Wissenschaften, Sitzungsberichte, **1915 (part 2)**, 844-847,

[6] A. Einstein, "Grundlage der allgemeinen Relativitätstheorie," Annalen der Physik (ser. 4), **49**, 769-822 1916

[7] K. Schwarzschild, "Über das Gravitationsfeld eines Massenpunktes nach der Einsteinschen Theorie," Sitzungsberichte der Deutschen Akademie der Wissenschaften zu Berlin, Klasse fur Mathematik, Physik, und Technik, 1916.

[8] S. W. Hawking,"Particle creation by black holes," Comm. Math. Phys. **43** (1975), no. 3 199-220.

[9] S. W. Hawking,"Breakdown of predictability in gravitational collapse," Phys. Rev. D **14** (1976) 2460-2473.

[10] J. D. Bekenstein, "Black holes and entropy," Phys. Rev. D **7**, 2333 (1973).

[11] S. W. Hawking, M. J. Perry and A. Strominger, "Soft Hair on Black Holes," Phys. Rev. Lett. **116**, 231301 (2016) hep-th/1601.00921.

[12] S. W. Hawking, M. J. Perry and A. Strominger, "Superrotation Charge and Supertranslation Hair on Black Holes," JHEP **05** 161 (2017) hep-th/1611.09175.

[13] S. Haco, S. W. Hawking, M. J. Perry and A. Strominger, "Black Hole Entropy and Soft Hair," hep-th/1810.01847

[14] A. Almheiri, D. Marolf, J. Polchinski and J. Sully, " Black Holes: Complementarity or Firewalls?," Journal of High Energy Physics **2013** (2013), no. 2 62 hep-th/1207.3123.

[15] A. Almheiri, D. Marolf, J. Polchinski, D. Stanford and J. Sully, "An apologia for firewalls," J. High Energy Phys. **2013** (2013), no. 9 hep-th/1304.6483.

[16] D. Marolf and J. Polchinski, " Gauge-Gravity Duality and the Black Hole Interior," Phys. Rev. Lett. **111** (2013) 171301hep-th/1307.4706.

[17] S. N .Gupta, "Gravitation and electromagnetism," Phys. Rev. **96**, 1683-1685 (1954),

[18] R. H. Kraichnan,"Quantum theory of the linear gravitational field," unpublished B.S. thesis, Massachusetts Institute of Technology,

[19] R. H. Kraichnan, "Special relativistic derivation of generally covariant gravitation theory," Phys. Rev. **98**, 1118-1122 (1955),

[20] R. H. Kraichnan, "Possibility of unequal gravitational and inertial mass," Phys. Rev. **101**, 482-488 (1956),

[21] S. Deser, "Self-interaction and gauge invariance," General Relativity and Gravitation, **1**, 9-18 (1970),

[22] S. Weinberg, "Derivation of gauge invariance and equivalence principle from Lorentz invariance of the S-matrix", Phys. Lett, **9**, 357-359 (1964),

[23] S. Weinberg, "Photons and gravitons in the S-matrix theory", Phys. Rev, **135**, B1049-B1056 (1964),

[24] J. Maldacena, "The Large N Limit of Superconformal field theories and supergravity," Theor. Math. Phys. **2** (1998) 231-252 hep-th/9711200.

[25] S. S. Gubser, I. R. Klebanov and A. M. Polyakov,"Gauge theory correlators from noncritical string theory," Phys. Lett. B **428** (1998) 105 doi:10.1016/S0370-2693(98)00377-3 hep-th/9802109.

[26] E. Witten,"Anti-de Sitter space and holography," Adv. Theor. Math. Phys. **2** (1998) 253 hep-th/9802150.

[27] S. Ryu and T. Takayanagi, "Holographic derivation of entanglement entropy from AdS/CFT," Phys. Rev. Lett. 96 (2006) 181602, hep-th/0603001.

[28] L. Susskind, "Computational Complexity and Black Hole Horizons," Fortsch. Phys. **64**, 24 (2016), Addendum: Fortsch. Phys. **64**, 44 (2016), hep-th/1402.5674, hep-th/1403.5695.

[29] L. Susskind, "Entanglement is not enough," Fortsch. Phys. **64** (2016) 49 hep-th/1411.0690.

[30] T. Hartman, "Entanglement Entropy at Large Central Charge," hep-th/1303.6955.

[31] A. L. Fitzpatrick, J. Kaplan and M. T. Walters, "Virasoro conformal blocks and thermality from classical background fields," J. High Energy Phys. **11** 200 (2015) hep-th/1501.05315.

[32] A. L. Fitzpatrick, J. Kaplan, D. Li and J. Wang,"On Information Loss in AdS_3/CFT_2," J. High Energy Phys. **05** 109 (2016) hep-th/11603.08925.

[33] C. T. Asplund, A. Bernamonti, F. Galli and T. Hartman, "Holographic entanglement entropy from 2d CFT: heavy states and local quenches," J. High Energy Phys. **02** 171 (2015) hep-th/1410.1392 .

[34] T. Anous, T. Hartman, A. Rovai and J. Sonner,"Black Hole Collapse in the 1/c Expansion," J. High Energy Phys. **07** 123 (2016) hep-th/1603.04856.

[35] J. Maldacena, J. Michelson and A. Strominger,"Anti-de Sitter Fragmentation," J. High Energy Phys. **02** 011 (1999) hep-th/9812073.

[36] G. Sárosi, "AdS_2 holography and the SYK model," PoS Modave **2017**, 001 (2018) hep-th/1711.08482.

[37] R. Jackiw, "Lower Dimensional Gravity," Nucl. Phys. B **252**, 343 (1985). NuclPhysB.252.343.

[38] C. Teitelboim, "Gravitation and Hamiltonian Structure in Two Space-Time Dimensions," Phys. Lett. **126B**, 41 (1983). PhysLettB.126.41.

[39] A. Almheiri and J. Polchinski, "Models of AdS_2 backreaction and holography," JHEP **1511** (2015) 014 hep-th/1402.6334.

[40] J. Maldacena, D. Stanford and Z. Yang, "Conformal symmetry and its breaking in two dimensional Nearly Anti-de-Sitter space," PTEP **2016**, no. 12, 12C104 (2016) doi:10.1093/ptep/ptw124 [arXiv:1606.01857 [hep-th]].

[41] S. Sachdev and J. Ye, "Gapless spin fluid ground state in a random, quantum Heisenberg magnet," Phys. Rev. Lett. **70**, 3339 (1993) cond-mat/9212030.

[42] A. Kitaev,"Hidden correlations in the hawking radiation and thermal noise", Talk at KITP, online.kitp.ucsb.edu/online/joint98/kitaev/, February, 2015.

[43] A. Kitaev,"A simple model of quantum holography", Talks at KITP online.kitp.ucsb.edu/online/entangled15/kitaev/

and online.kitp.ucsb.edu/online/entangled15/kitaev2/, April and May, 2015.

[44] J. Polchinski and V. Rosenhaus, "The Spectrum in the Sachdev-Ye-Kitaev Model," JHEP **1604** (2016) 001 hep-th/1601.06768.

[45] J. Maldacena and D. Stanford, "Remarks on the Sachdev-Ye-Kitaev model," Phys. Rev. D **94**, no. 10, 106002 (2016) hep-th/1604.07818.

[46] S. W. Hawking and S. F. Ross, "Duality between electric and magnetic black holes," Phys. Rev. D **52**, 5865 (1995) hep-th/9504019.

[47] S. Deser, M. Henneaux and C. Teitelboim, "Electric-magnetic black hole duality," Phys. Rev. D **55**, 826 (1997) hep-th/9607182.

[48] J. D. Brown, "Duality invariance of black hole creation rates," Phys. Rev. D **56**, 1001 (1997) hep-th/9702158.

[49] M. Rangamani and T. Takayanagi, *Holographic Entanglement Entropy*, Springer International Publishing, 2017.

[50] M. V. Raamsdonk, "Building up spacetime with quantum entanglement," Gen. Rel. Grav. **42** (2010) 2323-2329. [Int. J. Mod. Phys.D19,2429(2010)] hep-th/1005.3035.

[51] M. V. Raamsdonk, "Lectures on Gravity and Entanglement," Proceedings, Theoretical Advanced Study Institute in Elementary Particle Physics: New Frontiers in Fields and Strings (TASI 2015): Boulder, CO, USA, June 1-26, 2015 hep-th/1609.00026.

[52] D. Stanford and L. Susskind, "Complexity and Shock Wave Geometries," Phys. Rev. D **90**, no. 12, 126007 (2014), hep-th/1406.2678.

[53] A. R. Brown, D. A. Roberts, L. Susskind, B. Swingle and Y. Zhao, "Holographic Complexity Equals Bulk Action?," Phys. Rev. Lett. **116** (2016) no.19, 191301, hep-th/1509.07876.

[54] A. R. Brown, D. A. Roberts, L. Susskind, B. Swingle and Y. Zhao, "Complexity, action, and black holes," Phys. Rev. D **93** (2016) no.8, 086006, hep-th/1512.04993.

[55] D. A. Roberts, D. Stanford and L. Susskind, "Localized shocks," JHEP **1503** (2015) 051, hep-th/1409.8180.

[56] R. G. Cai, S. M. Ruan, S. J. Wang, R. Q. Yang and R. H. Peng, "Action growth for AdS black holes," JHEP **1609** (2016) 161, gr-qc/1606.08307.

[57] L. Lehner, R. C. Myers, E. Poisson and R. D. Sorkin, "Gravitational action with null boundaries," Phys. Rev. D **94**, no. 8, 084046 (2016) hep-th/1609.00207.

[58] S. Chapman, H. Marrochio and R. C. Myers, "Complexity of Formation in Holography," JHEP **1701** (2017) 062, hep-th/1610.08063.

[59] D. Carmi, R. C. Myers and P. Rath, "Comments on Holographic Complexity," JHEP **1703** (2017) 118, hep-th/1612.00433.

[60] D. Carmi, S. Chapman, H. Marrochio, R. C. Myers and S. Sugishita, "On the Time Dependence of Holographic Complexity," JHEP **1711** (2017) 188, hep-th/1709.10184.

[61] S. Chapman, H. Marrochio and R. C. Myers, "Holographic Complexity in Vaidya Spacetimes I," JHEP **1806**, 046 (2018) hep-th/1804.07410.

[62] S. Chapman, H. Marrochio and R. C. Myers, "Holographic complexity in Vaidya spacetimes. Part II," JHEP **1806**, 114 (2018) hep-th/1805.07262.

[63] P. A. Cano, R. A. Hennigar and H. Marrochio, "Complexity Growth Rate in Lovelock Gravity," Phys. Rev. Lett. **121**, no. 12, 121602 (2018) hep-th/1803.02795.

[64] A. R. Brown and L. Susskind, "The Second Law of Quantum Complexity," Phys. Rev. D **97**, no. 8, 086015 (2018) hep-th/1701.01107.

[65] A. Reynolds and S. F. Ross, "Complexity in de Sitter Space," Class. Quant. Grav. **34**, no. 17, 175013 (2017), hep-th/1706.03788.

[66] M. Moosa, "Evolution of Complexity Following a Global Quench," JHEP **1803** (2018) 031, hep-th/1711.02668 .

[67] B. Swingle and Y. Wang, "Holographic Complexity of Einstein-Maxwell-Dilaton Gravity," JHEP **1809**, 106 (2018) hep-th/1712.09826.

[68] M. Alishahiha, A. Faraji Astaneh, M. R. Mohammadi Mozaffar and A. Mollabashi, "Complexity Growth with Lifshitz Scaling and Hyperscaling Violation," JHEP **1807**, 042 (2018) hep-th/1802.06740.

[69] Y. Zhao, "Uncomplexity and Black Hole Geometry," Phys. Rev. D **97**, no. 12, 126007 (2018) hep-th/1711.03125.

[70] Z. Fu, A. Maloney, D. Marolf, H. Maxfield and Z. Wang, "Holographic complexity is nonlocal," JHEP **1802**, 072 (2018) hep-th/1801.01137.

[71] C. A. Agón, M. Headrick and B. Swingle, "Subsystem Complexity and Holography," hep-th/1804.01561.

[72] A. R. Brown, H. Gharibyan, A. Streicher, L. Susskind, L. Thorlacius and Y. Zhao, "Falling Toward Charged Black Holes," hep-th/1804.04156.

[73] A. R. Brown, H. Gharibyan, H. W. Lin, L. Susskind, L. Thorlacius and Y. Zhao, "The Case of the Missing Gates: Complexity of Jackiw-Teitelboim Gravity," hep-th/1810.08741.

[74] Z. Yang, "The Quantum Gravity Dynamics of Near Extremal Black Holes," hep-th/1809.08647.

[75] P. Caputa, N. Kundu, M. Miyaji, T. Takayanagi and K. Watanabe, "Anti-de Sitter Space from Optimization of Path Integrals in Conformal Field Theories," Phys. Rev. Lett. **119**, no. 7, 071602 (2017), hep-th/1703.00456.

[76] P. Caputa, N. Kundu, M. Miyaji, T. Takayanagi and K. Watanabe, "Liouville Action as Path-Integral Complexity: From Continuous Tensor Networks to AdS/CFT," hep-th/1706.07056.

[77] B. Czech, "Einstein Equations from Varying Complexity," Phys. Rev. Lett. **120** (2018) no.3, 031601, hep-th/1706.00965.

[78] A. Bhattacharyya, P. Caputa, S. R. Das, N. Kundu, M. Miyaji and T. Takayanagi, "Holographic Spacetimes as Quantum Circuits of Path-Integrations," hep-th/1804.01999.

[79] T. Takayanagi, "Path-Integral Complexity for Perturbed CFTs," JHEP **1807**, 086 (2018) hep-th/1808.09072.

[80] D. A. Roberts and B. Yoshida, "Chaos and complexity by design," JHEP **1704**, 121 (2017) doi:10.1007/JHEP04(2017)121 [arXiv:1610.04903 [quant-ph]].

[81] K. Hashimoto, N. Iizuka and S. Sugishita, "Time evolution of complexity in Abelian gauge theories," Phys. Rev. D **96** (2017) no.12, 126001, hep-th/1707.03840.

[82] R. A. Jefferson and R. C. Myers, "Circuit complexity in quantum field theory," JHEP **1710** (2017) 107, hep-th/1707.08570.

[83] S. Chapman, M. P. Heller, H. Marrochio and F. Pastawski, "Towards Complexity for Quantum Field Theory States," Phys. Rev. Lett. **120** (2018) no.12, 121602, hep-th/1707.08582.

[84] L. Hackl and R. C. Myers, "Circuit complexity for free fermions," JHEP **1807**, 139 (2018) hep-th/1803.10638.

[85] M. Guo, J. Hernandez, R. C. Myers and S. M. Ruan, "Circuit Complexity for Coherent States," JHEP **1810**, 011 (2018) hep-th/1807.07677.

[86] S. Chapman, J. Eisert, L. Hackl, M. P. Heller, R. Jefferson, H. Marrochio and R. C. Myers, "Complexity and entanglement for thermofield double states," hep-th/1810.05151.

[87] J. Couch, S. Eccles, W. Fischler and M. L. Xiao, "Holographic complexity and noncommutative gauge theory," JHEP **1803** (2018) 108, hep-th/1710.07833.

[88] L. Susskind and Y. Zhao, "Switchbacks and the Bridge to Nowhere," hep-th/1408.2823.

[89] K. Goto, H. Marrochio, R. Myers, L. Queimada, B. Yoshida, "Holographic Complexity Equals Which Action?,"hep-th/1901.00014.

[90] K. Goto, H. Marrochio, L. Queimada, B. Yoshida, "Holographic complexity in the Jackiw-Teitelboim Gravity," in preparation

[91] J. W. York, Jr., "Role of conformal three geometry in the dynamics of gravitation," Phys. Rev. Lett. **28** (1972) 1082, PhysRevLett.28.1082.

[92] G. W. Gibbons and S. W. Hawking, "Action Integrals and Partition Functions in Quantum Gravity," Phys. Rev. D **15** (1977) 2752, PhysRevD.15.2752.

[93] P. Nayak, A. Shukla, R. M. Soni, S. P. Trivedi and V. Vishal, "On the Dynamics of Near-Extremal Black Holes," JHEP **1809**, 048 (2018) hep-th/1802.09547.

[94] D. Brecher, J. He and M. Rozali, "On Charged Black Holes in Anti-de Sitter Space," JHEP **04**, 004 (2005) hep-th/0410214.

[95] B. Wang, C. Lin and E. Abdalla, "Quasinormal modes of Reissner-Nordström Anti-de Sitter black holes," Phys. Lett. B481, 79-88 (2000) hep-th/0003295.

[96] R. C. Myers and M. J. Perry, "Black Holes in Higher Dimensional Space-Times," Annals Phys. 172 (1986) 304.

[97] C. Montonen and D. Olive, "Magnetic monopoles as gauge particles?," Phys. Lett. **72B**, 117-120 (1977).

[98] H. W. Braden, J. D. Brown, B. F. Whiting and J. W. York, Jr., "Charged black hole in a grand canonical ensemble," Phys. Rev. D **42** (1990) 3376 PhysRevD.42.3376.

[99] A. Chamblin, R. Emparan, C. V. Johnson and R. C. Myers, "Charged AdS black holes and catastrophic holography," Phys. Rev. D **60** (1999) 064018 hep-th/9902170.

[100] A. Chamblin, R. Emparan, C. V. Johnson and R. C. Myers, "Holography, thermodynamics and fluctuations of charged AdS black holes," Phys. Rev. D **60** (1999) 104026 hep-th/9904197.

[101] U. Moitra, S. P. Trivedi and V. Vishal, "Near-Extremal Near-Horizons," hep-th/1808.08239.

[102] A. Almheiri and B. Kang, "Conformal Symmetry Breaking and Thermodynamics of Near-Extremal Black Holes," JHEP **1610**, 052 (2016) hep-th/1606.04108.

[103] D. Harlow and D. Jafferis, "The Factorization Problem in Jackiw-Teitelboim Gravity," hep-th/1804.01081.

[104] R. Emparan, C. V. Johnson and R. C. Myers, "Surface terms as counterterms in the AdS / CFT correspondence," Phys. Rev. **D60**, 104001 (1999).

[105] T. Hartman and J. Maldacena, "Time Evolution of Entanglement Entropy from Black Hole Interiors," JHEP **05**, 014 (2013) hep-th/11303.1080.

[106] J. Maldacena, D. Stanford and Z. Yang, "Diving into traversable wormholes," Fortsch. Phys. **65** (2017) no.5, 1700034 hep-th/1704.05333.

[107] G. Hayward, "Gravitational action for space-times with nonsmooth boundaries," Phys. Rev. D **47** (1993) 3275, PhysRevD.47.3275.

[108] D. Brill and G. Hayward, "Is the gravitational action additive?," Phys. Rev. D **50** (1994) 4914, gr-qc/9403018.

[109] J. Lin, "Entanglement entropy in Jackiw-Teitelboim Gravity," hep-th/1807.06575

[110] J. D. Brown and C. Teitelboim, "Dynamical Neutralization of the Cosmological Constant," Phys. Lett. B **195** (1987) 177. doi:10.1016/0370-2693(87)91190-7

[111] J. D. Brown and C. Teitelboim, "Neutralization of the Cosmological Constant by Membrane Creation," Nucl. Phys. B **297** (1988) 787. doi:10.1016/0550-3213(88)90559-7

[112] A. B. Zamolodchikov, "Expectation value of composite field T anti-T in two-dimensional quantum field theory," hep-th/0401146.

[113] F. A. Smirnov and A. B. Zamolodchikov, "On space of integrable quantum field theories," Nucl. Phys. B **915**, 363 (2017) hep-th/1608.05499.

[114] L. McGough, M. Mezei and H. Verlinde, "Moving the CFT into the bulk with $T\bar{T}$," JHEP **1804**, 010 (2018) hep-th/1611.03470.

[115] P. Kraus, J. Liu and D. Marolf, "Cutoff AdS_3 versus the $T\overline{T}$ deformation," JHEP **1807**, 027 (2018) hep-th/1801.02714.

[116] M. Taylor, "TT deformations in general dimensions," hep-th/1805.10287.

[117] T. Hartman, J. Kruthoff, E. Shaghoulian and A. Tajdini, "Holography at finite cutoff with a T^2 deformation," hep-th/1807.11401.

[118] J. Maldacena and X. L. Qi, "Eternal traversable wormhole," hep-th/1804.00491.

[119] K. Goto and Y. Kazama, "On the observer dependence of the Hilbert space near the horizon of black holes," hep-th/1803.01672.

[120] L. Susskind, L. Thorlacius and J. Uglum, "The Stretched horizon and black hole complementarity," Phys. Rev. D**48**, 3743 (1993) hep-th/9306069.

[121] C. R. Stephens, G. 't Hooft and B. F. Whiting, "Black hole evaporation without information loss," Class. Quant. Grav. **11**, 621 (1994) gr-qc/9310006.

[122] D. Marolf and M. Rangamani, "Causality and the AdS Dirichlet problem," JHEP **04**, 035, 2012, hep-th/1201.1233.

[123] T. Andrade, W. R. Kelly, D. Marolf and J. E. Santos, "On the stability of gravity with Dirichlet walls," Class. Quant. Grav. **32**, 235006, 2015, hep-th/1504.07580.

[124] J. Cardy, "Quantum Quenches to a Critical Point in One Dimension: some further results," J. Stat. Mech. **1602**, 023103, 2016, cond-mat.stat-mech/1507.07266.